INFORMATION TO USERS

This manuscript has been reproduced from the microfilm master. UMI films the text directly from the original or copy submitted. Thus, some thesis and dissertation copies are in typewriter face, while others may be from any type of computer printer.

The quality of this reproduction is dependent upon the quality of the copy submitted. Broken or indistinct print, colored or poor quality illustrations and photographs, print bleedthrough, substandard margins, and improper alignment can adversely affect reproduction.

In the unlikely event that the author did not send UMI a complete manuscript and there are missing pages, these will be noted. Also, if unauthorized copyright material had to be removed, a note will indicate the deletion.

Oversize materials (e.g., maps, drawings, charts) are reproduced by sectioning the original, beginning at the upper left-hand corner and continuing from left to right in equal sections with small overlaps.

Photographs included in the original manuscript have been reproduced xerographically in this copy. Higher quality 6" x 9" black and white photographic prints are available for any photographs or illustrations appearing in this copy for an additional charge. Contact UMI directly to order.

Bell & Howell Information and Learning
300 North Zeeb Road, Ann Arbor, MI 48106-1346 USA

UMI®
800-521-0600

A Feasibility Study for a Proactive Congestion Control for Broadband Networks

Periklis Tsingotjidis

A Thesis

in

The Department

of

Electrical and Computer Engineering

Presented in Partial Fulfilment of the Requirements
for the Degree of Doctor of Philosophy at
Concordia University
Montreal, Quebec, Canada

August 1997

ABSTRACT

A Proactive Approach to Congestion Control for Broadband Networks

Periklis Tsingotjidis, Ph. D.
Concordia University, 1997

The feasibility of a proactive congestion control approach for broadband networks, especially involving large propagation delays is examined. The method is based on network overload prediction from a current underload state, by exploitation of the traffic correlations that services being transported exhibit, and subsequent shaping of input traffic through a tunable leaky bucket technique. First passage time analysis for Markov processes and Markov drift processes is used to give a measure of congestion imminence, through the probability distribution for the time to overload. Applications both to real time services and delay tolerant services are discussed. The method is predicated on knowledge of the current source state and a method of estimating it from network measurements is also presented.

To the memory of my father

and to my mother

στη μνήμη του πατέρα μου, Στυλιανού

και τη μητέρα μου

δόξα τῶ Θεῶ

ACKNOWLEDGMENTS

I would like to express my sincere thanks to my thesis supervisor, Prof. Jeremiah F. Hayes, for his patience, and his sincere and democratic approach in guiding me through my studies, and my former colleague, Mr. Vassilios Koukoulidis, for his encouragement and discussions. Last, anyone, who by good and disinterested will, encourage me to finish this task but remains at this point anonymous.

CONTENTS

LIST OF FIGURES

CHAPTER 1
INTRODUCTION

Advances in optical and semiconductor technology as well as market demand for high bit rate services, such as various video services and LAN to LAN high speed data transfer, drove the International Telegraph and Telephone Consultative Committee (CCITT), to introduce the Broadband Integrated Services Digital Network (B-ISDN) concept [CCITT89]. B-ISDN was conceived as an extension to a previously defined narrow band service, and was set to be flexible in accommodating present and future services in terms of their bandwidth requirements, efficient in the use of its available resources, and finally less expensive. All services were envisaged to be integrated not only in the access network as the narrow band concept envisaged, but in the transport network as well. CCITT standardized a versatile packet switching technology [Turne83], known now as Asynchronous Transfer Mode (ATM), as the universal multiplexing and switching technology for broadband ISDN.

1.1 The Asynchronous Transfer Mode

ATM is a packet based technology, but it differs from conventional packet-switched technologies, such as X.25, in that functions such as error and flow control are not supported. The standard, as introduced by CCITT, propose a three layer Protocol Reference model (figure 1.1) [DePry93].

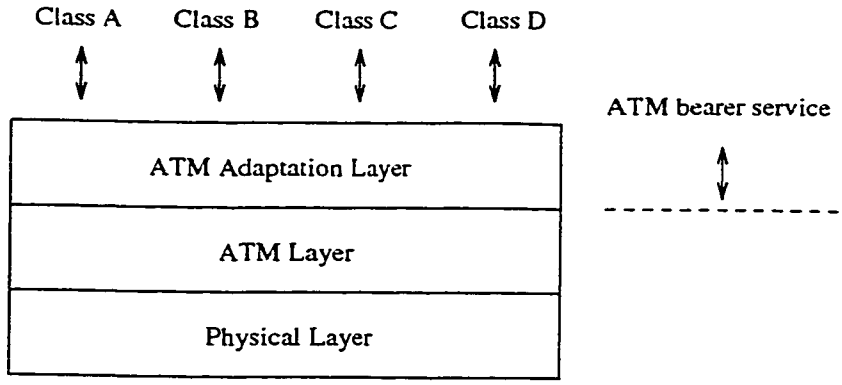

Figure 1.1: ATM Protocol Reference Model (User plane)

The physical layer of the ATM hierarchy defines the electrical or optical characteristics, as well as bit timing and line coding, for supporting the ATM technology on fiber as well as coaxial lines. It defines two transport methods: the first is based on the Synchronous Optical NETwork (SONET) or Synchronous Digital Hierarchy (SDH) standard; the second method has not been standardized, and uses special ATM layer units (cells), called "idle" cells, to create a frame like structure on the access line [DePry93, BaeS91].

SONET/SDH defines a complete digital multiplexing hierarchy, together with access link framing specifications for the User Network (UNI) and Network Node (NNI) interfaces. SONET starts its framing structure definition from the Synchronous Transfer Signal - Level 1 (STS-1), operating at a bit rate of 51.84 Mbits/s; SDH uses the Synchronous Transfer Module - Level 1 (STM-1) as the lower level in its multiplexing hierarchy at 155.52 Mbits/s. Both standards use a flexible multiplexing technique, introducing pointers to the frame payload. N low rate frames are first phase aligned and then byte-interleaved to form a STS-N frame. Frame alignment does not require any buffering, and is achieved through pointer recalculations. Any

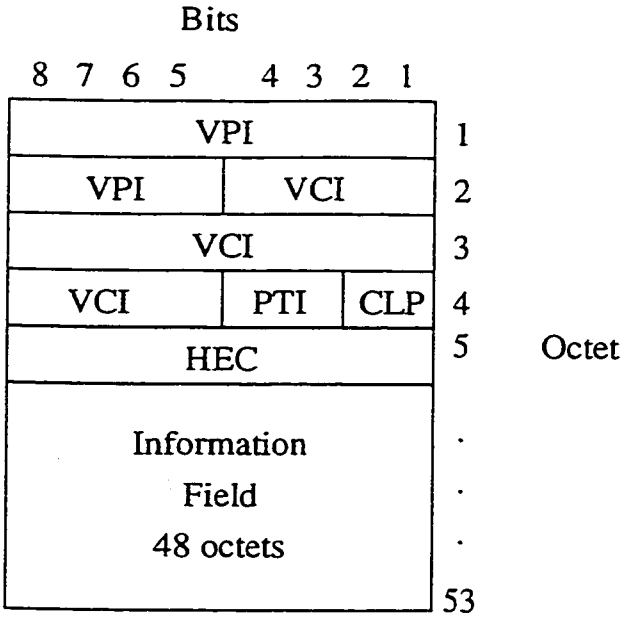

Figure 1.2: ATM cell structure at the Network to Network Interface (NNI) point. Every octet has 8 bits. VPI stand for the Virtual Path Identifier, VCI for the Virtual Circuit Identifier, CLP for the Cell Loss Priority bit, and HEC for the Header Error Control.

variations in frequency between consecutive frames is absorbed through simple pointer operations as well as byte stuffing [BallC89].

The second layer in the hierarchy is the ATM layer and it is responsible for routing and switching. It is based on a standardized fixed length protocol unit that comprises of 53 octets. Figure 1.2 depicts the cell structure for a NNI point; the cell structure at a UNI point differs slightly, to provide flow access control in multidrop access lines.

B-ISDN provides a connection oriented transport based on virtual circuits. Two types of virtual circuits are supported: Virtual Channels (VCs), and Virtual Paths (VPs). VCs are simple end-to-end virtual circuits. VPs stand in a higher conceptual layer, consisting of a bundle of VCs. VPs can simplify network resource management, through route precalculation, between certain source destination pairs, and connection state information prestorage. Moreover, the VP concept can improve network

utilization by facilitating the introduction of different grades of service in an ATM network [CoopP90], [WerAG92],[FriHW96]. The ATM cell header contains information for cell routing, in the form of Virtual Path and Virtual Channel Identifiers (VPI and VCI).

Services provided by the ATM layer are not tailored to any specific application. The third layer of the ATM protocol hierarchy, i.e. the ATM adaptation layer (AAL), enhances the service provided by the ATM layer according to the requirements of specific applications CCITT proposes 4 different classes of services at the AAL layer [KimSY94]. In general, class A is for constant bit rate services such as stream voice or video; class B is for variable bit rate services which require sender and receiver synchronization (i.e. variable bit rate video or packetized voice); classes C and D are reserved for non-constant bit rate applications without sender-receiver synchronization which are either connection oriented (e.g. frame relay) or connectionless (e.g. the Switched Multimegabit Data Service - SMDS).

1.2 The B-ISDN Service Model

To accommodate flexibly a variety of applications, B-ISDN, at the ATM layer level, was structured along a service model. In this section we summarize this model, explaining its structure from the point of view of applications.

Although the list of applications that B-ISDN will support can not be determined permanently, due to the inherent potential of B-ISDN to accommodate with flexibility unforeseen future applications, existing applications can be classified considering voice, video, image, and data in their conversational, messaging, distribution, and

retrieval mode [Garre96]. For instance, telephony belongs to the conversational (interactive) voice applications, e-mail and facsimile are data messaging applications, television is a video distribution service, and video on demand is a video retrieval application. The above applications imply in some way the human involvement; additionally there are important machine to machine applications such as LAN interconnection and LAN emulation.

Applications are characterized by the generation of different traffic patterns and have different quality of services requirements [Garre96]. In terms of traffic pattern, B-ISDN applications are considered "bursty". In loose terms this means that their bandwidth demands vary with time, i.e. voice with silence detection and variable bit rate conversational video. In more precise terms burstiness in traffic signifies cell arrivals that are time correlated. In this respect traditional computer communications and voice/video/text messaging and retrieval applications (e.g voice mail or video on demand) are even burstier.

Services also have diverse performance requirements, in terms of delay (maximum or average), delay variance and loss. Interactive applications such as conversational voice or video have maximum delay and delay variance requirements, but they are loss tolerant to some extent. An occasional lost cell can be tolerated; but, if that cell contained video frame synchronization information, then its loss is important. Distribution applications, e.g. television broadcasting, are not so strictly delay constrained, but they are affected by delay variance. Messaging and retrieval applications are more tolerant to average delay in different degrees, but there are loss intolerant; files transferred from remote file servers are required to be error free at the desti-

nation. Computer communication applications are generally sensitive to cell loss; of course the application might rely on higher level protocols to recover from the losses, at the expense of some delay incursion. However, compared to messaging services computer communications applications cannot tolerate excessive delays.

To meet the diverse performance requirements of the services being transported, B-ISDN is organized using a service model that provides several service categories. So far, the list of envisaged services include, the Constant Bit Rate (CBR), Available Bit Rate (ABR), unspecified Bit Rate (UBR) and the Variable Bit Rate (VBR) service, either in its real time or non-real time form. The list is not exclusive, and other service categories might be added to the service model as needed. A service category is simply a concept which suggests that there are important applications with common requirements and properties, and that some mechanisms exists that can provide appropriate QoS for these applications [Garre96].

CBR service guarantees a maximum cell delay transfer as well as a limited cell delay variation. Real time VBR service offers the same guarantees as the CBR service, with the addition of a cell loss rate guarantee. UBR is a "best effort" service, and as such does not offer any specific guarantees either in terms of delay on in terms of cell loss. Non real-time VBR service has been introduced in order to improve the delay and loss performance of the UBR service by offering some guarantees in terms of these performance figures. Finally, the ABR service can also be seen as a refinement of the UBR service, for applications that require very small amount of cell loss, but are extremely delay tolerant.

In order for these services to be provided on a fixed length packetized network

transport (ATM), some form of traffic and congestion control is required. According to CCITT, traffic control refers to all these functions that cooperate to prevent congestion, while congestion control refers to the functions that dissipate the effects of congestion once happened.

1.3 Traffic and Congestion Control in Broadband Networks

Congestion control methodologies for broadband networks can be classified in many ways. [YangR95] classify them according to a control theoretic approach. We follow roughly the same approach with differences in terminology and paying more attention to applications. We follow the following classification; we call all the algorithms that tend to control congestion with no feedback from the network as preventive. These algorithms comprise the open-loop algorithms in [YangR95]. Moreover, we divide all the close-loop algorithms (that control congestion using feedback from the network) according to whether the feedback is sent during the onset of congestion (reactive algorithms) or prior and in anticipation to it (proactive algorithms). Following we present each of the three congestion control classes alluded to above, drawing specific examples from existing congestion control proposals.

1.3.1 Preventive Controls

The most important algorithm of this class (although simple) is connection admission control. The network refuses access to incoming calls to guarantee the performance offered to currently subscribed calls. Whereas the method can be easily described, its implementation faces difficulties in the realm of ATM based broadband

networks. To determine the threshold where service to an additional call must be denied, we must first characterize the resources that a call occupies for a certain QoS delivered to it.

Real time services can not tolerate long delays, and therefore buffering for these services must be kept to a minimum; accordingly, bandwidth is the principal network resource that affects their performance, and connection admission control can be based on call bandwidth requirements. However, the characterization of the bandwidth requirements of a call, can be accomplished in different ways.

Call bandwidth needs can be characterized simply by peak bandwidth requirements, and admission control can be performed on a peak bandwidth demand basis. However, due to the inherent temporal variability of the bandwidth demands of some applications, peak bandwidth admission control might result in low bandwidth utilizations. Nevertheless, for the CBR service category, this is the only method applicable, and thus, CBR service admission control is identical with the admission control applied to circuit switched networks.

For real time VBR service category implementation, peak bandwidth admission control results in inefficient bandwidth utilization, as explained above. To increase the efficiency of the network resource utilization, bandwidth in this case is allocated on an equivalent bandwidth basis, a value that stands between the peak bandwidth demand of a call and its mean. Call equivalent bandwidths, on links where no buffering is performed, can be determined by a layered approach to preventive congestion control, where admission control is performed in various layers within a call [Hui88], [Hui91]. Alternatively, equivalent bandwidth on links where buffering is allowed can

be given approximately in [GueAN91]; approximations are based partially on the use of the fluid flow model [AniMS82]. Finally another approach to equivalent bandwidth calculation is given in [ElwaM93] based completely on the model of [AniMS82].

Equivalent bandwidth admission control treats all cells of a given call equally in terms of loss, and therefore offers a uniform grade of service across all cells within a call. Bandwidth utilization can be further increased, if the network offers more than one grade of service, either on a per call, or in per cell basis [KrHBG91]; e.g. we can offer one guaranteed grade, for cells that carry vital to the application information, and a second not guaranteed at all.

To offer discriminated service on a per cell basis, source generated traffic must be classified in at least two classes. For voice traffic, methods to achieve this are presented in [YinLS90]. These methods include embedded coding [BiaGS80] where the least significant bits of a voice sample after quantization and coding, are placed in different ATM cell payloads than the most significant ones. Garrett and al. [GarrV93] considers joint source/channel coding using embedded coding on a PCM coded video sequence as well.

The principle of grading the traffic generated by source according to its importance, can be coupled with a selective packet discard methodology at the network switching and multiplexing points. Selective discarding rejects lower priority packets at the entrance of the node when certain congestion thresholds are exceeded. Yang et al. [YangR95] classify this scheme, as an open loop congestion strategy with destination (intermediate node) control.

1.3.2 Reactive Controls

Reactive congestion control methodologies were employed initially in packet switched networks, that carried nontime critical data, in order to strike a good compromise between throttling users (throughput) and keeping the average delay per message at a reasonable level (and consequently packet loss) [BertG92]. A classic example of these algorithms is the window based flow control algorithms for data networks (e.g. Transmission Control Protocol).

Reactive controls need some kind of feedback from the network about impending congestion, and upon reception of such information, they react accordingly to diffuse it. In the TCP protocol, for instance, the sender learns about congestion in an implicit way (when an outstanding packet times out) and reacts by reducing its transmission window.

Reactive congestion control methodologies have been proposed in the broadband network environment as well. They can be used in support of the real time VBR ATM service category, in a closed loop feedback loop manner. Admission control normally limits the number of sources admitted into the network, to render the probability of congestion at a interior node of the network to be below a given threshold. In cases of congestion this scheme can be supplemented by selective cell discarding [YinLS90]. However, discarding cells in the interior of the network wastes resources by allocating them to traffic that later is discarded. Reactive closed loop controls reduce this effect, by discarding information at the entrance of the network [YinHl91].

Reactive congestion control methods were proposed for the ABR service as well.

The objective of ABR service is to use the available bandwidth (the bandwidth that remains on a link after the CBR and VBR traffic have been served) in an efficient and fair manner. Moreover, since it targets delay tolerant applications, it aims at zero or very low loss rate at the expense of delay [CheLS96]. There were two proposals for reactive controls to support ABR traffic; the first which is based on shaping the peak rate of connections in response to network feedback due to congestion, and was eventually adopted by the ATM Forum, is the rate-based flow control method [BonoF95]; the second is based on buffer space allocations inside the switches and per VC queueing (credit-based method [KungM95]).

1.3.3 Proactive Controls

The principal problem with reactive congestion control methods is that they are sensitive to the bandwidth delay product of a network. When congestion is detected inside the network and a signal is sent across it to the traffic sources at its entrance, it takes a one way propagation time for this signal to reach the periphery of the network where traffic sources lie. Moreover, even if with the immediate reception of this signal sources make adjustments to reduce their transmission rate, it takes another one way propagation time for these changes to be effective at the congested node. Throughout this round trip time losses might occur at the multiplexer. For real time services such as the VBR real time service (when it is operated in a statistical mode), which are loss tolerant, losses mean wastage of the network resources until the congested point of the network.

For delay insensitive traffic, losses should be eliminated with the provision of ap-

propriate buffer space at the nodes. However, the amount of buffering required to eliminate losses equals the bandwidth delay product of the network. This can be quite large, in current broadband networks where bandwidths can be in the hundreds of Mbits/sec range. The problem might be present in networks with somehow lower bandwidths but large round trip times. A major example of this class of networks are satellite networks. In Europe the Universal Mobile Communication System (UMTS) aims at developing tetherless access at variable bit rates of up to 144 Kbits/s to support N-ISDN (2B+D) basic services. Moreover access speeds up to the primary N-ISDN rate (2 Mbits/s) are under study, however, in a limited radio environments [Rapel95]. Satellites will extend this services to rural outdoor environments, where the deployment of terrestrial networks is not economically attractive [AnanP95]. Currently there are second generation mobile satellite systems operating at the Geosynchronous Earth Orbit (GEO), that offer data and voice services, mostly for maritime and aeronautical applications where relatively large terminals are used. For personal communications, the trend is to use small satellites operating at Low Earth Orbits (LEOs) or even Medium Earth Orbits (MEOs). LEOs further are divided in "small", operating at frequencies below 1 GHz and "big LEOs" operating at over 1 GHz. Services offered are either data or limited voice services.

Moreover, in parallel with the introduction of the narrowband access to ISDN services through UMTS, access to the broadband ISDN services is considered in Europe though the Mobile Broadband System (MBS) platform [Ferna95]. As with UMTS a similar satellite component of MBS exists. In this vein Spaceway, a wideband access satellite system supports asymmetric wideband access at 384 Kbits/s - 6 Mbits/s

at the uplink and 108 Mbits/s at the downlink, with hubless full mesh networking. Moreover it provides bandwidth on demand, using ATM switching on board.

For real time services, e.g. packet voice and conversational video buffering in case of congestion is not very helpful. Therefore losses are unavoidable during congestion, and selective packet discarding can be used [YinLS90]. Reactive controls, reduce the resources that are wasted carrying information that will later be discarded at a congested point in the network [YinHl91].

Proactive congestion controls are based on the prediction of overload, given a current underload network state and the subsequent transmission of feedback signals to the network input in the case of anticipated congestion; traffic adjustment at the network inputs take place in response to these feedback signals [HuLP95].

Evaluation of the efficiency of any traffic and congestion control method, as well as resource dimensioning and management, requires the postulation of traffic models for the various applications supported by B-ISDN, that capture the essential traffic characteristics to predict statistical multiplexing performance. In the next section we overview some of the source traffic models that appeared in the literature with special emphasis to the models used in this thesis.

1.4 Traffic Modeling Overview

A general characteristic of the traffic generated by B-ISDN applications is that it is correlated. Traffic correlation extends in different time scales [NoRSV91], [LeTWW94], and has been captured in different ways in various models.

For individual PCM coded voice sources with silence detection, simple renewal models, such as the well established binary On-Off model with uniform cell arrivals during the On times (fig. 1.3) [Brady69], have been employed. However, when more

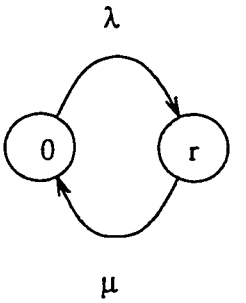

Figure 1.3: The continuous time binary On-Off source model

than one source are statistically multiplexed, correlative effects come into place, that renewal models can not capture. To facilitate analytical treatment of statistical multiplexing in these cases, the superposition of a set of voice sources has been modeled by a non-renewal process, that is based on a two state Markov process as well. This process is termed as the Markov modulated Poisson process (MMPP) [HeffL86] (figure 1.4), and differs from the previous On-Off model on the fact that, during sojourn time in any of the two Markov states cells are generated according to Poisson processes with rates γ and γ'. Finally, keeping the two-state Markovian model and ignoring completely the cell level traffic variations (in fact assuming that traffic arrive as a

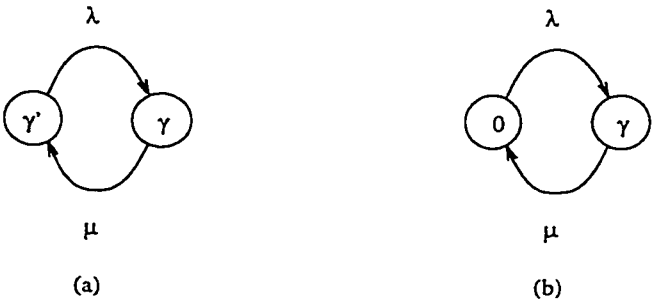

Figure 1.4: (a) The two state MMPP process; (b) the IPP process.

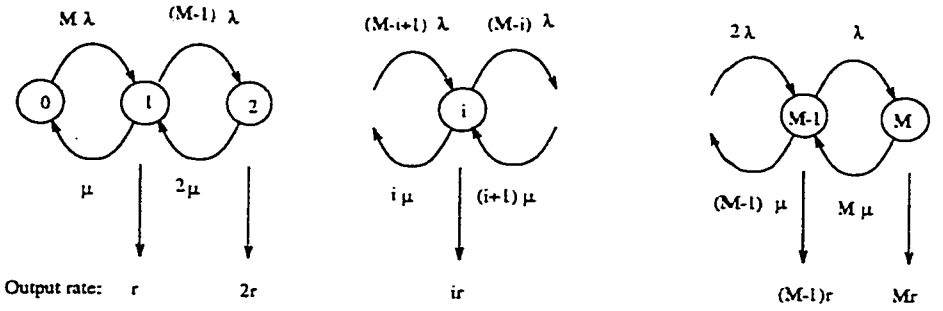

Figure 1.5: The birth-death process describing the Maglaris' video model.

fluid with fixed rate during On source periods), we arrive at the third voice model, the fluid model, introduced by Anick et al. [AniMS82].

Statistical video modeling follows two trends; there are researchers that advocate non-Markovian models, on the grounds that video traffic presents long-term dependencies [BSTW95]. However, Heyman et al. claim in [HeyL96b] that long range effects are significant only when multiplexer queues exhibit long busy periods, which might not be the case when multiplexers are equipped with small buffers, to limit maximum delay for time critical applications.

We will follow the last approach and we will use Markovian models for video traffic modeling; specifically we will use a fluid model developed by Maglaris et al., [MASKR88], where a birth and death process captures the rate variations of a variable bit rate videoconference connection (figure 1.5). More advanced, and of higher dimensionality, Markovian models for videoconference applications appear in [HeyTL96], and [HeyL96a] (discrete autoregressive of order one model). However, we feel, as in [GarrV93], that the Maglaris' model serves as a first order approximation for videoconferencing scene modeling, especially in capturing the essential short range dependence of video traffic, for traffic prediction purposes. For video applica-

tions other than videoconferencing, e.g. broadcast video distribution and video on demand, statistical source modeling is still an open issue [HeyL96a]. Video-sequence dependent Markovian models are proposed, but universal models, applicable to every video-sequence, could not be stated.

For real-time image transfer applications, we follow the approach of [Hui91], and we model image transfers using the On-Off model as well. For applications that are more delay tolerant, i.e. Ethernet traffic on Local Area Networks, and for data traffic in LAN interconnection services, the use of Markovian models is challenged in [LeTWW94], due to the long range traffic dependence observed in traffic traces involving this kind of applications. However, Norros [Norro95] proves that, at least for linear prediction purposes, knowing the infinite past of a long range dependent process, does not contribute to the future prediction of that same process, and only a finite past of the process, of duration equal in depth to the prediction horizon will suffice to give an accurate estimate. The above argument might be used to give a support to the use of short range dependent Markovian models for LAN traffic as well.

1.5 Thesis Outline

In this thesis we propose a proactive congestion control algorithm for broadband networks. The algorithm predicts the imminence of congestion inside the network, and accordingly modifies appropriate source parameters at the network input.

Chapter 2 deals with the problem of congestion prediction, when the network is loaded with real time services services only, and buffering is not allowed inside the

network. A measure of congestion imminence is given, by treating as overload the network state, where the sum of peak rates of all active sources equals the channel capacity, and considering the probability that such a network state is reached from a current underload state in a less than a network round-trip delay time. The passage to overload is treated as a first passage to a state problem for a Markov process. The dependence of the imminence of congestion on the number of admitted calls, and their statistical characteristics is explicitly described. This description in turn is used to devise in-call source parameter adjustments, such as peak source rate and active and idle period control. Finally, the proactive strategy is compared with the pure preventive control approach.

Chapter 3 characterizes the imminence of congestion when buffering is allowed inside the network. This case might correspond to networks loaded with delay tolerant services; however, the high speeds involved with B-ISDN allow buffering for services with end-to-end time constraints as well. The problem is treated as a fluid flow problem, and overload prediction is related to the first passage problem for a Markov drift process. The aim of the chapter is to present in-call source parameter controls towards a proactive congestion control methodology in the case of buffered statistical multiplexing.

Our proposed proactive control methodology (in chapters 2 and 3) is based on the layered approach for congestion control that appeared in [Hui88]. As such, it requires the knowledge of the current traffic levels in terms of currently active bursts in the system (for real time services). Prediction of congestion for delay sensitive services (chapter 3) requires additionally the knowledge of current buffer levels. In chapter 4

we propose a linear algorithm to estimate the current number of active traffic bursts in our system, from observations of cell counts on the output links of a switch for real time services.

CHAPTER 2
OVERLOAD PREDICTION FOR A BUFFERLESS RESOURCE

In this chapter the overload prediction for a statistical multiplexer loaded with real-time traffic is presented. The multiplexer is assumed to be working in the underload region, and prediction is performed by finding the probability that it will overload in a network round trip delay time.

Overload prediction assumes that the number and type of all sources that use the services of the multiplexer, their statistical characteristics, and the current source state, are known to us in advance. As far as the number of subscribed sources is concerned, their number can be registered during the call establishment phase. The statistical characteristics of the calls can be declared by the user during call set up negotiation with the network as well. Furthermore, the current network state, in terms of number of sources that are currently active and transmitting on the output channel, can be estimated, using e.g. Kalman filtering of cell count observations at the multiplexer output link (chapter 4).

Services can be approximated to one degree or another by Markovian models on the rate. This property can be used to predict the time to overload. We focus first on real time models for which overload occurs when the simultaneous rate is greater than

the available capacity. Buffering is used only when there are simultaneous arrivals. The time scales that are involved, allow us to use the fluid flow approximation. The basic question is whether the correlation times for realistic sources are such that congestion can be predicted and avoided.

Under the above assumptions, the probability distribution to overload can be found as the first passage distribution to a state for a Markov process. This distribution is known to be of the phase type [Nelso95]. For the special case that the Markov process is a one-dimensional birth and death process, the problem is addressed in [Keils64].

We divide this chapter in two parts: in the first part (section 2.1), the overload problem in the case where the multiplexer is loaded with a single type of sources (homogeneous case) is treated; in the second (section 2.2), we assume the existence of more than one type of sources (heterogeneous case). In the homogeneous case, the problem requires the determination of the first passage to a state time for a birth and death process, and therefore the formulation of [Keils64] applies. Similarly, the heterogeneous case involves the first passage time of a multidimensional birth and death process to a set of states. In both cases however, the probability distribution for the time to overload can be expressed as a summation of exponentially decaying terms, equal in number to the dimensionality of our problem (the product of the number of subscribed sources over all source types) [Keils65]. Section 2.1.1 develops the multiplexer model in detail for the homogeneous case, and introduces necessary notation. Section 2.1.2 develops the set of first order linear differential equations that the probability distribution for the time to overload satisfies, and gives their

solution in terms of the eigenvalues of our system. Consequently, section 2.1.3 uses this expression of the solution for the probability distribution for the time to overload, as a characterization of congestion imminence in a network round-trip time interval, and presents in-call parameter control methods to keep the probability of a congestion onset event in a network round-trip time interval at low levels. Similarly, section 2.2.1, presents the multiplexer model in a heterogeneous environment, and section 2.2.2 develops and solves the system of pertinent linear differential equations for the probability distribution for the time to overload in this case. Finally, the expression of the solution for the probability distribution for the time to overload is used in section 2.2.3 to extend proactive congestion control schemes in a heterogeneous source environment.

2.1 Single Source Type

2.1.1 Model Formulation

We envisage N identical connections sharing a part C of the capacity of a network link through the auspices of a statistical multiplexer. This capacity might correspond to the capacity allocated to a given VP in a link connecting two internal nodes in a terrestrial broadband ATM network, or a part of the downlink capacity in a broadband satellite system. Segregating the total capacity on a link, and allowing sources with similar characteristics and performance requirements share separate portions of the total capacity, may result in overall higher link utilization [CoopP90].

Each connection is associated with a source, residing at the periphery of the net-

work. Traffic emanating from a source reaches the multiplexer in t_p seconds, the

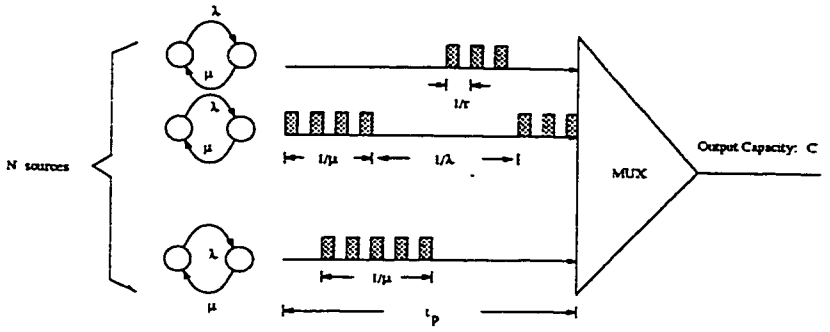

Figure 2.1: ATM statistical multiplexer loaded with N real-time applications at the Virtual Path (VP) level; VP capacity, C.

propagation delay between the network entrance and the location of the multiplexer (figure 2.1). Sources are of the On-Off type in the sense that their activity alternates between active and idle periods. During active periods they transmit cells with constant rate r. Active and idle source periods are exponentially distributed with rates μ and λ respectively (section 1.4).

The system operates in a statistical multiplexing mode, which relies upon the fact that not all sources are active at the same time. Let A_t be the number of active sources at time t. In accordance with the source independence assumption, A_t is characterized as a random process of the birth-death type. The transition probability for a birth in an incremental time interval Δt is

$$p_{a,a+1}(\Delta t) = (N-a)\lambda\Delta t + o(\Delta t), \tag{2.1}$$

where $p_{a,a+1}(\Delta t)$ stands for the conditional probability of $a+1$ sources being active at $t+\Delta t$, given that a sources were active at time t $p_{a,a+1}(\Delta t) = \Pr(A_{t+\Delta t} = a+1 \mid A_t = a)$. Similarly, the probability of a death and of no change in an incremental time

interval Δt are given as

$$p_{a,a-1}(\Delta t) = a\mu\Delta t + o(\Delta t) \tag{2.2}$$

$$p_{a,a}(\Delta t) = 1 - (N-a)\lambda\Delta t - a\mu\Delta t + o(\Delta t) \tag{2.3}$$

respectively.

A buffer at the input of the multiplexer temporarily stores cells that arrive simultaneously from different active sources. We assume that the buffer size is sufficient to handle simultaneous cell arrivals, but it is not large enough to handle overflow data when total arrival rate from all active sources, $A_t\ r$, is greater than the channel capacity C. The constraint on the buffer size is imposed from the nature of the services supported by the multiplexer, which, as it is stated in the chapter introduction, are of the delay intolerant type. Since buffering is considered negligible, the condition of total arrival rate from all active sources being grater than the VP capacity C can be considered as overload condition; thus,

$$\text{multiplexer overload condition:} \quad A_t\ r > C. \tag{2.4}$$

Normalizing C, the output channel capacity of the multiplexer, by r, the source rate in an active state, the above overload condition is written in terms of A_t as

$$\text{multiplexer overload condition:} \quad A_t > c, \tag{2.5}$$

with c the largest integer not exceeding $\frac{C}{r}$, $c \triangleq \lfloor \frac{C}{r} \rfloor$.

Furthermore, we position ourselves at the multiplexer site. We assume that the multiplexer currently (time t_0) is not overloaded. Moreover, the number of currently active bursts a_0 is known to us. We let T_{over} denote the time until overload is reached for the first time in the future given our current state (figure 2.2). We define the

Figure 2.2: A sample path of the system state A_t

conditional probability distribution for T_{over} given an initial number of active sources a_0 as

$$G_{a_0}(t) \triangleq \Pr(T_{over} \leq t \mid A_{t_0} = a_0). \tag{2.6}$$

There is a relation between T_{over}, and the round trip delay t_{rt} between the multiplexer and the entrance to the network $t_{rt} = 2\ t_p$. In the case when $T_{over} \leq t_{rt}$ cell loss is unavoidable, even if a choke signal is sent to the source at time t_0. First the choke signal needs t_p secs to reach the source, and within that time interval the source is unaware of the internal congestion; secondly, even when the source receives the signal and cooperates by performing some remedial action to vary the characteristics of the

input traffic, it takes another t_p seconds for these changes to effect the traffic situation at our link. We characterize the congestion in this case as imminent. On the other hand, when $T_{over} > t_{rt}$ the network operates in the safe region and no cell loss occurs. Congestion in this case is characterized as remote.

In this sense the conditional probability distribution for the time to overload, defined in equation (2.6), evaluated at the network round trip time, $G_{a_0}(t_{rt})$, gives a measure of the imminence of congestion. In the sequel we express $G_{a_0}(t_{rt})$ in terms of the input traffic parameters, such as the total number of subscribed sources N, their dynamics at the burst level, μ and λ, and their peak rate in active state r normalized by the channel capacity C.

2.1.2 Analysis

T_{over} can be identified as the first passage time for the birth-death process A_t from state a_0 to the state $c+1$, the state that is first entered when overload occurs. A standard procedure in first passage time to a state problems for Markov processes, is to treat the target Markov state as absorbing. Accordingly, we start by modifying our original process A_t, by considering state $c+1$ of the multiplexer, as absorbing. Figure 2.3, gives the state transition diagram of the new process, A'_t, that results after the above modification.

Further, we let $p_{a_0,c+1}(t)$ be the conditional probability that A'_t is at state $c+1$ at time t, given that initially it was at state a_0.

$$p_{a_0,c+1}(t) = \Pr(A'_t = c+1 \mid A'_{t_0} = a_0) \tag{2.7}$$

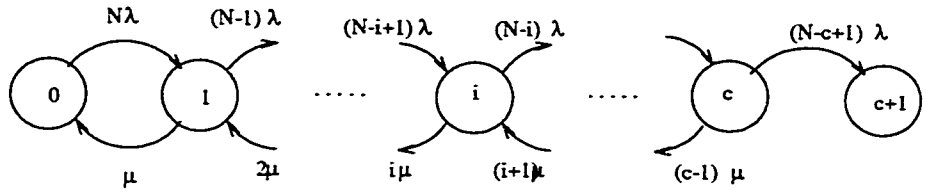

Figure 2.3: State transition diagram of the system process after the introduction of the absorbing state

Due to the fact that $c+1$ has been treated as absorbing, its occupation at time t means that $c+1$ either has been entered at time t for the first time, or its first entrance happened prior to time t and thereafter never exited. Thus, probability that absorption happens prior to time t equals the conditional probability of occupancy for state $c+1$,

$$\Pr(T_{over} \leq t \mid A_{t_0} = a_0) \;=\; p_{a_0,c+1}(t) \tag{2.8}$$

and consequently,

$$G_{a_0}(t) \;=\; p_{a_0,c+1}(t). \tag{2.9}$$

Then, determination of the first passage time distribution for the original process A_t entails finding the expression of the transition probability $p_{a_0,c+1}(t)$ for A'_t. Towards this end, we write down the Kolmogorov equations for the process A'_t. Since the transition probability to a fixed state (state $c+1$) from different initial states is required, the backward form of these equations is more appropriate to our problem.

The Backward Kolmogorov Equations

In contrast with the Forward Kolmogorov equations, where the rate of change of the probability of being in a certain state of a Markov process is related to the probability of being in other states, holding fixed the initial state of our Markov model, in the Backward Kolmogorov Equations we treat the current state as fixed and we relate the rate of change in probability of the current state varying the initial state [CoxM65].

We start by considering three points in time; t_0, $t_0 + \Delta t$, $t_0 + t + \Delta t$ with Δt an incremental time interval, $\Delta t \ll 1$. Without loss of generality since A'_t is time

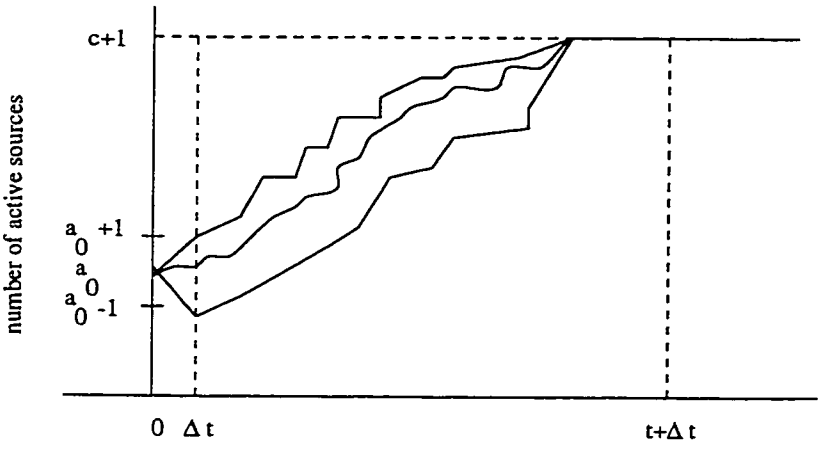

Figure 2.4: A sample path of the modified process A'_t.

homogeneous we can take $t_0 = 0$ (figure 2.4). We assume that initially A'_t is at an underload state a_0, $a_0 \in \{0, 1, 2, \ldots, c\}$ and at time $t_0 + t + \Delta t$ has reached the absorbing state $c + 1$. We relate the event of being at the overload state at time $t + \Delta t$ time units, given that at time zero we were at a_0 with all possible events at the intermediate time $t = t_0 + \Delta t$.

We reason as follows; state $c + 1$ can be reached in $t + \Delta t$ times units in three

mutually exclusive ways; (a) exactly one idle source becomes active; (b) exactly one active source becomes idle (only in case of $a_0 \geq 1$); (c) no change in the number of active sources; (d) more than one active sources become idle or more than one idle sources become active.

The probabilities of the above contingencies are given by equations (2.1) (2.2) and (2.3). Thus using the Chapman-Kolmogorov formulation,

$$p_{a_0,c+1}(t+\Delta t) = (N-a_0)\lambda\Delta t p_{a_0+1,c+1}(t) + a_0\mu\Delta t p_{a_0-1,c+1}(t)$$
$$+[1-(N-a_0)\lambda\Delta t - a_0\mu\Delta t]p_{a_0,c+1}(t) + o(\Delta t), \qquad \forall a_0 \in \{1,\ldots,c\} \quad (2.10)$$

The case for $a_0 = 0$ is treated separately, since no decrease in the number of active sources is possible at this state; The Chapman-Kolmogorov equation in this case is written as

$$p_{0,c+1}(t+\Delta t) = N\lambda\Delta t p_{1,c+1}(t) + [1-N\lambda\Delta t]p_{0,c+1}(t) + o(\Delta t). \quad (2.11)$$

Rearranging terms and dividing by Δt, we take the limit of (2.10) and (2.11) as Δt vanishes. Accordingly equation (2.10) gives

$$\frac{dp_{a_0,c+1}(t)}{dt} = (N-a_0)\lambda p_{a_0+1,c+1}(t) + a_0\mu p_{a_0-1,c+1}(t)$$
$$+[(N-a_0)\lambda - a_0\mu]p_{a_0,c+1}(t), \quad \forall a_0 \in \{1,2,\ldots,c\}, \quad (2.12)$$

and similarly equation (2.11)

$$\frac{dp_{0,c+1}(t)}{dt} = N\lambda p_{1,c+1}(t) - N\lambda p_{0,c+1}(t). \tag{2.13}$$

Equations for the Probability Distribution of the Time to Overload

Equations (2.12) and (2.13) describe the time evolution of the transition probabilities $p_{a_0,c+1}(t)$ for the truncated process A'_t. However, using equation (2.9) we can describe the dynamic behavior of the probability distribution for the time to overload for the original process A_t. Accordingly substituting (2.9) in (2.12) and (2.13) we get

$$\frac{dG_0(t)}{dt} = N\lambda G_1(t) - N\lambda G_0(t) \tag{2.14}$$

$$\frac{dG_{a_0}(t)}{dt} = (N-a_0)\lambda G_{a_0+1}(t) + a_0\mu G_{a_0-1}(t) - [(N-a_0)\lambda + a_0\mu]\, G_{a_0}(t)$$

$$a_0 \in \{1,\ldots,c\} \tag{2.15}$$

Equations (2.14) and (2.15) can be expressed in matrix form. However, before introducing matrix notation, we include with the set of equations (2.14) and (2.15) a degenerate equation for the probability distribution of the time to overload when we start from the overload state. Clearly,

$$\Pr(T_{over} \le t) = 1 \tag{2.16}$$

for all $t \ge 0$. Denoting the LHS of (2.16) by $G_{c+1}(t)$, according to our previous

notation, and differentiating both sides of (2.16) with respect to time t we have

$$\frac{dG_{c+1}(t)}{dt} = 0. \tag{2.17}$$

At this point setting $\rho = \frac{\lambda}{\mu}$, we are in the position to introduce the $(c+2) \times (c+2)$ matrix

$$\mathcal{Q} = \begin{pmatrix} -N\rho & N\rho & 0 & 0 & \cdots & 0 \\ & & \vdots & & & \\ i & -(N-i)\rho - i & (N-i)\rho & 0 & \cdots & 0 \\ & & \vdots & & & \\ \cdots & 0 & 0 & c & -(N-c)\rho - c & (N-c)\rho \\ 0 & 0 & 0 & 0 & 0 & 0 \end{pmatrix}. \tag{2.18}$$

Moreover, normalizing time by the mean period that a source stays in the active state, i.e. the average burst period $1/\mu$, $\tau = t\mu$, denoting by $\mathbf{G}(\tau)$ the column vector[1] $\mathbf{G}(\tau) = (G_0(\tau), G_1(\tau), \ldots, G_c(\tau), G_{c+1}(\tau))^T$. we express the set of equations (2.14) (2.15) and (2.17) as

$$\frac{d\mathbf{G}(\tau)}{d\tau} = \mathcal{Q}\mathbf{G}(\tau). \tag{2.19}$$

Solution of the Equations for the Probability Distribution

Equation (2.19) is a set of first order linear homogeneous differential equations;

[1] ^{T} indicates transpose; so, for example $\mathbf{G}(\tau)$ is a row vector.

its solution in terms of the exponential of the matrix $\mathcal{Q}$ is written as,

$$\mathbf{G}(\tau) = e^{\mathcal{Q}\tau}\mathbf{G}(0), \tag{2.20}$$

with $\mathbf{G}(0)$ the initial conditions for our problem.

$e^{\mathcal{Q}\tau}$ can be expressed as a sum involving the eigenvalues and eigenvectors of matrix $\mathcal{Q}$. Denoting by z_j, $j = 0, 1, \ldots c+1$ the eigenvalues of $\mathcal{Q}$ and by $\mathbf{V}_j$ and $\mathbf{U}_j$ its right and left eigenvectors respectively associated with the j^{th} eigenvalue, normalized such as

$$\mathbf{U}_j^T\mathbf{V}_k = \begin{cases} 1 & j = k \\ 0 & j \neq k \end{cases} \tag{2.21}$$

we write

$$\mathbf{G}(\tau) = \sum_{j=0}^{c+1} e^{z_j\tau}\mathbf{V}_j\mathbf{U}_j^T\mathbf{G}(0). \tag{2.22}$$

Resort to numerical techniques was necessary (QR method) for the calculation of the eigenvalues and eigenvectors of matrix $\mathcal{Q}$.

Equation (2.22) involves $\mathbf{G}(0)$, the vector of the probabilities to overload from any initial state to overload at zero time. However, this probability is always zero when the initial state is an underload state, a_0 = 0,1,...,c, and one when the initial state is the overload state itself. Therefore,

$$G_{a_0}(0) = \begin{cases} 0 & \text{for} \quad a_0 = 0, 1, \ldots, c \\ 1 & \text{for} \quad a_0 = c+1 \end{cases} \tag{2.23}$$

Allowing for $a_j = \mathbf{U}_j^T \mathbf{G}(0)$ and considering $\tau_{rt} = t_{rt}\mu$

$$\mathbf{G}(\tau_{rt}) = \sum_{j=0}^{c+1} a_j e^{z_j \tau_{rt}} \mathbf{V}_j, \tag{2.24}$$

Equation (2.24) gives the probability to overload in less than a network round trip time, and thus is a measure of the imminence of a congestion event. It depends, apart from the network round trip time, t_{rt}, on: the eigenvalues and eigenvectors of matrix $\mathcal{Q}$ and hence on the number of subscribed sources, N, and their in-call statistical characteristics, i.e. λ and μ; the number of underload states, $c+1$, and consequently on the ratio of the channel capacity, C, to the source peak rate r. In the sequel we use the above expression in a voice and a video multiplexing example.

Numerical Examples

Voice Call Multiplexing

We consider $N = 48$, 8-bit PCM coded voice sources with silence detection multiplexed onto a VP of capacity $C = 1.544$Mbits/sec. The mean burst duration of a voice call is taken to be $\frac{1}{\mu_{vo}} = 1.01$ secs, and the mean interburst period, $\frac{1}{\lambda_{vo}} = 1.38$ secs.

Figure 2.5 plots the probability of congestion onset in less than the round trip time, versus the network round trip delay for different values of initially active sources, a_0. The probability of congestion onset depends strongly on the network round trip time. For networks with short round trip delays between the place where the multiplexer is located and the network input, low values for the probability to overload are possible,

even when initially the number of active sources a_0 is close to the channel capacity c ($c \triangleq \lfloor \frac{C}{r} \rfloor$, as defined previously, is the channel capacity in terms of simultaneously active sources). For instance, consider Low Earth Orbit (LEO) satellite systems [WuMPP94]; Iridium [Grub91] has an operating height of its space components of 778 km above the earth's surface, resulting in a round trip delay between the earth

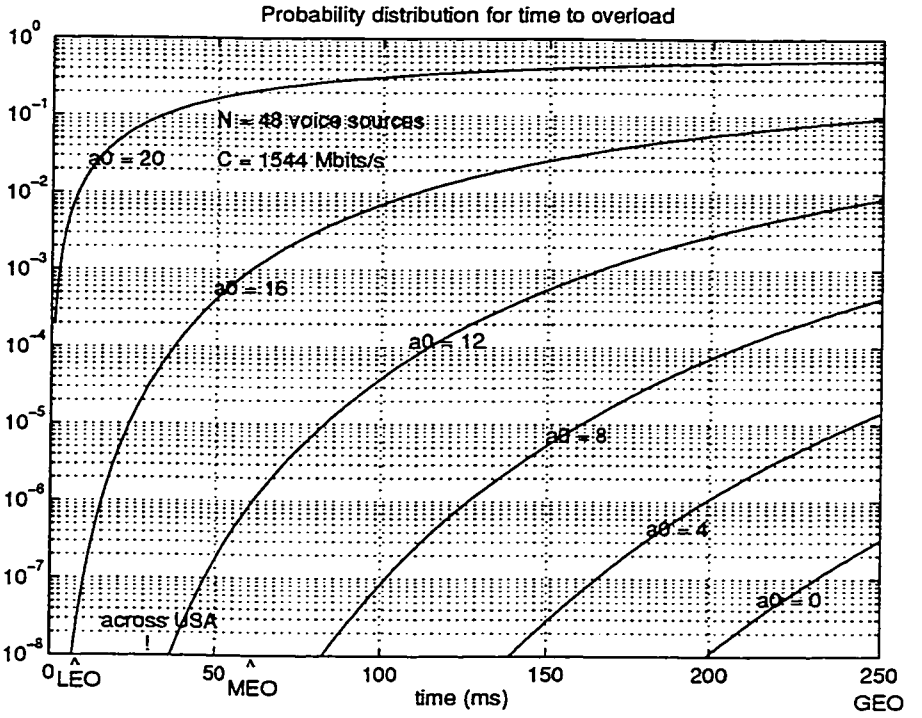

Figure 2.5: Conditional probability distribution for the time to overload for a statistical multiplexer loaded with voice sources with silence detection: a_0, initial multiplexer state in terms of active voice sources; output channel capacity, $C = 1.544$ Mbits/s; total number of voice sources, $N = 48$.

terminals and the satellite of 5.2 ms; Globalstar's [Viter92] "bent-pipe" transponders operate at inclined orbits in an altitude of 1400 km, introducing a round trip delay of 10 ms. The probability to overload in these cases is kept below 10^{-6} with an initial traffic profile ($a_0 = 16$), that is as high as 66.32% of the output channel capacity. Wide area terrestrial connections might be included in the above category, since

they introduce delays comparable to the LEO systems with a connection across USA presenting a 30 ms round trip time [Klein92].

As the network propagation delay increases, the initial network traffic profile, which guarantees a certain performance level, decreases gradually. Medium Earth Orbit (MEO) satellite channels, e.g. the Odyssey system, operating at 10370 km over the earth's surface [WuMPP94], have round trip propagation delays of 70 ms, and require less than $a_0 = 12$ voice sources to be active initially, to guarantee a 10^{-6} probability to overload. For longer propagation delays the situation aggravates; for geosynchronous earth orbit (GEO) satellite systems, characterized by a 250 ms round trip delay, a value of 10^{-6} for the probability to overload can not be met.

Video Call Multiplexing

As a second example, we assume N_{vi} video calls multiplexed on a OC-1 link ($C =$ 51.84 Mbits/s) supporting the first level of Synchronous Transport Signal (STS-1) of the SONET hierarchy. Video traffic in the form of ATM cells is transported in the payload of STS-1 frames. Video calls have identical characteristics such as peak bit rate of 10.57 Mbits/s, average bit rate of 3.9 Mbits/s, and bit rate autocovariance function which decays exponentially with time at a rate of 3.9 sec^{-1} [MASKR88]. According to the latter reference, each video call is equivalent to a set of M binary On-Off sources, which are called minisources in this context (section 1.4). We have chosen $M = 10$ minisources to represent one video call. Therefore, equation (2.24) applies in a straightforward manner, with $N = N_{vi}M$. In the case of $N_{vi} = 10$ video calls, figure 2.6 gives the probability to overload in less than a round trip time as

function of the network round trip delay. The initial state of the network in multiples of video sources at their peak rate is treated as a parameter. Considering first the LEO example as above, we see that the probability to overload is below 10^{-6} even when the initial network state is such that three video connections transmit at their peak rate. This corresponds in an initial multiplexer loading of 70.68%, which is almost the same

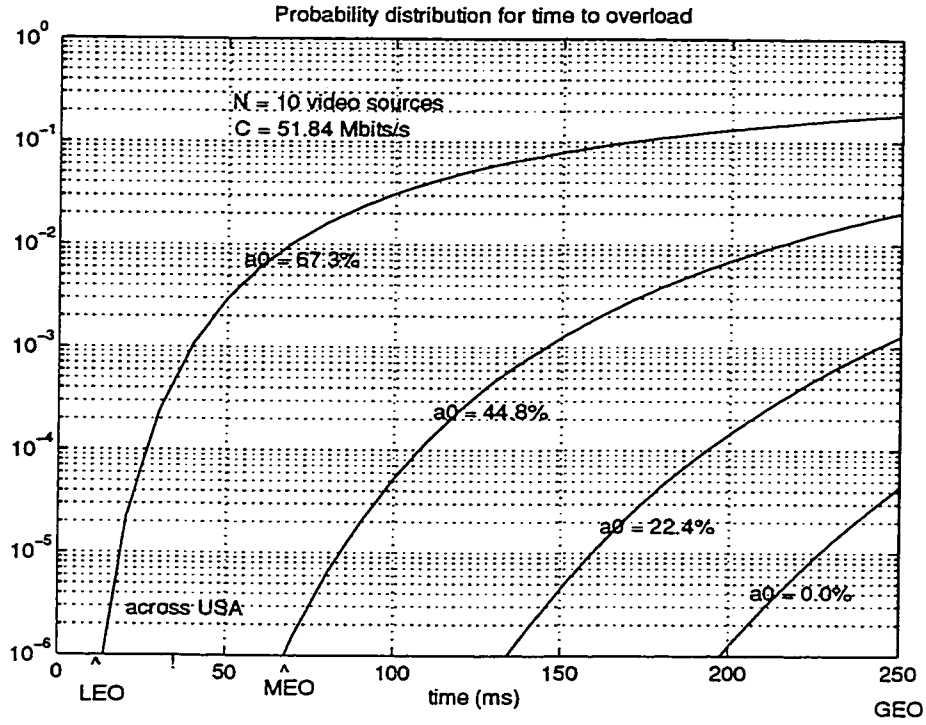

Figure 2.6: Conditional probability distribution for the time to overload for a variable bit rate video statistical multiplexer: a_0, initial channel occupancy as percentage of the output bandwidth; output channel capacity, $C = 51.84$ Mbits/s; total number of video sources, $N = 10$.

as the initial condition for the voice multiplexer in the previous example. However, the situation deteriorates in comparison to the voice multiplexing case as the network propagation delays increase. For MEO satellite systems the same performance in terms of the probability to overload in a channel round trip time is achieved with an initial loading of 44.8%, which is less than that of the voice multiplexer in the

example considered above. Finally, for geosynchronous satellites, a 10^{-6} probability to overload can not be achieved for any initial state.

Above we have described the increased difficulty in multiplexing video connections compared to voice; this difficulty becomes more pronounced if additionally we consider the multiplexer load, as the ratio of the average input bit rate to the channel capacity. The T1 link loaded with 48 voice sources (each one with activity ratio of 42.2%), results in a load of 92.7%; calculating this figure we have taken into consideration the ATM cell overhead. The OC-1 link supports 10 video calls, each one with an average rate of 3.9 Mbits/s. Given the SONET and the cell header overhead, the video multiplexer load becomes 87%. Thus, certainly the T1 link is loaded heavier with voice calls than the OC-1 link with video calls.

The reason for the increased difficulty in multiplexing video calls, is that video traffic is correlated over shorter periods of time in comparison to voice traffic. Comparing the decay rates of the bit rate autocorrelation functions for voice and video traffic we see that the decay rate for voice traffic ($\lambda_{vo} + \mu_{vo} = 1.7$ sec^{-1}) is greater than the one for video traffic (3.9 sec^{-1}).

2.1.3 Applications to Congestion Control

Preventive congestion control algorithms for broadband networks carrying real time services are designed using a layered approach [Hui88, Hui91]. Three traffic layers are considered; the cell, burst, and call level. Congestion is prevented by limiting the number of admitted calls N so as the blocking probability at the burst level is kept below a given threshold [StamH91].

Expression (2.24) gives another characterization of the performance of a network, in terms of the probability of overload or burst blocking in a network round trip time. Therefore it takes into account an additional parameter in characterizing network performance, namely the network round trip time. The above characteristic makes expression (2.24) useful in designing congestion control algorithms of the proactive type for broadband networks carrying real time services.

The objective of these algorithms is to keep congestion imminence, quantified by the probability of overload in a network round trip time, below a certain level ϵ

$$\Pr(T_{over} \leq t_{rt} \mid A_0 = a_0) = G_{a_0}(t_{rt}) \leq \epsilon. \tag{2.25}$$

However, from equation (2.24), the LHS of (2.25) is found to depend on the following parameters: (1) number of sources N multiplexed; (2) the sources characteristics at the burst level through the ratio $\rho = \frac{\lambda}{\mu}$; (3) the source peak rate during active periods, r, and the channel capacity C, through their ratio $\frac{r}{C}$; (4) the network round trip delay normalized by the mean burst length $\tau_{rt} = t_{rt}\mu$; (5) the current multiplexer load, represented by the initial number of active sources, a_0. Accordingly, condition (2.25) can be satisfied on a link with given capacity C and round trip time t_{rt}, in one of the following ways; (1) by limiting the number of admitted calls N (connection admission control), and (2) by modification of the in-call source characteristics, λ, μ, or r. Below, we give examples of the above methods applied to voice and video multiplexing.

Voice Call Multiplexing

We return to our example of N voice sources multiplexed on a T1 link. We consider two cases for the performance index ϵ; $\epsilon = 10^{-2}$, and $\epsilon = 10^{-5}$. We examine first the effect of the total number of admitted sources, N, and hence the admission control strategy, has on meeting (2.25).

Admission Control

From figure 2.5 we see that for a channel with given round trip delay time t_{rt}, the LHS of (2.25) is a monotonically increasing function of a_0. Therefore given a value for ϵ there would be a threshold value a_0^* for a_0 below which criterion (2.25) will be met and above which it will not. When the number of active sources a_0 is below a_0^*, congestion is not imminent and no feedback signals must be sent to the source; thus, intervals of the form $[0, a_0^*]$ constitute safe operating region for the statistical voice multiplexer.

For $\epsilon = 10^{-2}$, figure 2.7 depicts these safe operating regions for voice multiplexing as a function of, the network round trip delay, and the number of sources N admitted into the network. Note that the capacity of our link in terms of concurrently active sources is $c = 21$; this in accordance with the 10% reduction in the output channel capacity assumed due to the ATM cell header. For $N = 72$ admitted voice sources, the safe operating region for our multiplexer corresponds to region I. Decreasing the number of admitted calls results in extension of the safe operating region. In other words, the operation of the multiplexer meets the overload condition (2.25) for a greater set of initial conditions, and therefore the employment of remedial controls is

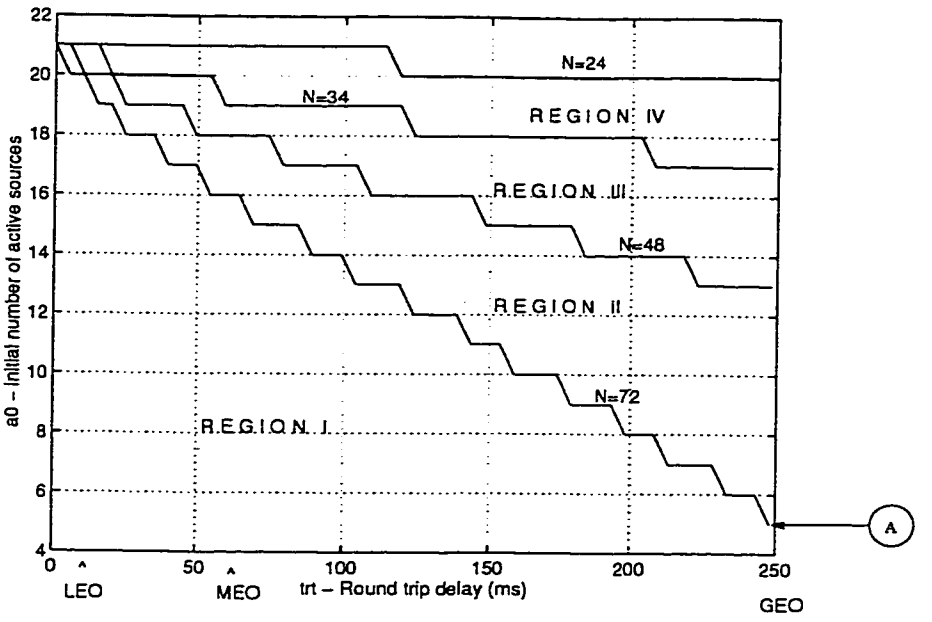

Figure 2.7: Safe operating regions for a statistical voice multiplexer as a function of N, the total number of admitted calls; output channel capacity, $C = 1.544$ Mbits/s; probability to overload in a round trip time, $\epsilon = 10^{-2}$.

less required. Region II corresponds to $N = 48$ admitted calls, region III to $N = 34$ and finally region IV to $N = 24$ voice calls. We note in passing that $N = 24$ and $N = 34$ are the number of voice calls that a preventive congestion control algorithm admits for a guaranteed burst blocking probability of 10^{-5}, and 10^{-2} respectively [Hui91, StamH91].

Besides the number of admitted calls, the network propagation delays affect the size of the safe regions for the multiplexer. We see that for very small propagation delays, i.e. LEO satellite systems, the probability of overloading in less than a round trip time is almost negligible, and therefore independent of the current network state a_0. A statistical voice multiplexer can operate in such a network, with almost no remedial actions taken by the sources. Only when N, the number of admitted sources, increases significantly, some corrective actions need to be taken for a very limited set

of initial states that are very close to the channel capacity.

For networks with greater propagation delays, the set of initial states that satisfy condition (2.25) decreases in size. This implies the necessity of remedial action deployment by the sources on a more regular basis. The question of the feasibility and the potentials of such remedial actions in effectively guaranteeing the performance requirement ϵ, for states a_0 of the multiplexer, not in the safe operating region, $a_0 > a_0^*$, is addressed below (section on in-call parameter control).

Safe operating regions for more stringent criteria for the probability to overload in a round trip time are smaller in size. Figure 2.8 depicts these regions for $\epsilon = 10^{-5}$. In this case, corrective measures are required in a greater extent. Moreover, it is

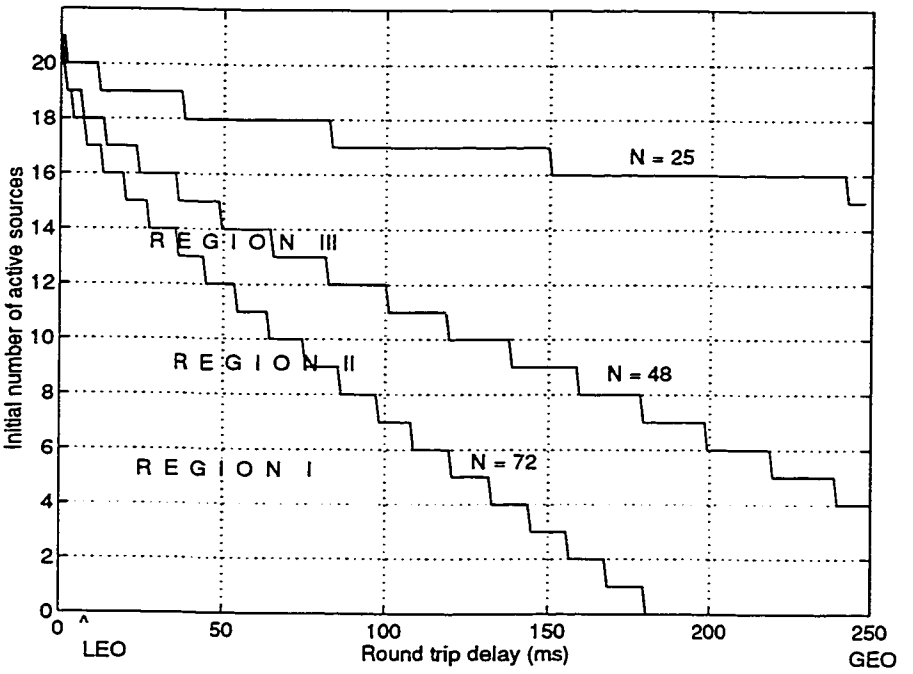

Figure 2.8: Safe operating regions for a statistical voice multiplexer as a function of N, the total number of admitted; output channel capacity, $C = 1.544$ Mbits/s; probability to overload in a round trip time, $\epsilon = 10^{-5}$.

characteristic, that for networks with large propagation delays, i.e. GEO satellite

systems, and for large number of admitted calls N, it is impossible to meet the $\epsilon = 10^{-5}$ requirement, starting from any initial state a_0. Voice multiplexing in these cases is impossible without the help of in-call parameter controls.

In-call Parameter Control

Given N, the number of the total admitted sources on the link, and t_{rt} the network round trip delay time, we saw that the set of states a_0 that satisfies the criterion (2.25) does not cover the total link capacity. Extending the safe operating regions in these cases, requires the use of in-call parameter controls, such as variation of the peak source rate r, and the transition probability rates λ and μ. The two last parameters, as was mentioned above, affect the performance of the multiplexer through their ratio $\rho = \frac{\lambda}{\mu}$, and therefore only the effect of ρ (or equivalently the source activity ratio $\frac{\rho}{1+\rho}$) in the design of a reactive control algorithm will be examined.

Therefore, fixing N and t_{rt} we can determine safe operating regions in the operation of the statistical multiplexer, in terms of the in-call parameters, i.e r and $\frac{\rho}{1+\rho}$. For instance, consider the case of a multiplexer loaded with $N = 72$ voice sources, operating in a network with large propagation delays ($t_{rt} = 250$ ms), i.e. a geosynchronous satellite system, and suppose that $a_0 = 5$ sources were active initially (point A in figure 2.7). We recall from figure 2.7, that this point lies at the boundary of the safe region of the multiplexer, i.e. the multiplexer meets the $\epsilon = 10^{-2}$ requirement for the probability to overload in a round trip time, when the number of initially active sources is less than five; in the case of a larger number of sources being active initially, this requirement is not fulfilled.

Figure 2.9 depicts the safe operating regions in terms of the in-call parameters, r

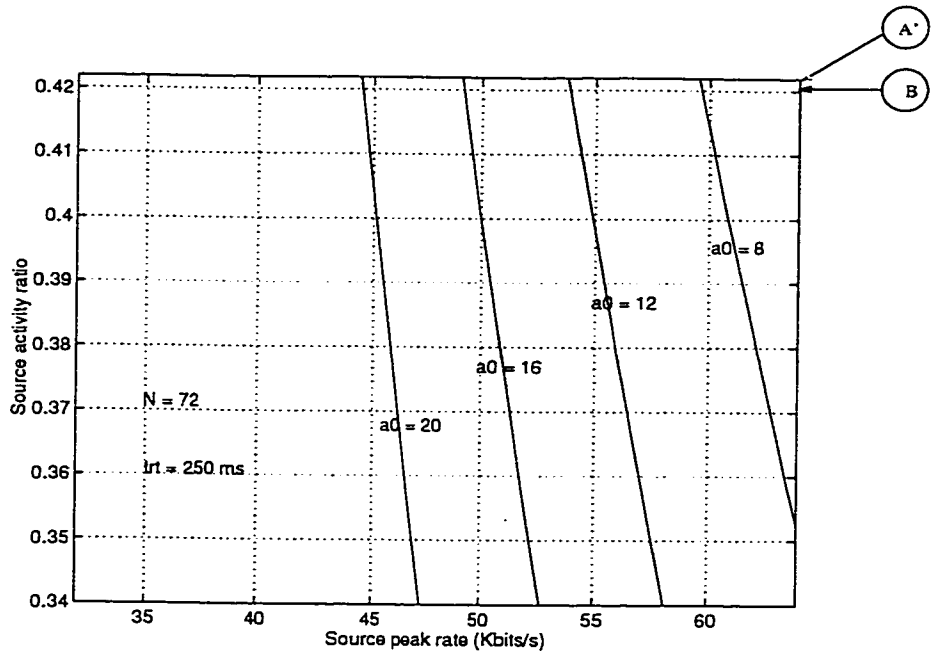

Figure 2.9: Safe in-call parameter operating regions for voice multiplexing as functions of a_0, the initial network state: total number of admitted sources, $N = 72$; source-multiplexer round trip time, $t_{rt} = 250$ ms; output channel capacity, $C = 1.544$ Mbits/s; probability to overload in a round trip time $\epsilon = 10^{-2}$.

and $\frac{\rho}{1+\rho}$ in this case. The upper right corner (point A') refers to point A in figure 2.9, with initially five active sources ($a_0 = 5$) and normal operating conditions for the voice sources, i.e. activity ratio of 42.2%, and peak rate of $r_0 = 64$ kbits/s. For greater values of initially active sources, either the peak rate r of the source, or its source activity ratio (or both) must be reduced to meet the requirement for probability to overload.

Delaying the transmission of a talkspurt, increases the source idle time, and therefore reduces the effective source activity ratio. This can be implemented with the use of a buffered leaky bucket [SiLCG89]. However, voice being a real time service cannot tolerate excessive delays, especially when channels characterized by long propagation

delays are involved, e.g. GEO satellite channels, and therefore the strategy of delaying the transmission of a talkspurt to reduce the effective source activity ratio is limited. Following [GoodW91], we may continue reducing the source activity ratio by reducing the mean on period of the source through cell discarding at the beginning of a talkspurt. This method will introduce front end clipping, an impairment in voice conversations that becomes annoying when cell drop rate exceeds a certain value. In [GoodW91], the amount of front end clipping is required to remain below 1 %. In these cases, the source activity ratio can only be reduced to 0.42% (point B in figure 2.9). Therefore, in our example the above methods of source activity control will not suffice to bring the operating point of our multiplexer within the safe region, and at the same time satisfy both delay and loss requirements for voice.

The other burst level parameter that could be varied to achieve our goals in meeting the probability to overload requirements for our multiplexer, is the source peak rate during active periods, r. One such method of reducing r at the entrance of the network is by selectively dropping cells. Moreover, such strategy can be combined with embedded coding to achieve further improvements in the perceived end-to-end voice quality. Embedded coding classify cells in more and less significant cell classes. Less significant cells are discarded at the input of the network at a variable rate, to reduce the effective peak rate of the talkspurts, to the point that the operating point of the multiplexer falls into the safe region. Yin et al. [YinLS90], apply the above method, with the discarding being performed at the multiplexer, and not at the network input, as we propose. Peak voice rate can be reduced up to 32 Kbits/s, e.g. following an even/odd sample strategy, where even speech samples are classified

as more significant, while odd samples as less.

Voice rate reduction is more effective than source activity ratio control, and with a rate of 58 Kbits/s (a 10% reduction in the original rate) is easy to bring the operating point of the multiplexer in the safe region (when the initial number of active sources is $a_0 = 8$). Of course, in cases where rate reduction alone is not enough, it can be combined with the above method of burst delaying and clipping.

We see above that inherent to our discussion is a lower level on the range of variation of the in-call control parameters (source activity ratio, $\frac{1}{1+\rho}$, and peak rate, r, in our example), below which the performance offered to the subscribed calls is considered unacceptable. In our example these levels might correspond to $r_{\min} = 32$ Kbits/s and $\frac{1}{1+\rho_{\min}} = 34\%$, as in figure 2.9. These lower bounds in terms of the in-call source parameters, will put bounds as well on the initial network state, a_0, that we could start from and be able to guarantee safe operation ($\Pr(T_{\text{over}}) < \epsilon$). For instance again from figure 2.9, we see that we could perform proactive controls for $a_0 > 5$ active sources, but not for indefinitely. As a_0 increases the range of values of the control parameters, r and $\frac{1}{1+\rho}$ reduces, and there would be a value for a_0 (greater than 20 active sources) above which overload happens with probability more than $\epsilon = 10^{-2}$ in a network round trip time.

This is the point that call admission control will come into place; it will guarantee that the probability of reaching a state a_0, from which the target probability to overload in a round trip time can not be satisfied even when the most stringent allowable in-call source parameter actions have been taken, is very low.

Similar discussion can be followed assuming the more stringent performance cri-

terion of $\epsilon = 10^{-5}$. Figure 2.10 depicts how a performance requirement of $\epsilon = 10^{-5}$ for the probability to overload in a round trip time can be met with in-call parameter

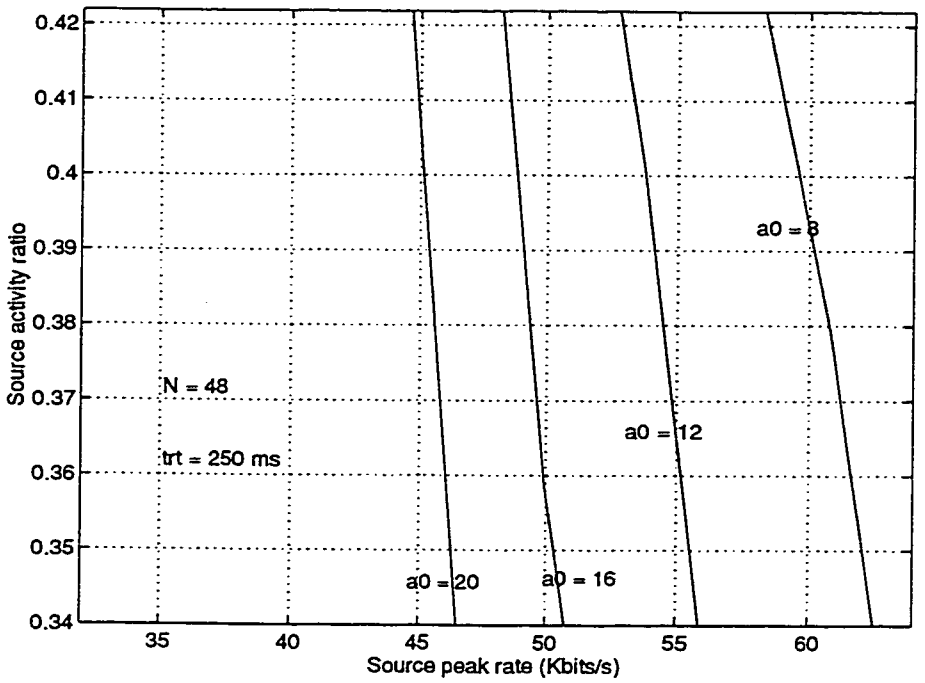

Figure 2.10: Safe in-call parameter operating regions as a function of a_0 the number of initially active sources; total number of admitted sources to the link, $N = 48$; source-multiplexer round trip time, $t_{rt} = 250$ ms; output channel capacity, $C = 1.544$ Mbits/s; probability to overload in a round trip time, $\epsilon = 10^{-5}$.

variation for $N = 48$ voice sources and a channel of round trip delay of 250 msec, can still be met, but with a bigger reduction in the source peak rate, or activity ratio.

Video Call Multiplexing

We continue by applying the ideas introduced above for voice call multiplexing, to video call multiplexing. We consider an OC-1 link, and N_{vi} video sources accessing it through a statistical multiplexer. Quality of the video service is expressed by the probability that overload occurs in a channel round trip time, ϵ. Two cases for ϵ are

considered; $\epsilon = 10^{-2}$ and $\epsilon = 10^{-5}$.

As in the case of voice multiplexing we consider the effect of admission control and round trip delay time on the feasibility of in-call parameter controls, that lie at the heart of proactive congestion control algorithms.

Admission Control

As in the previous voice multiplexing example, we first give the regions, such that when the multiplexer initial traffic level lies within, the probability that there will be an overload in a less than a round trip time is less or equal to $\epsilon = 10^{-2}$, without the intervention of any control action. Again, safe operating regions depend on the

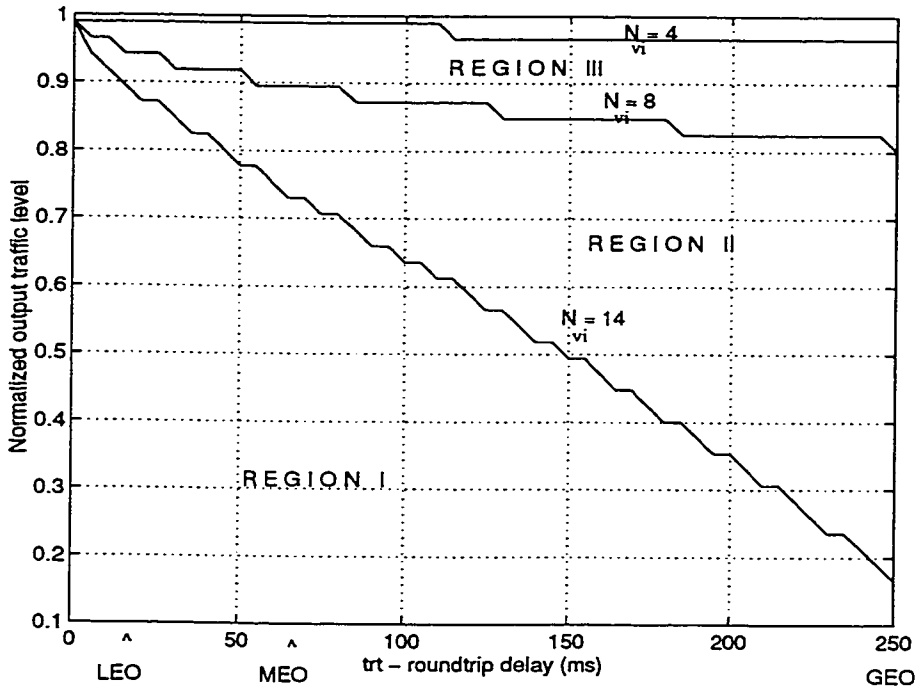

Figure 2.11: Safe operating regions for statistical variable bit rate video multiplexing as a function of N_{vi}, the total number of admitted video sources; output channel capacity, $C = 51.84$ Mbits/s; probability to overload in a round trip time, $\epsilon = 10^{-2}$.

number of admitted sources as well as on the channel round trip time. Figure 2.11 depicts these regions for $\epsilon = 10^{-2}$ with N_{vi}, the number of admitted video calls,

as a parameter. Initial traffic levels are given normalized to the multiplexer output channel capacity. Video multiplexing complying with the requirement of overflowing with probability less than $\epsilon = 10^{-2}$, in a less than a channel round trip time, is easy, for networks with short propagation delays, i.e. LEO satellite systems. As network propagation delay increases, multiplexing N_{vi} video sources on a OC-1 link, becomes more difficult, and it is achieved only when the initial traffic level on the link is relative low; for instance, for a GEO satellite system loaded with $N_{vi} = 10$ video sources, the probability to overload in a less than the link round trip time is kept below the $\epsilon = 10^{-2}$ level, only when the initial multiplexer loading in terms of simultaneously active video bursts, is below 20% of the output channel capacity.

Certainly, safe operating regions depend on N_{vi}, and decrease as the number of admitted to the network video calls is increased. For instance, for $N_{vi} = 14$ video calls admitted, and a geosynchronous satellite channel, it is almost impossible to achieve multiplexing with the required quality of service. For comparison, preventive congestion controls admit $N_{vi} = 9$ video sources, allowing a video burst blocking probability of 10^{-2}.

Figure 2.12 depicts similar results, in the case of a more stringent quality of service constraint, $\epsilon = 10^{-5}$. Under such a performance constraint, multiplexing becomes more difficult, a fact signified by smaller safe operating regions. $N_{vi} = 6$ is the number of video calls that a preventive congestion control algorithm admits allowing for a burst blocking probability of 10^{-5}.

In-call Parameter Control

As it is seen from figures 2.11 and 2.12, safe operation of the video multiplexer

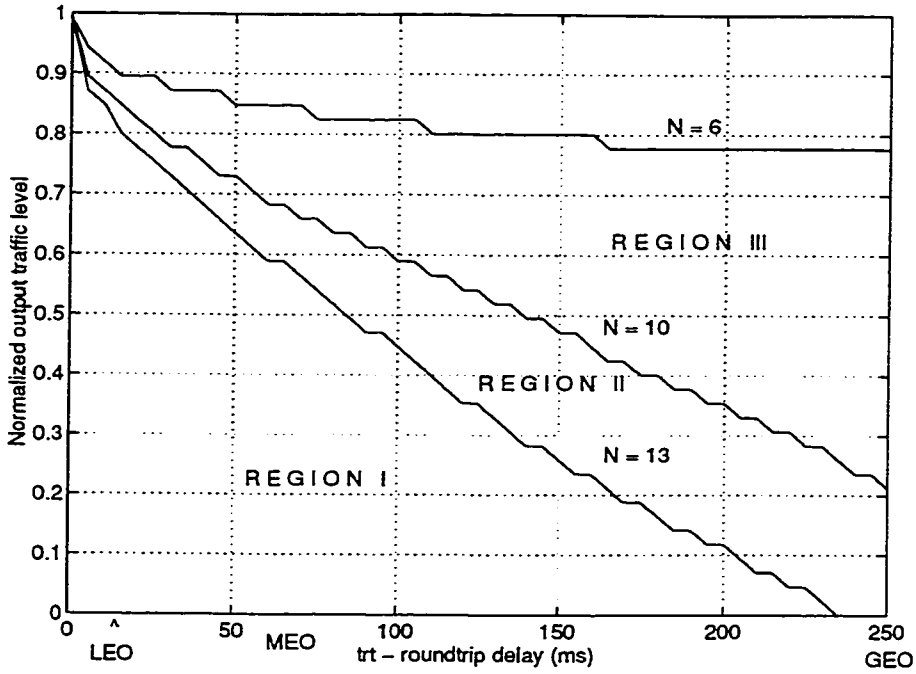

Figure 2.12: Safe operating regions for variable rate video sources, as a function of N_{vi}, the total number of admitted video calls; output channel capacity, $C = 51.84$ Mbits/s; probability to overload in a round trip time $\epsilon = 10^{-5}$.

depends on the output channel traffic levels in terms of active sources. In some cases these safe operating regions constitute a very small percentage of the total operating range of our statistical multiplexer. Given the channel propagation delay t_{rt} and the number of admitted video calls N_{vi}, in order to extend the safe operation regions to cover all initial traffic conditions, i.e. from 0% to 100% initial loading, some form of adjustment of the remaining call parameters, that modify the video burst characteristics, must be employed.

Adjustment of video burst characteristics can be achieved by delaying the beginning of a burst, or by reducing its duration, or by reducing its peak rate. Delaying

the transmission of a burst increases their interburst time, while dropping the beginning of a video burst results in shortening the burst duration; in both cases the video source activity ratio is decreased, which in turn results in a reduction of the probability to overload in a round trip time. Peak rate control can be performed by dropping a certain percentage of cells before transmission at the access link. The above operations can be performed at the network access points using a tunable leaky bucket scheme [SiLCG89]. Rate reduction can be combined with hierarchical video coding to further reduce the impact of cell loss dropping at the perceived end-to-end video quality. Alternatively it can be performed by the source using a traffic shaper buffer.

As an example, we consider $N_{vi} = 10$ video calls, on a network with round trip

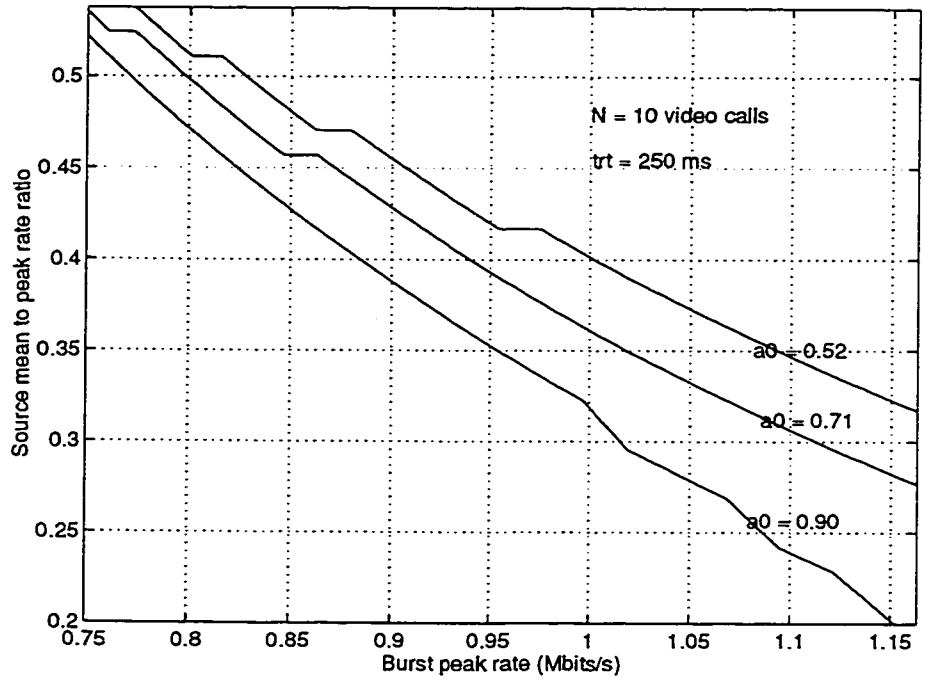

Figure 2.13: Safe operating regions for variable bit video calls, in terms of the burst peak rate and mean to peak source rate ratio, for different values of initial traffic levels ($N_{vi} = 10$ video sources, $t_{rt} = 250$ ms, output channel capacity $C = 51.84$ Mbits/s, probability to overload in a round trip time $\epsilon = 10^{-2}$).

delay time of 250 ms. According to figure 2.11 above, the probability to overload in a round trip delay remains below $\epsilon = 10^{-2}$, only when the initial traffic level at the multiplexer is not higher than 47% of the output link capacity.

As in the case of voice sources, we could extend the safe operating region of the multiplexer, for higher initial traffic levels, by modifying the peak rate during a burst r, or the mean burst or interburst periods. Figure 2.13 gives the required adjustments that must be performed to these parameters, when the initial multiplexer traffic level is above 47%, in order to meet the probability to overload within a round trip time constraint. Points in the plot that lie below and to the left of the solid lines, correspond to in-call parameter values that satisfy the constraint for $\epsilon = 10^{-2}$.

Comparison with Static Congestion Control

Preventive congestion controls are usually designed assuming a layered traffic level, [Hui88]. For a channel of a given capacity C, and On-Off sources of given in-call characteristics, such as their peak On rate r and mean On and Off sojourn times, $\frac{1}{\mu}$,, $\frac{1}{\lambda}$ respectively, the number of subscribed sources N is limited in order to meet a certain performance requirement for the burst blocking probability. Consequently, connection admission control for real time services depends on the steady state characteristics of the multiplexed calls, such as the steady state probability that a source is in the On state $\pi_{on} = \frac{\lambda}{\lambda+\mu}$, and the peak to link ratio of a call $\frac{r}{C}$.

Similarly, proactive congestion controls for real time services are designed within a layered congestion control framework. However, instead of a constraint on the burst

blocking probability, proactive congestion controls are designed to meet a probability to overload within the round trip time of the channel constraint. As such they involve an additional parameter, namely the round trip time of the channel.

We compare the two approaches of congestion control, by examining the number of sources that each method admits into the network. This is in accordance with the fact that the number of admitted sources is related to the channel utilization. Towards this end, we consider our voice multiplexing example, and in figure 2.14 we plot the number of voice sources that a proactive congestion control algorithm admits

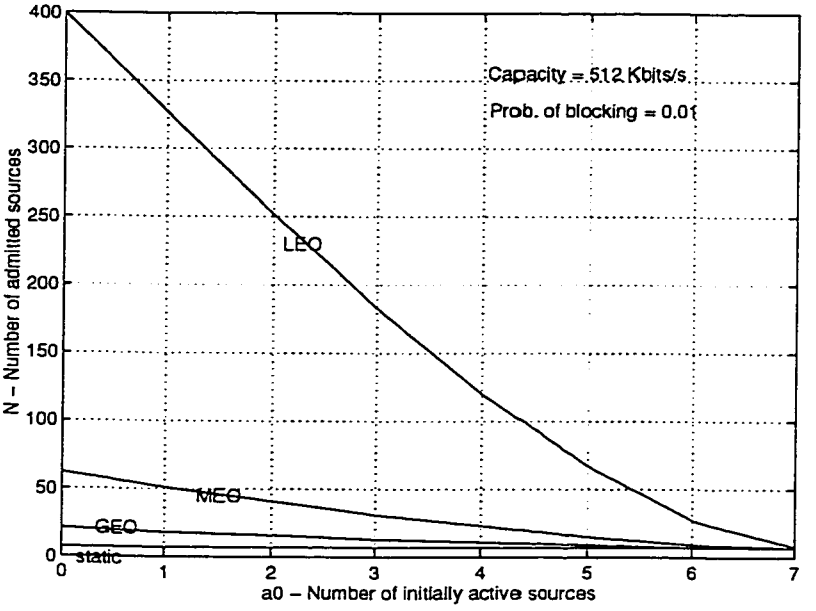

Figure 2.14: Comparison between admission control under a static and a dynamic congestion control scheme, for voice sources.

in order to keep a burst blocking probability in a round trip time of $\epsilon = 10^{-2}$. Three cases are presented depending on the channel round trip time, i.e. one for LEO, one for MEO and one for GEO links. A characteristic of the proactive approach is that the number of admitted calls depends on the initial network state in terms of simultaneously active sources.

Static preventive controls [Hui88, StamH91], admit a fixed number of sources that is independent on the initial state of the network. In contrast proactive algorithms in general have the potential of admitting more sources into the network. however, when the initial state of the network is very close to its capacity, i.e. for high values of a_0, the number of admitted sources drops to the number allowed by pure peak rate admission control. We suppose that there is enough elasticity in the services transported to introduce in-call parameter controls when the initial state a_0 is high, to allow the admission of more sources than the peak admission control strategy does.

2.2 Multiple Source Types

2.2.1 Model Formulation

We extend the model introduced in section 2.1 to the multiclass source case, where L different classes of sources share the output channel capacity C of the multiplexer (figure 2.15). This capacity might correspond, as in the single source type case, to the capacity of a Virtual Path on a link, that has been allocated to these L classes of sources. Each class consists of N_l sources, $l \in \{1, 2, \ldots, L\}$ of the On-Off type. Moreover, sources of the l^{th} type are characterized by transition probability rates λ_l and μ_l, and peak transmission rates during active periods r_l.

We let the number of active sources of each type describe the state of our system. Accordingly, our system state becomes a vector, $\mathbf{A}_t = (A_{1,t}, A_{2,t}, \ldots, A_{L,t})$, with $A_{l,t}$ being the number of active sources of class l, at time t. $\mathbf{A}_t$ is a L-dimensional birth-

death process. Given the vector $\mathbf{a} = (a_1, \ldots, a_l, \ldots, a_L)$ we define $\mathbf{a}_l^+$ and $\mathbf{a}_l^-$ as:

$$\mathbf{a}_l^+ = (a_1, a_2, \ldots, a_l + 1, \ldots, a_L), \tag{2.26}$$

$$\mathbf{a}_l^- = (a_1, a_2, \ldots, a_l - 1, \ldots, a_L). \tag{2.27}$$

Then, the transition probability for a birth of class l source in an incremental time

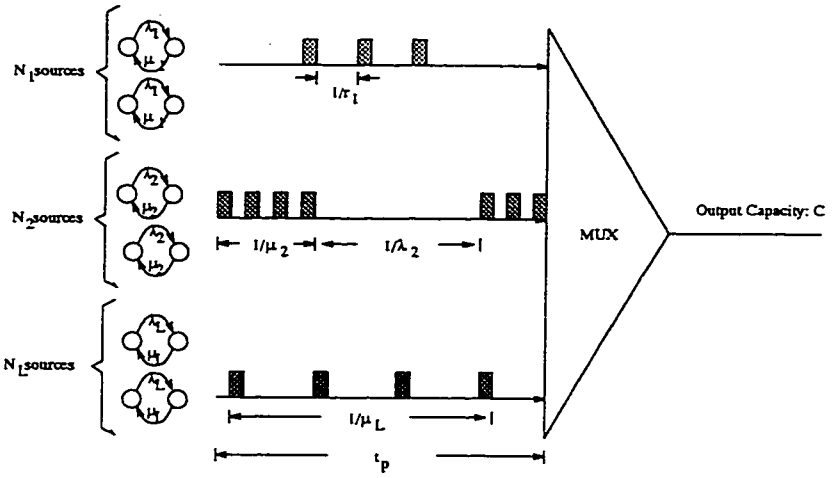

Figure 2.15: ATM statistical multiplexer loaded with multiple types of delay sensitive sources

interval $\Delta t \ll 1$, $p_{\mathbf{a},\mathbf{a}_l^+}(\Delta t) = \Pr\left(\mathbf{A}_{t+\Delta t} = \mathbf{a}_l^+ \mid \mathbf{A}_t = \mathbf{a}\right)$ is given as,

$$p_{\mathbf{a},\mathbf{a}_l^+}(\Delta t) = (N_l - a_l)\lambda_l \Delta t + o(\Delta t). \tag{2.28}$$

Similarly, the probability of an active source of class l switching into the idle state in Δt, is given as

$$p_{\mathbf{a},\mathbf{a}_l^-}(\Delta t) = a_l \mu_l \Delta t + o(\Delta t). \tag{2.29}$$

Equations (2.28) and (2.29) apply for an increase or decrease in the number of active sources in an incremental time interval Δt. Finally, there is a possibility of no change in the number of active sources in Δt, an event with probability,

$$p_{\mathbf{a},\mathbf{a}}(\Delta t) = 1 - \sum_{l=1}^{L}(N_l - a_l)\lambda_l \Delta t - \sum_{l=1}^{L} a_l \mu_l \Delta t + o(\Delta t). \tag{2.30}$$

All l traffic types are assumed to be delay sensitive and therefore buffering at the multiplexer is limited only in scheduling traffic that arrives simultaneously. In this sense, overload occurs when the total information arrival rate from all active sources, exceeds the output channel capacity C,

$$\text{multiplexer overload condition} \qquad \sum_{l=1}^{L} A_{l,t} r_l > C. \tag{2.31}$$

Let, as in the single source type case, T_{over} be the time of the first overload occurrence, given a present underload state $\mathbf{a}_0 = (a_{1,0}, a_{2,0}, \ldots, a_{L,0})$, where $a_{l,0}$, $l \in \{1, 2, \ldots, L\}$ are the initial numbers of active sources of each class. We are interested in the probability distribution for the time to reach overload denoted as

$$G_{\mathbf{a}_0}(t) \triangleq \Pr(T_{over} \leq t \mid \mathbf{A}_0 = \mathbf{a}_0). \tag{2.32}$$

As in the homogeneous case, $G_{\mathbf{a}_0}(t_{rt})$ gives a measure of congestion imminence.

2.2.2 Analysis

Given an initial network state $\mathbf{a}_0 = (a_{1,0}, a_{2,0}, \ldots, a_{L,0})$, T_{over} is the first passage

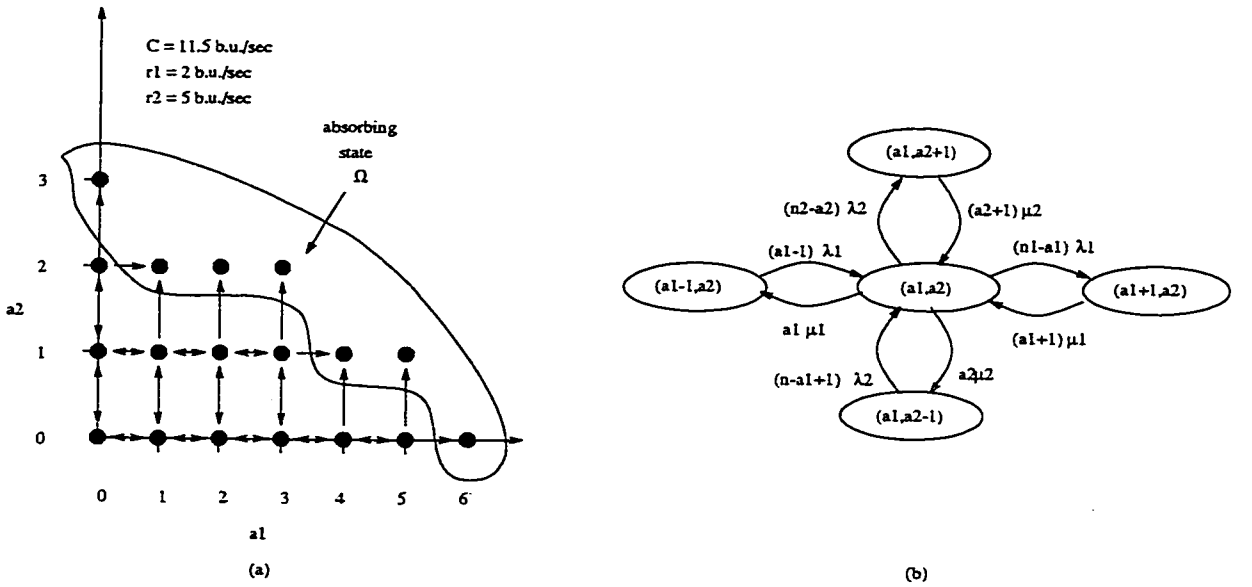

Figure 2.16: (a) State transition diagram for a multiplexer loaded with $L = 2$ types of sources (b) Detailed local state transitions.

time to a any state of the Markov process $\mathbf{A}_t$, that satisfies the multiplexer overload condition in (2.31). We denote by Ω this set of states,

$$\Omega \triangleq \{\mathbf{a} = (a_1, a_2, \ldots, a_L) : \sum_{l=1}^{L} a_l r_l > C\} \tag{2.33}$$

Following the standard methodology for first passage to a state problems, we treat the overload states as absorbing. Unlike the homogeneous case, the set Ω of absorbing states is entered from the underload in more than one states. This can be seen in the example for $L = 2$ types of sources in figure 2.16. We let Ω' be the subset of Ω that contains all the states that are entered first upon absorption. Then, the probability that any state $\mathbf{w} \in \Omega'$ is occupied at time t means that absorption happened either at t or before, and therefore

$$\Pr(T_{over} \leq t \mid \mathbf{A}_0 = \mathbf{a}_0) = \sum_{\mathbf{w} \in \Omega'} p_{\mathbf{a}_0 \mathbf{w}}(t);$$

moreover, using our notation in (2.32)

$$G_{\mathbf{a}_0}(t) = \sum_{\mathbf{w} \in \Omega'} p_{\mathbf{a}_0 \mathbf{w}}(t) \qquad \mathbf{a}_0 \in \bar{\Omega}; \tag{2.34}$$

$\bar{\Omega}$ denotes the complement of Ω, the set of overload states, and thus is the set of underload states.

We denote the new process that results after the introduction of the absorbing state as $\mathbf{A}'_t$. According to (2.34) determination of the first passage time to overload entails finding the transitional probabilities $p_{\mathbf{a}_0 \mathbf{w}}(t)$ from any underload state $\mathbf{a}_0$ to any first entered overload state $\mathbf{w}$ for the modified process $\mathbf{A}'_t$. A standard procedure towards this is to use the backward Kolmogorov equations for $\mathbf{A}'_t$.

The Backward Kolmogorov equations

The procedure for writing the Backward Kolmogorov equations for $\mathbf{A'}_t$ parallels to a great extent the procedure followed in the single dimensional case. The difference here is that absorption can happen in more than one state.

We fix a state $\mathbf{w} \in \Omega'$ which is entered upon absorption. Furthermore, we assume that at time $t + \Delta t$ this state is occupied, implying that absorption happened at state $\mathbf{w}$ before any other state in Ω'. We consider two more points in time, one at time 0, and the other at time $t = \Delta t$. Using the Chapman-Kolmogorov formulation we sum on all possible combinations of states that are visited at the intermediate time Δt, in

the path from an initial underload state $\mathbf{a}_0$ at time 0, to the overload state $\mathbf{w}$ at time $t + \Delta t$

$$p_{\mathbf{a}_0,\mathbf{w}}(t + \Delta t) = \sum_{\mathbf{a}} p_{\mathbf{a}_0,\mathbf{a}}(\Delta t) p_{\mathbf{a},\mathbf{w}}(t) \qquad \mathbf{a}_0 \in \bar{\Omega}. \tag{2.35}$$

Since $\mathbf{A}'_t$ retains the birth-death structure of $\mathbf{A}_t$ for states that are not absorbing, only states with one more or one less active source of a given class are reachable in an incremental time interval Δt from an initial state $\mathbf{a}_0$. However, transitions to an absorbing state $\mathbf{w}'$ other than $\mathbf{w}$ in the initial time Δt must be excluded from the summation in (2.35). This is because if absorption takes place in the first Δt seconds at a state $\mathbf{w}'$ other than $\mathbf{w}$, then state $\mathbf{w}$ would never be visited in the next t seconds, since $\mathbf{w}'$ would never be exited as being absorbing as well. But this last statement entails that

$$p_{\mathbf{w}',\mathbf{w}}(t) = 0 \tag{2.36}$$

Accordingly, in expanding the summation in (2.35) we should include terms with $\mathbf{a} = \mathbf{w}' \in \Omega' - \{\mathbf{w}\}$, bearing in mind that they vanish according to (2.36).

Then by introducing the indicator function of the event $a_l > 0$, $I_{\{a_l>0\}}(\mathbf{a})$,

$$I_{\{a_l>0\}}(\mathbf{a}) = \begin{cases} 1 & \text{if} \quad a_l > 0 \\ 0 & \text{if} \quad a_l = 0 \end{cases}$$

we expand the RHS of equation (2.35) and we write

$$p_{\mathbf{a}_0,\mathbf{w}}(t+\Delta t) = \sum_{l=1}^{L} p_{\mathbf{a}_0,\mathbf{a}_{0,l}^{+}}(\Delta t)\, p_{\mathbf{a}_{0,l}^{+},\mathbf{w}}(t) + \sum_{l=1}^{L} I_{\{a_l>0\}}(\mathbf{a}_0)\, p_{\mathbf{a}_0,\mathbf{a}_{0,l}^{-}}(\Delta t)\, p_{\mathbf{a}_{0,l}^{-},\mathbf{w}}(t) + p_{\mathbf{a}_0,\mathbf{a}_0}(\Delta t)\, p_{\mathbf{a}_0,\mathbf{w}}(t). \quad (2.37)$$

where $\mathbf{a}_{0,l}^{+}$ and $\mathbf{a}_{0,l}^{-}$ follow the notation introduced in (2.27). The first summation in the RHS of the above corresponds to a class l source becoming active, while the second one to the event of an active call of class l becoming idle. Finally the last term corresponds to no change in the number of active sources.

Continuing we substitute in (2.37) the transition probabilities given by (2.28) (2.29) and (2.30). Accordingly, (2.37) becomes

$$p_{\mathbf{a}_0,\mathbf{w}}(t+\Delta t) = \sum_{l=1}^{L}(N_l - a_{0,l})\lambda_l \Delta t\, p_{\mathbf{a}_{0,l}^{+},\mathbf{w}}(t) + \sum_{l=1}^{L} a_{0,l}\mu_l \Delta t\, p_{\mathbf{a}_{0,l}^{-},\mathbf{w}}(t) + \left[1 - \sum_{l=1}^{L}(N_l - a_{0,l})\lambda_l \Delta t - \sum_{l=1}^{L} a_{0,l}\mu_l \Delta t\right] p_{\mathbf{a}_0,\mathbf{w}}(t). \quad (2.38)$$

Rearranging terms, dividing by Δt, and taking the limit as $\Delta t \to 0$, (2.38) results in the backward Kolmogorov equations for $p_{\mathbf{a}_0,\mathbf{w}}(t)$,

$$\frac{dp_{\mathbf{a}_0,\mathbf{w}}(t)}{dt} = \sum_{l=1}^{L}\left[(N_l - a_{0,l})\lambda_l p_{\mathbf{a}_{0,l}^{+},\mathbf{w}}(t) + a_{0,l}\mu_l p_{\mathbf{a}_{0,l}^{-},\mathbf{w}}(t)\right] - \sum_{l=1}^{L}[(N_l - a_{0,l})\lambda_l + a_{0,l}\mu_l] p_{\mathbf{a}_0,\mathbf{w}}(t). \quad (2.39)$$

Considering the fact that $p_{\mathbf{w},\mathbf{w}}(t) = 1$ and $p_{\mathbf{w}',\mathbf{w}}(t) = 0$ for any state $\mathbf{w}' \in \Omega' - \{\mathbf{w}\}$,

we can write:

$$\frac{dp_{\mathbf{a}_0,\mathbf{w}}(t)}{dt} = 0 \qquad \mathbf{a}_0 \in \Omega' \tag{2.40}$$

Equations for the Probability Distribution of the Time to Overload

Equations (2.39) and (2.40) describe the time evolution of the transition probabilities $p_{\mathbf{a}_0,\mathbf{w}}(t)$ for the truncated process $\mathbf{A}'_t$. Using equation (2.34) we can describe the dynamic behavior of the probability distribution for the time to overload for the original process $\mathbf{A}_t$. Towards this end, we take summation of both sides of (2.39) over all states $\mathbf{w}$ in Ω'; thus, (2.39) becomes

$$\begin{aligned}\frac{dG_{\mathbf{a}_0}(t)}{dt} &= \sum_{l=1}^{L}\left[(N_l - a_{0,l})\lambda_l G_{\mathbf{a}^+_{0,l}}(t) + a_{0,l}\mu_l G_{\mathbf{a}^-_{0,l}}(t)\right] \\ &\quad - \sum_{l=1}^{L}[(N_l - a_{0,l})\lambda_l + a_{0,l}\mu_l]G_{\mathbf{a}_0}(t). \end{aligned} \tag{2.41}$$

Similarly from equation (2.40) we get a degenerate form of the probability distribution for the time to overload when the initial state is any of the first entered overload states,

$$\frac{dG_{\mathbf{a}_0}(t)}{dt} = 0 \qquad \mathbf{a}_0 \in \Omega' \tag{2.42}$$

There exists one equation like (2.41) above, for every initial underload state and like (2.42) for every overload state that is first visited upon absorption. We follow the approach of the previous section 2.1, and organize these equations in a matrix

form. Towards this end, we need a way to enumerate all the underload states $\mathbf{a_0}$ of our system. We choose the lexicographic ordering,

$$\mathbf{a_0} \prec \mathbf{a_0'} \quad \text{iff} \quad \exists i, a_{0,1} = a'_{0,1}, \ldots, a_{0,i-1} = a'_{0,i-1}, a_{0,i} < a'_{0,i}, \tag{2.43}$$

and we denote by $\mathcal{F}$, the mapping

$$\begin{array}{cccccccccc} & 1 & , & 2 & , & \ldots & , & s & \ldots & , & n \\ \mathcal{F}: & \updownarrow & & & & & & \updownarrow & & & \updownarrow \\ & (0,0,\ldots,0) & \prec & (0,0,\ldots,1) & \prec & \ldots & \prec & \mathbf{a_0} & \ldots & \prec & (c_1,0,\ldots,0) \end{array} \tag{2.44}$$

between the states $\mathbf{a_0} \in \bar{\Omega}$ and the first n positive integers. $c_1 = \lfloor \frac{C}{r_1} \rfloor$ is the capacity of the output channel in terms of the number of simultaneous active sources of type 1.

We denote by $\mathbf{G}(t)$ the column vector $\mathbf{G}(t) = (G_1(t), \ldots, G_s(t), \ldots, G_n(t), G_{n+1}(t))^T$, where $G_s(t)$, $s = 1, 2, \ldots, n$, stands for $G_{\mathbf{a_0}}(t)$, with s the order of $\mathbf{a_0}$ in the lexicographic mapping $\mathcal{F}$. We enumerate the overload state as the $(n+1)^{\text{th}}$ state. Consequently, we arrange equations (2.41) and (2.42) into matrix form

$$\frac{d\mathbf{G}(t)}{dt} = \mathcal{Q}'\mathbf{G}(t), \tag{2.45}$$

with $\mathcal{Q}'$ being a $n+1 \times n+1$ matrix. Matrix $\mathcal{Q}'$ contains the coefficients of functions $G_{(.)}(t)$ in the above representation, but it does not have a simple representation as the relevant matrix in the single source type case.

Solution of the Equations for the Probability Distribution

Equation (2.45) is a set of first order differential equations. We will give its solution in a form similar to the one for the single source type case. Denoting by $z'_1, z'_2, \ldots, z'_n$ the eigenvalues of matrix Q' and by $\mathbf{V}'_j$ and $\mathbf{U}'_j$ its normalized right and left eigenvectors respectively, associated with the eigenvalue z'_j,

$$\mathbf{U}'^T_j \mathbf{V}'_k = \begin{cases} 1 & j = k \\ 0 & j \neq k \end{cases} \tag{2.46}$$

the solution of (2.45) is written as

$$\mathbf{G}(t) = \sum_{j=1}^{n+1} e^{z'_j t} \mathbf{V}'_j \mathbf{U}'^T_j \mathbf{G}(0). \tag{2.47}$$

with $\mathbf{G}(0)$ standing for the initial conditions for our problem, namely the probability that the multiplexer overloads in time $t = 0$.

Clearly, the multiplexer overloads immediately, only if it starts from the overload state;

$$G_s(0) = \begin{cases} 1 & s = n+1 \\ 0 & \text{otherwise} \end{cases} \tag{2.48}$$

Finally, substituting a_j for $\mathbf{U}^T_j \mathbf{G}(0)$ in (2.47), and evaluating it at t_{rt}, the network

round trip time, we write

$$\mathbf{G}(t_{rt}) = \sum_{j=1}^{n+1} a_j e^{z_j t} \mathbf{V}_j. \tag{2.49}$$

The element $G_s(t_{rt})$ of $\mathbf{G}(t_{rt})$ where s is the order of a_0 according to the mapping $\mathcal{F}$, is a measure of congestion imminence in a network with round trip time of t_{rt}, and initial state $\mathbf{a}_0 = (a_{0,1}, a_{0,2}, \ldots, a_{0,L})$.

Numerical Example

We consider a 51.84 Mbit/s OC-1 link supporting $N_{\text{vi}} = 2$ video calls (i.e. each

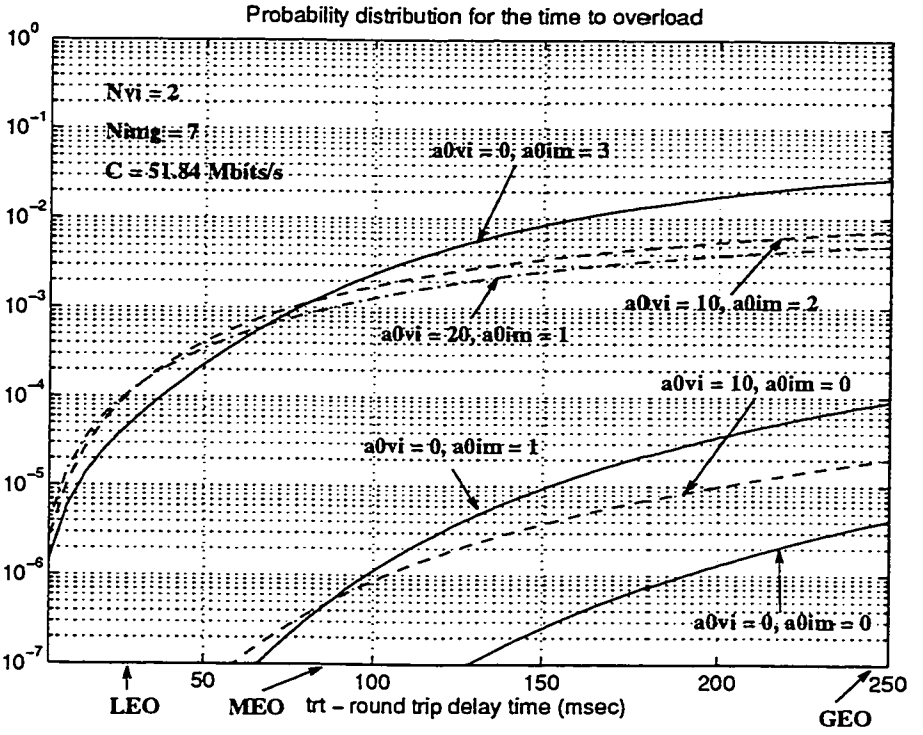

Figure 2.17: Probability distribution for the time to overload for a statistical multiplexer loaded with image and video traffic, for different values for the initial state $\mathbf{a}_0 = (a_{0\text{im}}, a_{0\text{vi}})$; number of admitted video sources, $N_{\text{vi}} = 2$; number of admitted image sources, $N_{\text{im}} = 7$.

video call consists of the video part of a videophone call, or of a videoconference) and $N_{im} = 7$ image transfer calls (i.e. medical image transfer sessions). The characteristics

of the video calls are as described above in section 2.1.2. During image transfer sessions, images having an average size of 10 Mbits are transmitted at a peak rate of $r_{\text{im}} = 10$ Mbits/s. According to this the mean transmission time for an image is $\frac{1}{\mu_{\text{im}}} = 1$sec. Each image transmission is followed by an idle period of $\frac{1}{\lambda_{\text{im}}} = 10$sec.

Figure 2.17 gives the probability distribution for the time to overload for different initial channel utilizations. We see that in the heterogeneous traffic case, the probability distribution for the time to overload does not only depend on the initial output channel occupancy, but on the particular mix of this occupancy in terms of active sources of the various classes.

2.2.3 Applications to Congestion Control

We treat, as above for the homogeneous case, the probability distribution for the time to overload evaluated at the network round trip time $\mathbf{G}(t_{rt})$, as a QOS parameter. Equation (2.49) relates this parameter with the other parameters of our model: number of admitted calls of each class, $N_1, N_2, \ldots, N_L$; the in-call parameters of these calls, r_l, λ_l, μ_l; the source-multiplexer round-trip time, t_{rt}; and the initial number of active sources from each class $a_{0,l}$.

Thus, (2.49) is useful in designing congestion control algorithms. Towards this end, we first set a quality of service requirement for $\mathbf{G}(t_{rt})$:

$$G_s(t_{rt}) < \epsilon, \tag{2.50}$$

for every element $G_s(t)$ of $\mathbf{G}(t)$. Accordingly, meeting (2.50), on a channel with a

given round trip time t_{rt}, depends on N_1, N_2, ..., N_L (admission control), and on r_l, λ_l, μ_l (in-call parameter control).

Admission Control

Figure 2.18 plots the regions, in terms of the initially active sources of each class, for our video-image multiplexing example that comply with requirement (2.50) (Regions I and II). When the multiplexer operates within these regions, overload in a round trip time happens with probability less than ϵ. Since the multiplexer state is two-dimensional both the initial number of images sources $a_{0_{\text{im}}}$, as well as the initial number of video minisources $a_{0_{\text{vi}}}$ is relevant in the determination of these regions.

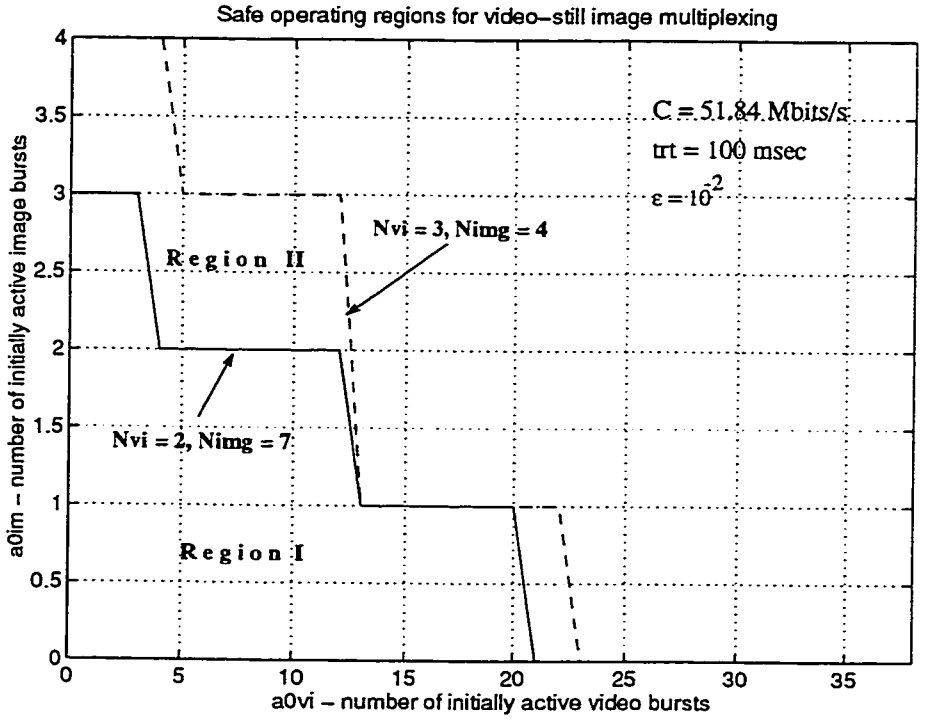

Figure 2.18: Multiplexer safe operating regions in terms of initially active video and image bursts, for different number of admitted sources, N_{vi}, and N_{im}; channel round trip time $t_{\text{rt}} = 100$ msec.

We use $\epsilon = 10^{-2}$ as the value of the acceptable probability to overload in a

network round trip time. Moreover, three video calls and four image sessions, $N_{\text{vi}} = 3$, $N_{\text{im}} = 4$, corresponds to a an admissible load under a preventive congestion control strategy that guarantees a 10^{-2} burst blocking probability [Hui88], while the case of $N_{\text{vi}} = 2$, $N_{\text{im}} = 7$ does not [DzioR87].

In-call Parameter Control

To extend the safe operating regions of the multiplexer such as condition (2.50) is satisfied for every feasible initial combination of bursts in active state, control of in-call parameters can be employed. In a heterogeneous source environment in-call parameter control results in a multitude of parameters that can be varied; these include the durations of burst or interburst intervals, and the peak burst rate r_l, of every source type.

Interburst intervals, $\frac{1}{\lambda_l}$, are varied by delaying the burst submissions into the network. In our video-image multiplexing example this can be achieved, either at the source level by a shaper buffer [ReiRH96], or at the network entrance by a buffered leaky bucket scheme [ElwaM91]. Similarly, burst duration, $\frac{1}{\mu_l}$, can be decreased by dropping cells at the beginning of a burst; this can also be achieved at the network access, if we consider a bufferless access regulator. Moreover, a combination of the two above methods could be employed, using a buffered access regulator with a limited buffer capability.

Interburst or burst duration variation result in a change of the source activity ratio. The extent to which either or both methods could be employed, would depend on the application; for instance, interactive applications are not amenable to interburst

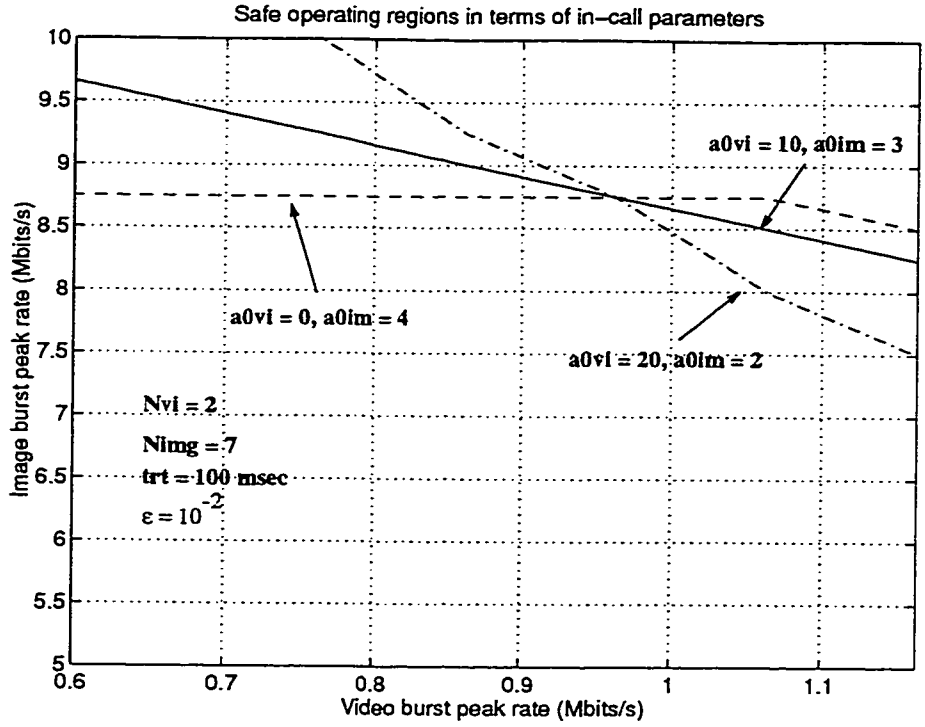

Figure 2.19: Multiplexer safe operating regions in terms of burst peak rates.

duration variation by delaying a burst, while loss sensitive applications are sensitive to consecutive cell loss in different degrees.

Finally, the peak burst rate can be decreased, by periodical cell dropping at a network access. For our example at hand, rate reductions can also be achieved by traffic shaping, e.g. by using coarser quantization during video encoding [ReiRH96]. Moreover, to reduce the effects of cell dropping in received video or still image quality, rate reductions can be combined with multilayer coding [ChiaA96]. Figure 2.19 depicts the rate adjustments that should be performed to meet the required value of the QOS constraint for our example.

CHAPTER 3
OVERLOAD AND UNDERLOAD PREDICTION FOR A BUFFERED RESOURCE

In this chapter the overload prediction for a statistical multiplexer loaded with delay tolerant services is presented. Since delay is not a critical performance requirement of the services supported, the multiplexer is equipped with a buffer of non-negligible size. This stands in contrast to the previous chapter, where the multiplexer buffering was very limited, and for practical purposes has been ignored.

However, the buffer existence does not necessarily preclude the use of the multiplexer in supporting voice and video applications; for high speed output channels, queueing delay becomes very small even when the multiplexer is equipped with high capacity buffers. For instance, an NTSC video frame would carry around 5-50 Kbytes of information, which on a OC-3 optical link corresponds to a transmission time of tenths to hundreths of a msec. Therefore, even a buffer of several Mbytes will result in a delay somewhat less than a second on these links.

As in the previous chapter, we assume knowledge of the total number of subscribed sources, and of their statistical characteristics. Moreover, the current activity level of the sources, sending traffic to the multiplexer is supposed to be known as well. In contrast with the previous chapter, where the source state is estimated from output

channel measurements, as explained in chapter 4, in this chapter we assume that this knowledge comes from monitoring directly the activity of the input to the multiplexer lines. Besides the source state, in this chapter we require knowledge of the buffer occupancy of the multiplexer, as well. Similarly, we assume that this is achieved by an appropriate method of buffer occupancy monitoring.

Moreover, overload prediction is predicated on the fact that network traffic presents short range dependencies, and Markovian traffic models are able to capture it. As we saw in the two previous chapters, this assumption can be justified for voice and video services.

Our interest in predicting overload, is to characterize the imminence of congestion in the case of a multiplexer with a buffer. Specifically, we advocate that the probability distribution to overload in a network round-trip time, serves as a quantitative measure of congestion imminence. This in accordance with the fact, that the network round trip time is the reaction time of our system. This chapter is concerned with the derivation of an analytic expression of the probability distribution for the time to overload for a buffered statistical multiplexer in terms of the network and source parameters. Subsequently, we use the results to give examples of proactive congestion avoidance strategies.

Congestion avoidance in a buffered statistical multiplexer is the first requirement in the operation of the statistical multiplexer; multiplexing efficiency is the second one. It is usually related to empty buffer conditions and therefore a requirement for efficient buffer multiplexing is to keep the probability of buffer underloading at low levels. As such, besides the probability distribution for the time to overload,

the probability distribution for the time to underload is of importance as well in our approach for the secondary reason of multiplexing efficiency. This can be developed in a similar manner, in the context of this chapter.

The development of the material of this chapter is based to a great extent on the fluid traffic model, first developed by Anick et al. [AniMS82], as is the material in chapter 2. Anick et al. [AniMS82] used the fluid model to derive steady state results for the complementary probability distribution for the buffer content. In our case, we are not interested in steady state results, but in the first passage times for the buffer to overflow or underflow. Gaver et al. [GaveL82], treats the mean first passage time to underload for a buffer that empties at a rate that varies according to Markov Process, in a mixed data-voice multiplexing application for an infinite source model. Ren and Kobayashi [RenKo95] treat the transient behavior of the Anick et al. model. Weiss, [Weis86], obtains approximate expressions for the mean time until the buffer exceeds a prescribed level, as a by-product of his asymptotic analysis using large deviations on the model of Anick et al. His approximations are valid when the multiplexer operates below its stability point. While our interest is in such cases, we will be considering cases where the multiplexer operates beyond its stability point as well.

This chapter is organized as follows; in the next section we give the formulation of the model of the multiplexer, defining any quantities of interest. In section 3.2, we treat the problem of multiplexer overload, and we give the probability distribution for the time to overload as solution to a set of partial differential equations. Section 3.2.4, adapting the procedure of [RenKo95], gives the solution of these equations in a

Laplace transform form. Section 3.3 discusses the multiplexer underload problem; it is found that it reduces to the overload problem by a proper change of variables. In section 3.4 we return to the overload problem, and we derive the moments of the first passage time to overload for our statistical multiplexer as solutions to inhomogeneous sets of first order linear ordinary differential equations. Their general solution are given explicitly in section 3.4.2, adapting the results of [AniMS82]. Sections 3.4.3 and 3.4.4 specialize these results for the first two moments. Finally in section 3.4.5 we give numerical results for the moments of the first passage time to overload for specific examples.

3.1 Model Formulation

We assume the same model for the input traffic as in chapter 2 (homogeneous case), namely, N identical On-Off sources. These share the capacity C of a VP through the auspices of a statistical multiplexer. The main difference in this chapter

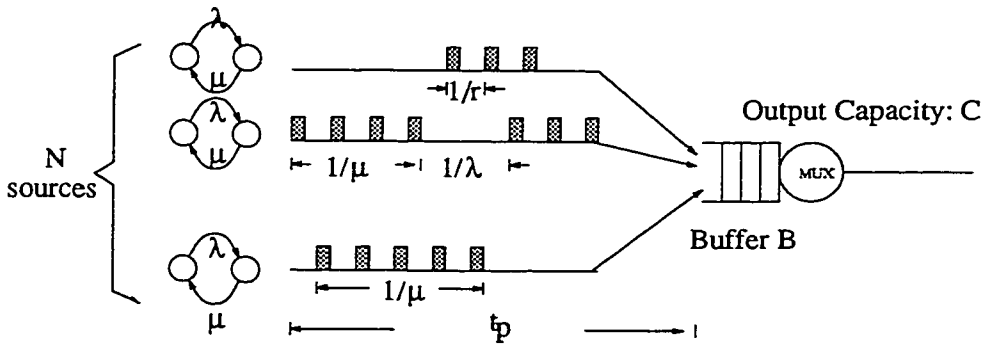

Figure 3.1: The multiplexer at the Virtual Path (VP) level; N identical binary On-Off sources are multiplexed in a VP of allocated capacity C and buffer space B.

is that the multiplexer is equipped with a buffer of finite capacity B (figure 3.1). The buffer stores input traffic arriving at a rate in excess of the output channel capacity.

We consider the fluid flow approach in modeling the buffer content of the multiplexer; towards this end we assume that buffer content is a continuous variable and we denote its value at time t by X_t. This could be justified considering the small size of cells, in comparison to the available buffer size B. Furthermore, we denote the number of active sources at time t by A_t. We define the state of our system as the two dimensional vector

$$S_t = (A_t, X_t) \quad A_t \in \{0, 1, 2, \ldots, N\} \quad X_t \in [0, B]\,. \tag{3.1}$$

S_t consists of one discrete and one continuous element, and its state space is a set of lines (figure 3.2).

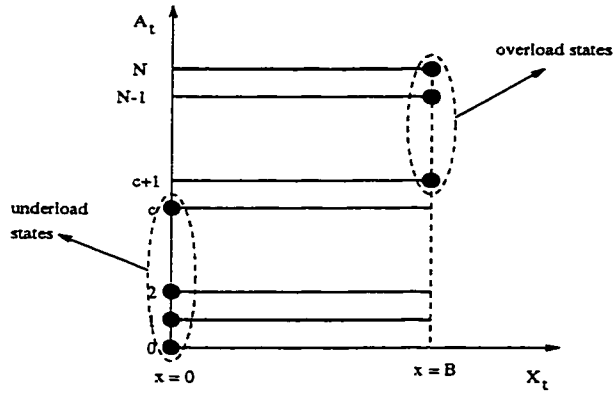

Figure 3.2: The state space of the multiplexer.

S_t belongs to the class of Markov process with a drift [Mitra88]. These processes consists of two element subprocesses; one that is a Markov process (A_t in our case), and a second that varies piecewise deterministically with a rate that depends on the current value of the Markov process (X_t in our case). For instance, the rate of change

for X_t given $A_t = a$, in our case, is given as

$$\frac{dX_t}{dt} = \begin{cases} \max\{0, -(C - ar)\} & \text{when} \quad X_t = 0 \\ -(C - ar) & \text{when} \quad 0 < X_t < B \\ \min\{0, -(C - ar)\} & \text{when} \quad X_t = B \end{cases} ; \tag{3.2}$$

buffer content can only increase when the buffer is empty, and similarly it can only decrease when it is full. For intermediate values of the buffer content ($0 < X_t < B$) changes in both directions of the buffer content are possible.

We further characterize our system state S_t, by giving its transition probabilities in an incremental time interval $\Delta t \ll 1$. Towards this end, we define $p_{i,j}(y, x; t)$ as the conditional joint probability density of j, the number of active sources, and x the buffer content, at time t, given i active sources and buffer content of y, at time 0,

$$p_{i,j}(x_0, x; t) \triangleq \Pr(A_t = j, X_t = x \mid A_0 = i, y < X_0 \leq y + \Delta y). \tag{3.3}$$

Notice, that to make the presentation of the material easier, we defined the probability density conditioned on a event that can be easily assigned a probability measure. Accordingly,

$$\Pr(A_t = j, x < X_t \leq \Delta x \mid A_0 = i, x_0 < X_0 \leq x_0 + \Delta x_0) = p_{i,j}(x_0, x; t)\Delta x. \tag{3.4}$$

Recalling that A_t evolves as a birth-death process, the transition probabilities for S_t

in an incremental time interval Δt are

$$p_{a_0,a_0+1}(x_0, x_0 - (C - a_0 r)\Delta t; \Delta t)\Delta x = (N - a_0)\lambda \Delta t + o(\Delta t) \quad (3.5)$$

for an idle source becoming active during the Δt time interval,

$$p_{a_0,a_0-1}(x_0, x_0 - (C - a_0 r)\Delta t; \Delta t)\Delta x = a_0 \mu \Delta t + o(\Delta t), \quad (3.6)$$

for an active source becoming idle in the same time interval, and finally

$$p_{a_0,a_0}(x_0, x_0 - (C - a_0 r)\Delta t; \Delta t)\Delta x = 1 - (N - a_0)\lambda \Delta t - a_0 \mu \Delta t + o(\Delta t), \quad (3.7)$$

for no change in the number of active sources. In all above cases, the buffer content changes by $-(C - a_0 r)\Delta t$, a quantity that can be positive or negative depending on the value of a_0.

Two events in the operation of the multiplexer are of importance in our discussion. The first one is buffer overflow, which occurs when the total information arrival rate from all active sources , rA_t, is greater than the capacity of the channel, C, and the buffer content is at its its upper limit B, and therefore cannot store the surplus input traffic, $rA_t - C$. We characterize this condition as overload for the multiplexer, and normalizing the output channel capacity by the peak source rate, r, and letting c, as in chapter 2, to denote the largest integer not exceeding the normalized channel

capacity, $c \triangleq \lfloor \frac{C}{r} \rfloor$, we write:

$$\text{multiplexer overload condition:} \quad A_t \in \{c+1, c+2, \ldots, N\}, \quad X_t = B. \quad (3.8)$$

Similarly, the event of the buffer content depletion, which occurs when the total information arrival rate from all active sources, rA_t, is less than the channel capacity and the buffer is empty, $X_t = 0$, constitutes an underload condition for our multiplexer

$$\text{multiplexer underload condition:} \quad A_t \in \{0, 1, 2, \ldots, c\}, \quad X_t = 0. \quad (3.9)$$

We assume that at an initial time t_0, the multiplexer state is (A_{t_0}, X_{t_0}), such that $A_{t_0} = a_0$, and $x_0 < X_{t_0} \leq x_0 + \Delta x_0$. We further assume that x_0 and a_0 are such that, neither the overload condition (3.8), nor the underload one (condition (3.9)) is satisfied at time t_0. In other words, $x_0 \neq 0$ and $x_0 \neq B$, or if initially we assume an empty buffer, then a_0 should be an "up" state [1]; similarly if initially we assume a full buffer, then the initial state of the sources must be a "down" state.

Ignoring for the moment the lower buffer limit, implicitly assuming that buffer content can resume negative values as well, we denote by T_{over} the time until overload happens for the first time after t_0. T_{over}, defined in this sense, serves as an approximation to the actual first time to overload for the multiplexer. More precisely, T_{over} overestimates this time, since allowing the buffer content to decrease indefinitely, it takes longer to fill up again to reach its upper limit. However, assuming a large buffer

[1] We term source states $a_0 > c$ as "up" states; similarly sources states such that $a_0 \leq c$ are called "down" states.

size B, and that the the average offered to the multiplexer load is greater than its handling capacity $\frac{N\lambda r}{\lambda+\mu} > C$, the probability of the buffer occupancy reaching the zero level is very small, and hence the discrepancy, introduced by the ignorance of the lowest buffer level, between T_{over} and the actual time to overload, becomes small.

In a similar fashion, ignoring the fact that the buffer capacity is finite, but realizing that it has a lower limit at $X_t = 0$, we define T_{under} as the time until underload happens for the first time. T_{under} overestimates the actual time to underload; however, if the buffer size were large, and that the average offered to the multiplexer load were less that its handling capacity, $\frac{N\lambda r}{\lambda+\mu} < C$, the discrepancy between T_{under} and the actual time to underload becomes negligible.

We define the conditional probability distribution for T_{over} given the system initial state (a_0, x_0) as

$$G^{+}_{a_0}(x_0, t) \triangleq \lim_{\Delta x_0 \to 0} \Pr\left(T_{over} \leq t \mid A_{t_0} = a_0, x_0 < X_{t_0} \leq x_0 + \Delta x_0\right), \quad (3.10)$$

and the conditional probability distribution for T_{under}

$$G^{-}_{a_0}(x_0, t) \triangleq \lim_{\Delta x_0 \to 0} \Pr\left(T_{under} \leq t \mid A_{t_0} = a_0, x_0 < X_{t_0} \leq x_0 + \Delta x_0\right).$$

The above functions evaluated at the system reaction time, i.e. the network round trip time, t_{rt}, give a measure of the congestion imminence or underloading imminence respectively. In the sequel we focus on evaluating $G^{+}_{a_0}(x_0, t)$, and $G^{-}_{a_0}(x_0, t)$.

3.2 Probability Distribution for the Time to Overload

In this section we derive the dynamic equations that describe the time evolution of the probability distribution for the time to overload, and attempt their solution. We were able to give an analytic expression of the solution in a Laplace transform form.

3.2.1 Preliminaries

We start by defining the overload set of states, Ω_{over}, as the set of states of the multiplexer that satisfy the overload condition (3.8). However, since X_t is continuous, and we we can not assign properly probabilities to events like $X_t = B$, we augment the definition of the overload states of our multiplexer, by considering states in the vicinity of the states satisfying the above conditions (3.8); finally,

$$\Omega_{over} \triangleq \{(a,x):\ a \in \{c+1, c+2, \ldots, N\}, B - \Delta x < x \leq B\} \qquad (3.11)$$

where Δx is an incremental buffer interval.

Accordingly, T_{over} can be identified as a first passage time to a state $(a,x) \in \Omega_{over}$, for the Markov drift process S_t. A common method in treating such problems is to modify the process at hand, namely S_t, by introducing an absorbing state. Towards this end, we consider Ω_{over} as being absorbing. Let S'_t be our state process after the above modification. S'_t retains the structure of S_t for all other states except the absorbing one, and therefore equations (3.5), (3.6) and (3.7) describing the transition

probabilities of S_t in an incremental time interval Δt hold for the description of the transition probabilities of S'_t as well, except when the starting state (a_0, x_0) is one of the absorbing states, i.e, $(a_0, x_0) \in \Omega_{over}$.

The event, that the absorbing state is occupied at time t, signifies that absorption happened at some time before t, and thus the probability distribution for the time to overload for the initial Markov drift process, S_t, equals the conditional probability that Ω_{over} of the truncated process S'_t, is occupied at time t,

$$G^+_{a_0}(x_0, t) = \lim_{\Delta x_0 \to 0} \Pr(S'_t \in \Omega_{over} \mid A_0 = a_0, x_0 < X_0 \leq x_0 + \Delta x_0). \qquad (3.12)$$

Ω_{over}, is not a single state; therefore when absorption happens, i.e. Ω_{over} is visited for the first time, absorption can happen in any of its component states, (a, x), $B - \Delta x < x \leq B$, $a = c+1, c+2, \ldots, N$. Using the notation of equation (3.3), $p_{a_0,a}(x_0, B; t)\Delta x$, gives the probability that state (a, x), $B - \Delta x < x \leq B$ is occupied at time t, or in other words it gives the probability that absorption happens by time t and the first state entered upon absorption is state (a, x). Summing on all component states of Ω_{over}, equation (3.12) becomes,

$$G^+_{a_0}(x_0, t) = \lim_{\Delta x_0 \to 0} \sum_{a=c+1}^{N} p_{a_0,a}(x_0, B; t)\Delta x \qquad (3.13)$$

Equation (3.13) expresses the probability distribution for the to overload, $G^+_{a_0}(x_0, t)$, in terms of the transition probabilities $p_{a_0,a}(x_0, B; t)\Delta x$ for the truncated Markov drift process, S'_t. Thus, evaluation of the former depends on finding an expression of the

latter. In turn, the expression for $p_{a_0,a}(x_0, B; t)\Delta x$ will be given from the dynamic equations for the process S'_t. Towards this end, we need to develop the dynamic equations that $p_{a_0,a}(x_0, B; t)\Delta x$ satisfies.

3.2.2 The Backward Equations

The development of the backward equations for $p_{a_0,a}(x_0, B; t)\Delta x$, follows a standard procedure. First, we consider three points in time: the initial time t_0, which for ease of presentation it is considered to be zero, $t_0 = 0$; the intermediate incremental time Δt, $\Delta t \ll 1$; and at last the final time $t + \Delta t$. Secondly, we assume that at time $t + \Delta t$, the multiplexer is in one of the absorbing states (a, x), $B - \Delta x < x \leq B$, $a \in \{c+1, c+2, \ldots, N\}$. Then, using the Chapman-Kolmogorov formulation we sum on all possible paths at the intermediate time Δt, that brought the multiplexer from state (A_0, X_0) at time zero, to the absorbing state (a, x) at time $t + \Delta t$.

Before writing the Chapman-Kolmogorov equations, we enumerate the possible events, E_i, that can happen in the initial incremental time interval Δt: event E_1, an additional source becomes active, and consequently at time Δt, $a_0 + 1$ sources are active, and the buffer content changes to $x_0 - (C - a_0 r)\Delta t$; event E_2 a source becomes idle, leaving at time Δt $a_0 - 1$ active sources and the buffer level at $x_0 - (C - a_0 r)\Delta t$; E_3, no change in the number of active sources occurs, and thus, at time Δt a_0 sources are active, and the buffer content is at level $x_0 - (C - a_0 r)\Delta t$.

Then, introducing the indicator function of an event E,

$$I_E(i) = \begin{cases} 1 & \text{if } i \in E \\ 0 & \text{if } i \notin E \end{cases},$$

for unification of presentation, we are in the position to express the Chapman-Kolmogorov equations for $p_{a_0,a}(x_0, x; t + \Delta t)\Delta x$,

$$\begin{aligned} & p_{a_0,a}(x_0, x; t + \Delta t)\Delta x = \\ & \quad I_{\{N>a_0\}}(a_0) p_{a_0,a_0+1}(x_0, x_0 - (C - a_0 r)\Delta t; \Delta t)\, \Delta x\, p_{a_0+1,a}(x_0 - (C - a_0 r)\Delta t, B; t)\Delta x \\ & \quad + I_{\{a_0>0\}}(a_0) p_{a_0,a_0-1}(x_0, x_0 - (C - a_0 r)\Delta t; \Delta t)\Delta x\, p_{a_0-1,a}(x_0 - (C - a_0 r)\Delta t, B; t) \\ & \quad + p_{a_0,a_0}(x_0, x_0 - (C - a_0 r)\Delta t; \Delta t)\Delta x\, p_{a_0,a}(x_0 - (C - a_0 r)\Delta t, B; t)\Delta x. \end{aligned} \tag{3.14}$$

$I_{\{N>a_0\}}(a_0)$ nullifies the first term in the RHS of (3.14), when the number of active sources a_0 is equal to N, and therefore no additional source can become active, and $I_{\{a_0>0\}}(a_0)$ nullifies the second term, when the number of active sources is zero, and therefore it is impossible to decrease.

S'_t has the same structure as S_t for states not in the set of absorbing states, Ω_{over}. Therefore, the probabilities of the events E_1, E_2 and E_3 are also given by equations (3.5), (3.6), and (3.7) respectively. Substituting these probabilities in equation (3.14), we have,

$$p_{a_0,a}(x_0, x; t + \Delta t)\Delta x =$$

$$I_{\{N>a_0\}}(a_0)(N - a_0)\lambda\Delta t\, p_{a_0+1,a}(x_0 - (C - a_0 r)\Delta t, B; t)\Delta x$$

$$+ I_{\{a_0>0\}}(a_0)a_0\mu\Delta t\, p_{a_0-1,a}(x_0 - (C - a_0 r)\Delta t, B; t)$$

$$+ [1 - (N - a_0)\lambda\Delta t - a_0\mu\Delta t]\, p_{a_0,a}(x_0 - (C - a_0 r)\Delta t, B; t)\Delta x \qquad (3.15)$$

3.2.3 Dynamic Equations for the Probability Distribution

Equation (3.15) gives the probability that state (a, B) of the process S'_t is occupied at time $t + \Delta t$, which in turn express the probability that absorption happens and the first state entered upon absorption is (a, B). Summing over all states (a, B) that belong to the overload state Ω_{over}, taking limits as $x_0 \to 0$, and using equation (3.13), we get an equation for the probability distribution for the time to overload $G^+_{a_0}(x_0, t + \Delta t)$

$$G^+_{a_0}(x_0, t + \Delta t) =$$

$$I_{\{N>a_0\}}(a_0)G^+_{a_0+1}(x_0 - (C - a_0 r)\Delta t, t)(N - a_0)\lambda\Delta t$$

$$+ I_{\{a_0>0\}}(a_0)G^+_{a_0-1}(x_0 - (C - a_0 r)\Delta t, t)a_0\mu\Delta t$$

$$+ G^+_{a_0}(x_0 - (C - a_0 r)\Delta t, t)[1 - (N - a_0)\lambda\Delta t - a_0\mu\Delta t] \qquad (3.16)$$

Further, we apply Taylor series expansion of the functions $G^+_{(.)}(x, t)$ around the point

(x_0, t),

$$G^+_{a_0}(x_0, t+\Delta t) = G^+_{a_0}(x_0, t) + \frac{\partial G^+_{a_0}(x_0,t)}{\partial t}\Delta t + o\left((\Delta t)^2\right) \quad (3.17)$$

$$G^+_{a_0+1}(x_0 - (C - a_0 r)\Delta t, t) = G^+_{a_0+1}(x_0, t) - (C - a_0 r)\Delta t \frac{\partial G^+_{a_0+1}(x_0,t)}{\partial x_0} \quad (3.18)$$

$$G^+_{a_0-1}(x_0 - (C - a_0 r)\Delta t, t) = G^+_{a_0-1}(x_0, t) - (C - a_0 r)\Delta t \frac{\partial G^+_{a_0-1}(x_0,t)}{\partial x_0} \quad (3.19)$$

$$G^+_{a_0}(x_0 - (C - a_0 r)\Delta t, t) = G^+_{a_0}(x_0, t) - (C - a_0 r)\Delta t \frac{\partial G^+_{a_0}(x_0,t)}{\partial x_0} \quad (3.20)$$

Substituting equations (3.17) - (3.20) in (3.16) and keeping only up to linear terms in Δt, we finally get,

$$\begin{aligned} &\frac{\partial G^+_{a_0}(x_0,t)}{\partial t} + \frac{\partial G^+_{a_0}(x_0,t)}{\partial x_0}(C - a_0 r) = \\ &\quad I_{\{N>a_0\}}(a_0) G^+_{a_0+1}(x_0,t)(N-a_0)\lambda + I_{\{a_0>0\}}(a_0) G^+_{a_0-1}(x_0,t) a_0 \mu \\ &\quad - G^+_{a_0}(x_0,t)[(N-a_0)\lambda + a_0\mu] \end{aligned} \quad (3.21)$$

There is one equation like (3.21) for every initial source state a_0; we can arrange equations (3.21) in to a matrix form. Towards this end, we define the vector $\mathbf{G}^+(\xi_0, \tau)$, with elements the functions $G^+_{a_0}(\xi_0, \tau)$, $a_0 = 0, 1, 2, \ldots, N$

$$\mathbf{G}^+(\xi_0, \tau) = \left(G^+_0(\xi_0,\tau), G^+_1(\xi_0,\tau), \ldots, G^+_N(\xi_0,\tau)\right)^T,$$

the $(N+1)\times(N+1)$ matrix

$$\mathcal{Q}=\begin{pmatrix} -N\rho & N\rho & \dots & 0 & 0 & 0 \\ 1 & -(N-1)\rho-1 & (N-1)\rho & \dots & 0 & 0 \\ \vdots & \vdots & \vdots & \vdots & \vdots & \vdots \\ 0 & 0 & \dots & (N-1) & -(N-1)-\rho & \rho \\ 0 & 0 & \dots & \dots & N & -N \end{pmatrix},$$

and the diagonal matrix $\mathcal{C}$

$$\mathcal{C}=-\text{diag}\left\{-\frac{C}{r},1-\frac{C}{r},2-\frac{C}{r},\dots,N-\frac{C}{r}\right\},$$

where $\tau=t\mu$, $\xi_0=x_0\frac{\mu}{r}$, and $\rho=\frac{\lambda}{\mu}$. Then (3.21) is written as,

$$\frac{\partial \mathbf{G}^+(\xi_0,\tau)}{\partial\tau}+\mathcal{C}\frac{\partial \mathbf{G}^+(\xi_0,\tau)}{\partial\xi_0} \;=\; \mathcal{Q}\mathbf{G}^+(\xi_0,\tau). \tag{3.22}$$

Equation (3.22) is a set of linear first order partial differential equations. Before attempting its solution we must state its necessary boundary and initial conditions.

We start with the boundary conditions. Since we have treated the set of states Ω_{over} in (3.11) as absorbing, any state $(a,x)\in\Omega_{over}$ if entered is never exited. Moreover, assuming that initially we start from an overload state, $a_0\in\{c+1,\,c+2,\,\dots,\,N\}$ and $B-\Delta x<x_0\le B$, the probability of exiting this state is zero and therefore

$$p_{a_0,a_0}(B,B;t)\Delta x=1, \qquad a_0=c+1,c+2,\dots,N \tag{3.23}$$

Furthermore (3.23) entails that the probability of any other state visited, even the rest of the overload states, is zero

$$p_{a_0,a}(B,B;t)\Delta x = 0, \quad a_0 = c+1, c+2, \ldots, N \quad a \neq a_0 \tag{3.24}$$

Therefore fixing a_0, and putting equation (3.23) and (3.24) together, by summing over all overload states we get

$$\sum_{a=c+1}^{N} p_{a_0,a}(B,B;t)\Delta x = 1 \qquad a_0 = c+1, c+2, \ldots, N. \tag{3.25}$$

Then using (3.13) and after performing the necessary variable changes, and limit operations, (3.25) gives,

$$G^{+}_{a_0}(B',\tau) = 1 \quad a_0 = c+1, c+2, \ldots, N \quad \tau > 0, \tag{3.26}$$

with $B' = B\frac{\mu}{r}$ the normalized buffer length. Equation (3.26) expresses the boundary conditions that hold at the upper buffer boundary.

We continue with the initial conditions. We argue as follows; overload can not be reached immediately ($t = 0$) unless the multiplexer starts from it initially,

$$p_{a_0,a}(x_0,B;0)\Delta x = \begin{cases} 1 & a_0 = a, x_0 \geq B \\ 0 & \text{otherwise} \end{cases} \qquad a = c+1, \ldots, N. \tag{3.27}$$

Thus $p_{a_0,a}(x_0, B; 0^-)\Delta x = 0$, and accordingly summing up over all states in Ω_{over},

$$\sum_{a=c+1}^{N} p_{a_0,a}(x_0, B; 0^-)\Delta x = 0 \qquad a_0 = c+1, \ldots, N. \tag{3.28}$$

Using once more (3.13), and performing the necessary variable changes equation (3.28) gives

$$G^+_{a_0}(\xi_0, 0^-) = 0, \qquad a_0 \in \{c+1, \ldots, N\} \tag{3.29}$$

and in matrix form is expressed as

$$\mathbf{G}^+(\xi_0, 0^-) \;=\; \mathbf{0}. \tag{3.30}$$

3.2.4 Laplace Transforms of the Probability Distribution

Proceeding towards the solution of (3.21), we resort to the Laplace transform method; towards this end, we first define the Laplace transform, $\mathbf{\Gamma}^+(\xi_0, s)$, of $\mathbf{G}^+(\xi_0, \tau)$ as

$$\mathbf{\Gamma}^+(\xi_0, s) \;\triangleq\; \left(\Gamma^+_0(\xi_0, s), \Gamma^+_1(\xi_0, s), \ldots, \Gamma^+_N(\xi_0, s)\right)^T$$

where $\Gamma^+_{a_0}(\xi_0, s)$ are the individual Laplace transforms of each element in $\mathbf{G}^+(\xi_0, \tau)$

$$\Gamma^+_{a_0}(\xi_0, s) = \int_{0^-}^{\infty} G^+_{a_0}(\xi_0, \tau) e^{-s\tau} d\tau.$$

Then, taking Laplace transforms of both sides of equation (3.22), we have

$$\mathcal{C}\frac{d\mathbf{\Gamma}^{+}(\xi_0,s)}{d\xi_0} = [\mathcal{Q}-s\mathcal{I}]\,\mathbf{\Gamma}^{+}(\xi_0,s)+\mathbf{G}^{+}(\xi_0,0^{-}) \tag{3.31}$$

$\mathcal{I}$ being the $(N+1)\times(N+1)$ identity matrix.

Considering that $\mathbf{G}^{+}(\xi_0,0^{-}) = 0$ from conditions (3.30), equation (3.31) is a homogeneous system of first order linear differential equations. To find its solution, we follow a standard procedure for solving homogeneous linear differential equations [TeneP63], and we express its general solution in spectral form, using the eigenvalues $\zeta_i(s)$, and the eigenvectors $\mathbf{f}_i(s)$ and $\mathbf{h}_i(s)$ of matrix $\mathcal{C}^{-1}[\mathcal{Q}-s\mathcal{I}]$,

$$\zeta_i(s)\mathcal{C}\mathbf{f}_i(s) = [\mathcal{Q}-s\mathcal{I}]\,\mathbf{f}_i(s), \tag{3.32}$$

$$\zeta_i(s)\mathbf{h}_i(s)^{T}\mathcal{C} = \mathbf{h}_i(s)^{T}[\mathcal{Q}-s\mathcal{I}]\,. \tag{3.33}$$

Thus,

$$\mathbf{\Gamma}^{+}(\xi_0,s)=\sum_{i=0}^{N}u_i(s)e^{\zeta_i(s)(\xi_0-B')}\mathbf{f}_i(s). \tag{3.34}$$

Coefficients $u_i(s)$, will be determined from the initial conditions for our problem, $\mathbf{\Gamma}^{+}(B',s)$. Setting $\xi_0 = B'$ in the expression (3.34), and multiplying on the left the resulting expression first with $\mathcal{C}$ and then with $\mathbf{h}_i(s)^{T}$, we get,

$$u_i(s)=\frac{\mathbf{h}_i(s)^{T}\mathcal{C}\mathbf{\Gamma}^{+}(B',s)}{\mathbf{h}_i(s)^{T}\mathcal{C}\mathbf{f}_i(s)} \qquad i=0,1,\ldots N. \tag{3.35}$$

Equations (3.26) determine the $N - c$ elements of vector $\mathbf{\Gamma}^+(B', s)$; indeed, taking Laplace transforms of the conditions in (3.26), we have

$$\Gamma^+_{a_0}(B', s) = \frac{1}{s} \quad a_0 = c+1, c+2, \ldots, N. \tag{3.36}$$

To determine the remaining $c + 1$ of its elements, we rely on arguments on the stability of the expression (3.34). $G^+_{a_0}(\tau, \xi_0)$, as a probability distribution function, is bounded by 1, for $\tau > 0$ and $\xi_0 > 0$. Therefore, any terms in the expression (3.34), involving negative eigenvalues, i.e. $\zeta_i(s) < 0$, $Re\{s\} > 0$, must be canceled by requiring the coefficient of the corresponding term to vanish,

$$u_i(s) = 0, \qquad \forall i, z_i(s) < 0. \tag{3.37}$$

Using expression (3.35), conditions (3.37) can be considered as a system of equations in the unknown elements of the vector $\mathbf{\Gamma}^+(B', s)$,

$$\mathbf{h}_i(s)^T C \mathbf{\Gamma}^+(B', s) = 0 \qquad \forall i, z_i(s) < 0. \tag{3.38}$$

In our case, for a multiplexer being loaded beyond its stability point, the number of equations in (3.38) matches exactly the number of unknown coefficients of $\mathbf{\Gamma}^+(B', s)$ (see next section). Thus, (3.38) can be considered as a linear system in the unknown elements of $\mathbf{\Gamma}^+(B', s)$.

3.2.5 Properties of the Eigenvalues and Eigenvectors

Adapting the results of Ren and Kobayashi, [RenKo95], in appendix A, the eigenvalues $\zeta_i(s)$ of $\mathcal{C}^{-1}[\mathcal{Q} - s\mathcal{I}]$ are given as solutions to a set of quadratic equations of the form

$$\alpha(k,s)\zeta^2 + \beta(k,s)\zeta + \delta(k,s) = 0 \qquad k = 0, 1, \ldots, N, \tag{3.39}$$

with

$$\begin{aligned}
\alpha(k,s) &\triangleq \left(\frac{N}{2} - k\right)^2 - \left(\frac{N}{2} - \frac{C}{r}\right)^2, \\
\beta(k,s) &\triangleq -2(1-\rho)\left(\frac{N}{2} - k\right)^2 + N\left(\frac{N}{2} - \frac{C}{r}\right)(1+\rho) + 2s\left(\frac{N}{2} - \frac{C}{r}\right), \\
\delta(k,s) &\triangleq -(1+\rho)^2\left[\left(\frac{N}{2}\right)^2 - \left(\frac{N}{2} - k\right)^2\right] - N(1+\rho)s - s^2.
\end{aligned} \tag{3.40}$$

Equations (3.40), for the coefficients of the quadratic, are the same as the ones in [RenKo95]; only the sign of $\beta(k,s)$, the coefficient of the linear term in (3.39) is opposite. This in turn results in a set of eigenvalues for our problem of the same magnitude, as in [RenKo95], but of opposite sign. This is in accordance with the fact that Ren and Kobayashi treat the forward equations for the same problem as ours, while we treat the backward equations. Moreover, setting $s = 0$, the set of quadratics (3.39), becomes similar to the relevant set of quadratics in [AniMS82], with only the coefficient of the linear term, $\beta(k,0)$ in our case, to have opposite sign. This is once more due to the particular kind of our equations in contrast to [AniMS82].

For every k, each quadratic in the above set (3.39) has two solutions; however,

looking at the coefficients of them (equation (3.40)), we see that they are symmetric with respect to k, around $\frac{N}{2}$, i.e. setting k and $N-k$ in the equations (3.39) results to the same coefficients. Moreover, we find that the determinant of the above quadratics $\beta(k,s)^2 - 4\alpha(k,s)\delta(k,s)$, can be written after some algebraic manipulations as

$$\beta(k,s)^2 - 4\alpha(k,s)\delta(k,s) = \\ 4\left(\frac{N}{2}-k\right)^2\left[\left[s+(N-\frac{C}{r})\rho+\frac{C}{r}\right]^2+4\rho(k-\frac{C}{r})(N-k-\frac{C}{r})\right] \quad (3.41)$$

Hence, the set of the solutions of the above quadratics, and as a consequence the set of all eigenvalues of our system can be written using a single formula for the solutions of the quadratics

$$\zeta(k,s) = (1-\rho) - \frac{\left(\frac{N}{2}-\frac{C}{r}\right)\left[s+\left(N-\frac{C}{r}\right)\rho+\frac{C}{r}\right]+\left(\frac{N}{2}-k\right)\sqrt{\Delta(k,s)}}{\left(\frac{N}{2}-k\right)^2-\left(\frac{N}{2}-\frac{C}{r}\right)^2}, \quad (3.42)$$

with

$$\Delta(k,s) = \left[s+(N-\frac{C}{r})\rho+\frac{C}{r}\right]^2+4\rho(k-\frac{C}{r})(N-k-\frac{C}{r}). \quad (3.43)$$

Setting $s = 0$, in the above formula (3.42) we get the negative of the roots in [AniMS82].

Further properties of the eigenvalues, that we will use later, are stated in the following theorem, which stands as an adaptation of the theorem in [RenKo95] to our case. One main difference in our case, as stated above is that our eigenvalues

are of the opposite sign. The other difference comes from the fact that Ren and Kobayashi considered a stable system; in contrast, we allow input arrival rates to our multiplexer, that are greater than its capacity, i.e. $\frac{N\rho r}{1+\rho} > C$.

Theorem 1. *I. There are exactly $N+1$ distinct eigenvalues.*

II. From these

a. $N-c-1$ are positive, i.e. $Re\{\zeta_i(s)\} > 0$ for all $Re\{s\} > 0$

b. $c+1$ are negative, i.e. $Re\{\zeta_i(s)\} < 0$ for all $Re\{s\} > 0$

c. There is one eigenvalue that corresponds to $\zeta(0,s)$ that is strictly positive i.e. $Re\{\zeta_i(s)\} > 0$ for all $Re\{s\} > 0$

The proof of the above theorem is given in appendix A.

3.3 Probability Distribution for the Time to Underload

In parallel with the system introduced in in section 3.1 (figure 3.1), we could consider a dual complementary system, where traffic is generated during the idle source periods, while during active periods sources are silent. We also could assume, that this set of sources feeds a multiplexer with output channel capacity of $\tilde{C} = Nr - C$ (figure 3.3). When A_t sources in the original system are active, $I_t = N - A_t$ are idle and consequently supply the fictitious multiplexer of the dual system with work. When $I_t r > \tilde{C}$, or in terms of the variables of the primal system, when $A_t r < C$, the dual multiplexer can not handle the work that is offered to it, and overflows any excess work into a buffer of capacity B. We denote by $\tilde{X}_t$ the content of this buffer.

We see that when the dual system is overloaded, and consequently the content of its buffer increases, our original system is underloaded and its buffer content X_t

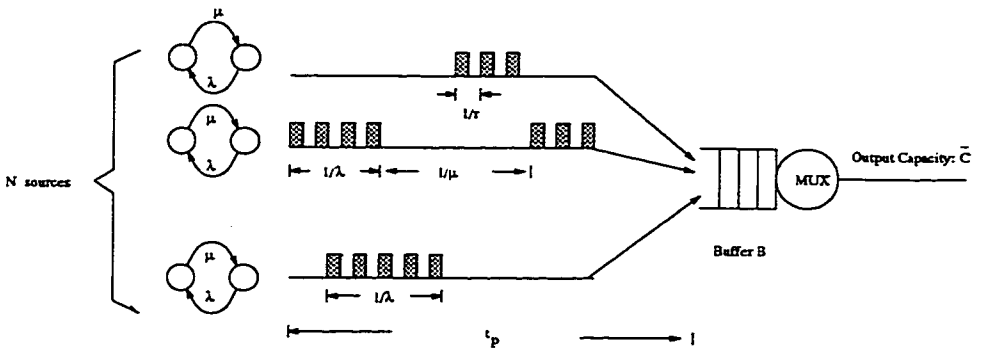

Figure 3.3: The dual system that serves for the calculation of the probability to underload for the primary system.

decreases, with the sum $X_t + \tilde{X}_t$ remaining constant. We assume that an empty buffer for the primal system, corresponds to a full buffer for the dual. Thus, $\tilde{X}_t = B - X_t$.

The underload condition for the multiplexer in the original system is given in (3.9). This condition expressed in the variables of the dual, corresponds to

$$I_t \in \{N, N-1, \ldots, N-c\}, \quad \tilde{X}_t = B, \tag{3.44}$$

Normalizing the output channel capacity $\tilde{C}$ of the dual multiplexer by the On source rate r, $c' \triangleq \lfloor \frac{C'}{r} \rfloor$ and relating it with c, the corresponding quantity of the primal system, we have $c' = N - c - 1$. Thus, condition (3.44) can be restated as

$$I_t \in \{N, N-1, \ldots, c'+1\}, \quad \tilde{X}_t = B, \tag{3.45}$$

This condition has exactly the same form as the overload condition in (3.8), and can

be considered as an overload condition for the dual system.

Considering the state of the dual system as $\tilde{S}_t = (I_t, \tilde{X}_t)$, the transition probabilities in an incremental time interval Δt have the same form as equations (3.5), (3.6) and (3.7) with the role of λ and μ interexchanged. Starting from an initial number of $I_0 = i_0$ idle sources and $\tilde{X}_t = x_0'$, the number of idle sources can increase by one if one active source from the $N - i_0$ becomes idle, an event with probability

$$p_{i_0,i_0+1}(\tilde{x}_0, x_0' - (C' - i_0 r)\Delta t; \Delta t)\Delta x \;=\; (N - i_0)\mu\Delta t + o(\Delta t). \qquad (3.46)$$

Similarly, an idle source can become active in Δt; then,

$$p_{i_0,i_0-1}(x_0', x_0' - (C' - i_0 r)\Delta t; \Delta t)\Delta x \;=\; i_0\lambda\Delta t + o(\Delta t); \qquad (3.47)$$

finally there can be no change in the number of idle sources, and the probability of this event is

$$p_{i_0,i_0}(x_0', x_0' - (C' - i_0 r)\Delta t; \Delta t)\Delta x \;=\; 1 - (N - i_0)\mu\Delta t - i_0\lambda\Delta t + o(\Delta t) \qquad (3.48)$$

In all cases, the available buffer space changes with rate $(C' - i_0 r) = -(C - a_0 r)$ the net buffer outflow rate.

From the above we see that the underload problem for our multiplexer is reduced to an overload problem for a dual system. That comprises of the same number of sources, and its multiplexer has the same buffer size B as the original system. The only differences between the two systems come from the fact that sources have their

dynamics in terms of idle and active periods interexchanged and that the multiplexer of the dual operates on a reduced capacity output channel. Thus, with suitable changes in notation, our solution to the problem of first passage to overload presented in section 3.2 serves as a solution to the first passage to underload problem.

3.4 Moments of the Time to Overload

Equation (3.34) gives Laplace transform of the probability distribution of the first passage time to overload. We leave for future work the overcoming of the numerical problems that we have encountered inverting the Laplace transform. In this section we use this result to find the moments of the time to overload. These moments allow us to derive safe operating regions analogous to those obtained in the previous chapter for systems handling real time traffic.

3.4.1 Dynamic Equations for the Moments of the Time to Overload

We start by defining the n^{th} moment of the time to overload. Since we normalized time by the mean on time $\frac{1}{\mu}$ of a source, we prefer to give the definition in the normalized time units; accordingly, we define the normalized n^{th} moment of the time to overload as,

$$m^{+}_{n,a_0}(\xi_0) \triangleq \mu^n E[T^n_{over} \mid A_0 = a_0, \xi_0 < X_0 \leq \xi_0 + \Delta\xi_0] \qquad n = 1, 2, \ldots . \quad (3.49)$$

Moreover, we define the column vectors, $\mathbf{M}^{+}_{n}(\xi_0)$, with elements the n^{th} moments for

the time to overload from each initial source state a_0,

$$\mathbf{M}_n^+(\xi_0) \triangleq \left(m_{n,0}^+(\xi_0), m_{n,1}^+(\xi_0), \ldots, m_{n,N}^+(\xi_0)\right)^T \qquad n = 1, 2, \ldots.$$

Then, we return to equation (3.31), the dynamic equation for the Laplace transform of the probability distribution for the time to overload, $\mathbf{\Gamma}^+(\xi_0, s)$. We further introduce the probability density for the time to overload $\mathbf{g}^+(\xi_0, \tau)$, and its Laplace transform $\gamma^+(\xi_0, s)$. Accordingly we have,

$$\gamma^+(\xi_0, s) = s\mathbf{\Gamma}^+(\xi_0, s) - \mathbf{G}^+(\xi_0, 0^-) \tag{3.50}$$

We expand each element of the vector $\gamma^+(\xi_0, s)$, $\gamma_{a_0}^+(\xi_0, s)$, in a Taylor series around $s = 0$,

$$\gamma_{a_0}^+(\xi_0, s) = 1 + \frac{d\gamma_{a_0}^+(\xi_0, 0)}{ds}s + \frac{d^2\gamma_{a_0}^+(\xi_0, 0)}{2!ds^2}s^2 + \ldots + \frac{d^n\gamma_{a_0}^+(\xi_0, 0)}{n!ds^n}s^n + \ldots. \tag{3.51}$$

Substituting in (3.51) the expression that gives the moments of a random variable around zero, from the Laplace transform of its probability density, $m_{n,a_0}^+(\xi_0) = (-1)^n \frac{d^n\gamma_{a_0}^+(\xi_0,s)}{ds^n}|_{s=0}$, we write,

$$\gamma_{a_0}^+(\xi_0, s) = 1 - m_{1_{a_0}}^+(\xi_0)s + \frac{m_{2_{a_0}}^+(\xi_0)}{2!}s^2 + \ldots + (-1)^n\frac{m_{n_{a_0}}^+(\xi_0)}{n!}s^n + \ldots. \tag{3.52}$$

We use the relation (3.50) and (3.52) (with $\mathbf{G}^+(\xi_0, 0^-) = 0$) to arrive at series expres-

sion for the probability distribution for the time to overload,

$$\Gamma^{+}_{a_0}(\xi_0, s) = \frac{1}{s} - m^{+}_{1_{a_0}}(\xi_0) + \frac{m^{+}_{2_{a_0}}(\xi_0)}{2!}s + \ldots + (-1)^n \frac{m^{+}_{n_{a_0}}(\xi_0)}{n!}s^{n-1} + \ldots . \tag{3.53}$$

Finally, substituting (3.53) in (3.34) and equating like terms we get the following dynamic equations for the moments,

$$\mathcal{C}\frac{d\mathbf{M}^{+}_1(\xi_0)}{d\xi_0} = \mathcal{Q}\mathbf{M}^{+}_1(\xi_0) + \mathbf{1} \tag{3.54}$$

$$\mathcal{C}\frac{d\mathbf{M}^{+}_n(\xi_0)}{d\xi_0} = \mathcal{Q}\mathbf{M}^{+}_n(\xi_0) + n!\mathbf{M}^{+}_{n-1}(\xi_0) \qquad n = 2, 3, \ldots . \tag{3.55}$$

$\mathbf{1}$ a $N+1$ column vector with all elements equal to one, $\mathbf{1} = (1, 1, \ldots, 1)^T$. By introducing the convention $\mathbf{M}^{+}_0(\xi_0) = \mathbf{1}$, we can consolidate equations (3.54) and (3.55) to

$$\mathcal{C}\frac{d\mathbf{M}^{+}_1(\xi_0)}{d\xi_0} = \mathcal{Q}\mathbf{M}^{+}_1(\xi_0) + n!\mathbf{M}^{+}_{n-1}(\xi_0) \qquad n = 1, 2, 3, \ldots . \tag{3.56}$$

Equation (3.56) constitute a set of first order linear differential equations. They have to be augmented by boundary conditions. From equation (3.26) the probability distribution for the time to overload, starting from an "up" source state and a full buffer is always one. Therefore, all moments for the time to overload are zero for

these starting states must be zero,

$$m^{+}_{n,a_0}(B') = 0 \quad n = 1, 2, \ldots \quad a_0 = c+1, \ldots, N \tag{3.57}$$

3.4.2 Solution of the Equations for the Moments

At this point we have a set of first order linear differential equations for the moments of the time to overload of all order, together with their boundary conditions. Equation (3.56), conditioned on the previous knowledge of $\mathbf{M}^{+}_{n-1}(\xi_0)$, is an inhomogeneous system of linear first order differential equations. Therefore, its general solution consists of the sum of the general solution $\mathbf{M}^{+}_{n_{gh}}(\xi_0)$ of the homogeneous system,

$$\mathcal{C}\frac{d\mathbf{M}_n{}^{+}(\xi_0)}{d\xi_0} = \mathcal{Q}\mathbf{M}_n{}^{+}(\xi_0) \qquad n = 1, 2, 3, \ldots, \tag{3.58}$$

and of a particular solution $\mathbf{M}^{+}_{n_{pi}}(\xi_0)$ of the inhomogeneous system (3.56) [TeneP63].

The general solution for the homogeneous equation (3.58) is expressed in terms of the eigenvalues z_i and the right eigenvectors $\bar{\phi}_i$ of matrix $\mathcal{C}^{-1}\mathcal{Q}$ as

$$\mathbf{M}^{+}_{n_{gh}}(\xi_0) = \sum_{i=0}^{N} u_{ni} e^{z_i(\xi_0 - B')} \bar{\phi}_i. \tag{3.59}$$

where u_{ni} are constants that are determined from the conditions at $\xi_0 = B'$. z_i and $\bar{\phi}_i$ are derived in appendix A.

Furthermore, using the method of variation of parameters [TeneP63], and the expression of the solution (3.59) for the homogeneous set of equations we get a particular

solution for (3.56) (appendix C):

$$\mathbf{M}^{+}_{n_{p_i}}(\xi_0) = n! \sum_{i=0}^{N} \left[\left(\int \frac{\bar{\psi}_i^T \mathbf{M}^{+}_{n-1}(\xi_0)}{\bar{\psi}_i^T C \bar{\phi}_i} e^{-z_i \xi_0} d\xi_0 \right) e^{z_i \xi_0} \right] \bar{\phi}_i. \tag{3.60}$$

To simplify notation, we denote the term in brackets of the above expression (3.60) by $d_{n,i}(\xi_0)$,

$$d_{n,i}(\xi_0) \triangleq \left(\int \frac{\bar{\psi}_i^T \mathbf{M}^{+}_{n-1}(\xi_0)}{\bar{\psi}_i^T C \bar{\phi}_i} e^{-z_i \xi_0} d\xi_0 \right) e^{z_i \xi_0}. \tag{3.61}$$

Then, combining (3.59) and (3.60) the general solution for $\mathbf{M}^{+}_{\mathbf{n}}(\xi_0)$ is

$$\mathbf{M}^{+}_{n}(\xi_0) = \sum_{i=0}^{N} u_{ni} e^{z_i(\xi_0 - B')} \bar{\phi}_i + n! \sum_{i=0}^{N} d_{n,i}(\xi_0) \bar{\phi}_i. \tag{3.62}$$

Constants u_{ni} will be determined from the conditions at the upper buffer level, $\mathbf{M}^{+}_{\mathbf{n}}(B')$. Setting $\xi_0 = B'$ in the general solution (3.62), and multiplying both its sides on the left, first by matrix C and subsequently by the i^{th} left eigenvector $\bar{\psi}_i^T$ we get

$$u_{ni} = \frac{\bar{\psi}_i^T C \mathbf{M}^{+}_{n}(B')}{\bar{\psi}_i^T C \bar{\phi}_i} - n! d_{n,i}(B'). \tag{3.63}$$

Determination of u_{ni} depends on the complete knowledge of the vector $\mathbf{M}^{+}_{n}(B')$, the n^{th} moment of the time to overload starting from a full buffer for all initial source states. The boundary conditions (3.57), corresponding to the moments of the time to overload starting from an "up" source state, determine the $N - c$ elements of this vector. The remaining $c + 1$ elements are determined by considerations of the

boundness of the solution.

Clearly, in order for (3.62) to remain bounded, terms in the summation involving negative eigenvalues should be excluded. Therefore we require the coefficients of all such terms in the expression of the solution (3.62) to vanish, i.e.

$$u_{ni} = 0 \quad \text{for} \quad z_i < 0. \tag{3.64}$$

Moreover, we know from appendix A, that exactly $c+1$ eigenvalues are negative. Thus, the above condition (3.64) results in $c+1$ linear conditions in the $c+1$ unknown elements of $\mathbf{M}_n^+(B')$,

$$\bar{\psi}_i^T C \mathbf{M}_n^+(B') = \left(\bar{\psi}_i^T C \bar{\phi}_i\right) n! d_{n,i}(B') \qquad \forall i : z_i < 0, \tag{3.65}$$

and can be solved numerically. Labeling the eigenvalues z_i in a way that indices, $0, 1, \ldots, c$ correspond to negative eigenvalues, and indices $c+1, \ldots, N-1$ the positive ones, and $z_N = 0$, we can express (3.62) as

$$\mathbf{M}_n^+(\xi_0) = \sum_{i=c+1}^{N} u_{ni} e^{z_i(\xi_0 - B')} \bar{\phi}_i + n! \sum_{i=0}^{N} d_{n,i}(\xi_0) \bar{\phi}_i. \tag{3.66}$$

We continue by treating particular cases of (3.66), that correspond to different moments. We start by the mean time to overload.

3.4.3 The Mean Time to Overload

In the case of the mean time to overload, $n = 1$ in our previous notation, expression

(3.66) that gives the mean time to overload simplifies further. First, the particular solution of the inhomogeneous equation consists of constant terms and a single term that depends linearly on ξ_0. More specifically, $d_{1,i}(\xi_0)$ is written as

$$\begin{aligned} d_{1,i}(\xi_0) &= \left(\int \frac{\bar{\psi}_i^T \mathbf{1}}{\bar{\psi}_i^T C \bar{\phi}_i} e^{-z_i \xi_0} d\xi_0 \right) e^{z_i \xi_0} \\ &= \begin{cases} -\frac{k_i}{z_i} & i = 0, 1, 2, \ldots, N-1 \\ k_N \xi_0 & i = N \end{cases} \end{aligned} \tag{3.67}$$

where $k_i = \frac{\bar{\psi}_i^T \mathbf{1}}{\bar{\psi}_i^T C \bar{\phi}_i}, i = 0, 1, 2, \ldots, N$, and according to our convention concerning the ordering of the eigenvalues z_i, $z_N = 0$. Using (3.67), the mean time to overload ($n = 1$ in equation (3.66)) becomes:

$$\mathbf{M}_1^+(\xi_0) = \sum_{i=c+1}^{N-1} u_{1i} e^{z_i(\xi_0 - B')} \bar{\phi}_i - \sum_{i=0}^{N-1} \frac{k_i}{z_i} \bar{\phi}_i + (u_{1N} + k_N \xi_0) \bar{\phi}_N. \tag{3.68}$$

For large buffers, and with a buffer starting level, ξ_0, much lower than the buffer full capacity, i.e. for large $B' - \xi_0$ differences, the exponentials in (3.68) vanish, and thus the mean time to overload becomes

$$\mathbf{M}_1^+(-\infty) = u_{1N} \bar{\phi}_N - \sum_{i=0}^{N-1} \frac{k_i}{z_i} \bar{\phi}_i + k_N \xi_0 \bar{\phi}_N \tag{3.69}$$

Furthermore, from equation (3.63), we can express u_{1N} as $u_{1N} = c_{1N} - k_N B'$, where

we have put c_{1N} for $\frac{\bar{\psi}_N^T C \mathbf{M}_1^+(B')}{\bar{\psi}_N^T C \bar{\phi}_N}$. Accordingly,

$$\mathbf{M}_1^+(-\infty) = c_{1N}\bar{\phi}_N - \sum_{i=0}^{N-1} \frac{k_i}{z_i}\bar{\phi}_i + k_N(\xi_0 - B')\bar{\phi}_N \tag{3.70}$$

Thus, the mean time to overload for large buffers depends linearly on the initially available free buffer space $\xi_0 - B'$.

3.4.4 The Mean Square of the Time to Overload

Equation (3.66) for the mean square of the time to overload is

$$\mathbf{M}_2^+(\xi_0) = \sum_{i=c+1}^{N} u_{2i} e^{z_i(\xi_0 - B')}\bar{\phi}_i + n! \sum_{i=0}^{N} d_{2,i}(\xi_0)\bar{\phi}_i. \tag{3.71}$$

In contrast to the case of the mean, expression $d_{2,i}(\xi_0)$, $i = 0, 1, 2, \ldots, N$, that determines the particular solution of the relevant differential equation for the mean square, does not have a simple expression. From equation (3.61) $d_{2,i}(\xi_0)$ depends on the mean $\mathbf{M}_1^+(\xi_0)$,

$$d_{2,i}(\xi_0) = \left(\int \frac{\bar{\psi}_i^T \mathbf{M}_1^+(\xi_0)}{\bar{\psi}_i^T C \bar{\phi}_i} e^{-z_i \xi_0} d\xi_0 \right) e^{z_i \xi_0}. \tag{3.72}$$

In turn looking at the expression for the mean time to overload from equation (3.69), we see that it has a complex dependence on ξ_0. In particular $M_1(\xi_0)$ involves exponentials in ξ_0, constant terms as well as linear in ξ_0 terms; thus, we expect that the particular solution of the equation for the mean square, which is determined by $d_{2,i}(\xi_0)$, will involve similar terms, plus additional terms with quadratic dependence

on ξ_0. More specifically, substituting for the mean $\mathbf{M}_1^+(\xi_0)$ in (3.72), performing the necessary integrations, and using the values of the projections of the left eigenvectors to the right ones, $\kappa_{ij} \triangleq \frac{\bar{\psi}_i^T \bar{\phi}_i}{\bar{\psi}_i^T C \bar{\phi}_i}$, $i, j = 0, 1, 2, \ldots, N$,

we have (a) for $i \neq N$:

$$\begin{aligned} d_{2,i}(\xi_0) &= \sum_{\substack{j=c+1 \\ j\neq i}}^{N-1} \frac{u_{1j}\kappa_{ij}}{z_j - z_i} e^{z_j(\xi_0 - B')} + u_{1i}\kappa_{ii}\xi_0 e^{z_i(\xi_0 - B')} \\ &\quad + \frac{1}{z_i}\left[\sum_{j=0}^{N-1} \kappa_{ij}\frac{k_j}{z_j} - u_{1N}\kappa_{iN}\right] - \frac{1}{z_i} k_N \kappa_{iN}\left(\xi_0 + \frac{1}{z_i}\right) \end{aligned} \tag{3.73}$$

and (b) for $i = N$,

$$\begin{aligned} &d_{2,N}(\xi_0) = \\ &\sum_{j=c+1}^{N-1} \frac{u_{1j}\kappa_{Nj}}{z_j} e^{z_j(\xi_0 - B')} + \left[\kappa_{NN}u_{1N} - \sum_{j=0}^{N-1} \kappa_{Nj}\frac{k_j}{z_j}\right]\xi_0 + k_N\kappa_{NN}\frac{\xi_0^2}{2} \end{aligned} \tag{3.74}$$

3.4.5 Numerical Results

We conclude this section by giving an example illustrating the application of the above results in calculating the mean and the mean square of the time to overload for a buffered statistical multiplexer. Towards this end, we consider $N = 23$ On-Off sources multiplexed on an OC-3 channel of $C = 51.84$ Mbits/s through a statistical multiplexer, having a buffer of $B = 100$ Kbytes at its input. The peak rate of each source when active is considered to be $r = 10$ Mbits/s, and their peak to the mean ratio is 3. Figure 3.4 depicts the mean time for the buffer to overflow, with the initial number of active sources a_0, treated as a parameter. Similarly, figure 3.5 gives the

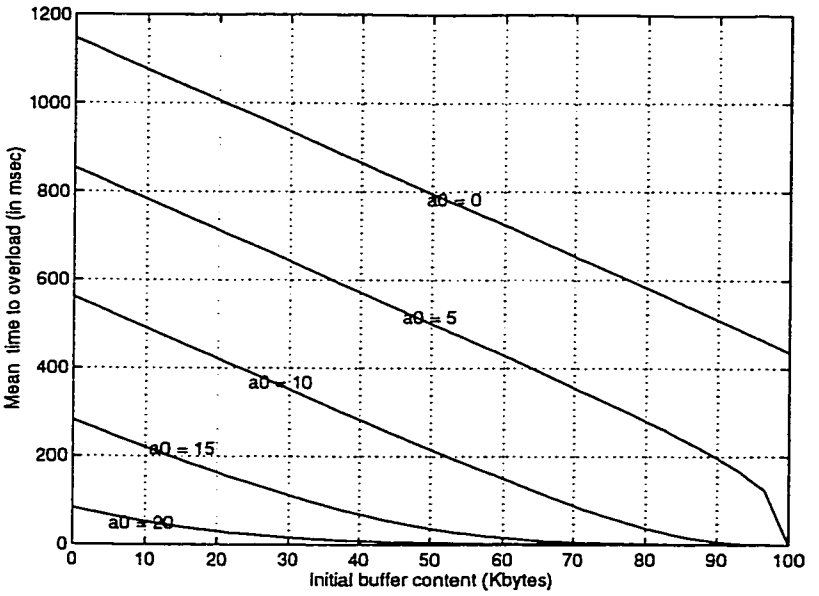

Figure 3.4: Mean time to overload for a multiplexer with a buffer $B = 100$ Kbytes, loaded with $N = 23$ data source (output channel capacity $C = 51.84$ Mbits/s). Peak source rate when On: 10 Mbits/s, peak to mean ratio: 5.

mean square for the same example.

In figure 3.6 we plot the square coefficient of variation $\frac{(\sigma^+_{1,a_0}(x_0))^2}{(m^+_{1,a_0}(x_0))^2}$ for the time to overload for the above multiplexing example. The coefficient is greater than one, except when the initial number of active sources is very small (comparable to the normalized channel capacity c). Hence, an exponential probability distribution fails to be a valid model for the conditional probability for the time to overload $G^+_{a_0}(x_0, t)$, except when a_0 is comparable to c.

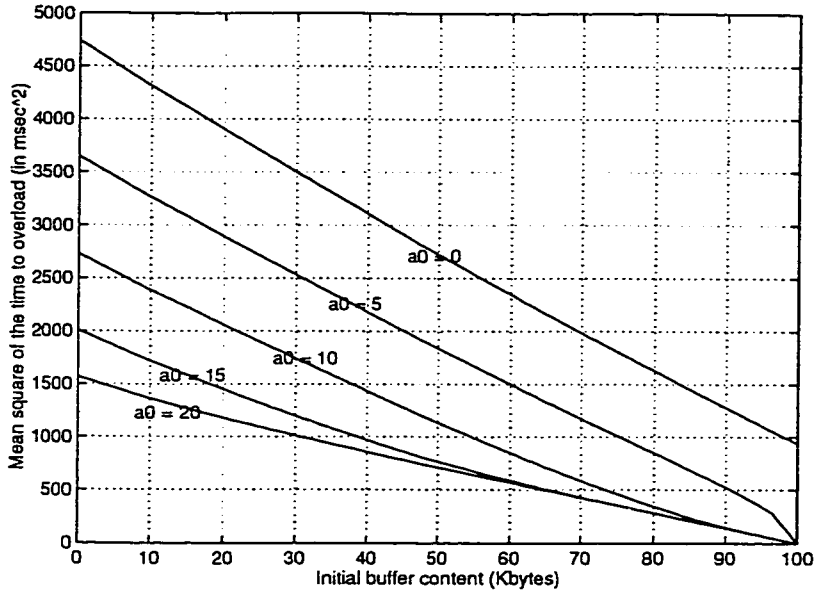

Figure 3.5: Mean square of the time to overload for a multiplexer with a buffer $B = 100$ Kbytes, loaded with $N = 23$ data source (output channel capacity $C = 51.84$ Mbits/s). Peak source rate when On: 10 Mbits/s, peak to mean ratio: 5.

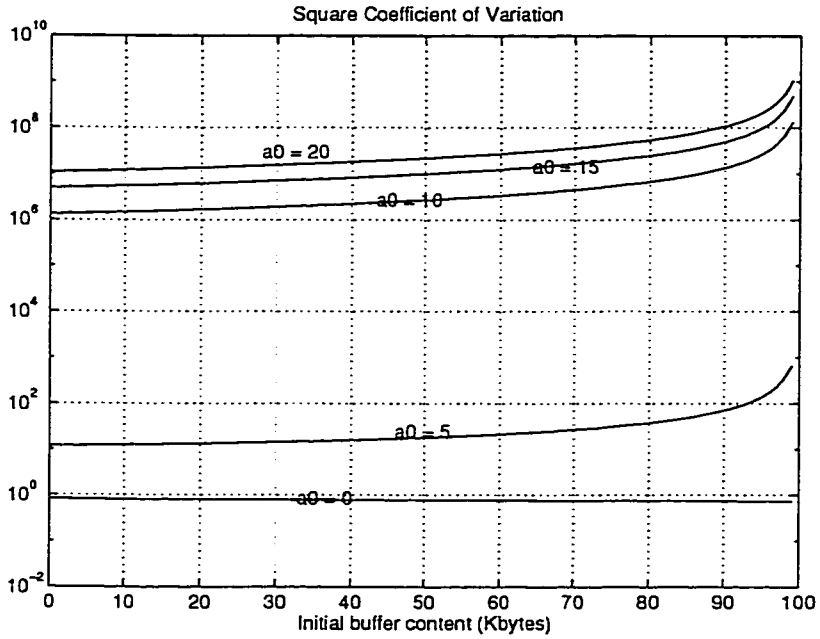

Figure 3.6: The square coefficient of variation of the time to overload for a statistical multiplexer, for various initial buffer contents, x_0, and for an initial source $a_0 = 0$: buffer, $B = 100$ Kbytes; number of sources, $N = 23$; output channel capacity, $C = 51.84$ Mbits/s; peak source rate when On, $r = 10$ Mbits/s; peak to mean ratio: 5.

CHAPTER 4
NETWORK STATE ESTIMATION USING KALMAN FILTERING

In this chapter we estimate the activity level of a set of connections multiplexed on a Virtual Path through a statistical multiplexer. We assume that connections carry real-time traffic, and are of the On-Off type; therefore, their activity level is determined by the total number of connections that are active at a given point in time. Estimation is based on data, selected from monitoring the cell activity on the VP at consecutive time intervals of fixed duration, and it is predicated on the fact that traffic encountered in ATM networks has memory, that is captured by Markov chain models.

The problem is treated as the tracking of the state of a Markov chain through noisy cell count observations. The Markov chain characterizes the number of active traffic sources at every point in time. During active periods sources transmit cells on the VP. Thus, cell count observations are related to the number of sources that are active. However this relationship is not one to one; we model the ambiguity, in determining the state of the Markov chain through cell counts, as noise introduced by the measurement process. We estimate the state of the Markov chain, describing the number of active sources on the link, using linear estimation algorithms. We

limit ourselves to linear algorithms, for their implementation simplicity, and real time operation when brought to a recursive form (Kalman filtering).

This chapter is organized as follows; the next section treats the estimation of the network state in the case of a single source type being multiplexed on the VP (homogeneous case). This is performed by assuming two models for the cell traffic on the VP; the first assumes a uniform spacing of the cells during active source periods (binary On-Off model), while the second assumes a probabilistic model of cell arrivals within a traffic burst (IPP model). Section 4.1.1 presents the network model and the cell count observation model in the case of On-Off source modeling. Similarly section 4.1.2 develops the same models under IPP source modeling. In both cases we assume general non Additive White Gaussian Noise (AWGN) models for the cell count observation process and a Markov chain model for the network state; however, restricting ourselves to linear network state estimation algorithms, we may replace the observation model with an AWGN model, and the network state process by a Gauss-Markov process (first order discrete autoregressive process). This model replacement is also described in section 4.1.1 for the On-Off source model and in section 4.1.2 for the IPP model. After the above modification, the estimation problem is in a form that Kalman filtering can be applied in a natural fashion. Section 4.1.3 describes the Kalman recursive algorithm, and presents results from the application of the algorithm in voice and video multiplexing examples. In section 4.2, network state estimation is extended to the case when more than one source classes are multiplexed on the same VP. The introduction of more than one type of sources into our model gives to the estimation problem a new dimension, since not only the number of active

sources is unknown, but their type as well. In the heterogeneous case, we follow steps that parallel our treatment of the homogeneous case; in section 4.2.1 we present the network state process and cell count observation models. We further replace these models with a Gauss-Markov network state evolution model, and an AWGN cell count observation model. Finally, in 4.2.2 we present and evaluate the performance of the Kalman filter in a mixed video-image transfer example.

Kalman filtering for the tracking of the state of an MMPP was performed by Snyder [Snyde75]. Such a technique finds application in the field of optical receivers, employing direct detection for decoding the information bits transmitted over an optical channel from photon count information over a bit period [GitHW92]. Our approach, [TsiHK94], was inspired by the work of Snyder. Recently, a Kalman filter, for a similar problem as ours, has been developed in [KolAH94] in a different manner.

4.1 Single Source Type

4.1.1 State Estimation Using the On-Off Source Model

System Description

We assume as in chapter 2 a link where N sources of the binary On-Off type (figure 4.1) are multiplexed. Sources are of the delay sensitive type, and therefore, multiplexing is performed at the input of the link on a statistical basis with very limited buffering (only to schedule simultaneous arrivals) to minimize queueing delay.

Further, we let time being slotted into consequentive intervals of length w. The

probability that a binary On-Off source becomes active during the time interval w, given that it was idle before, is

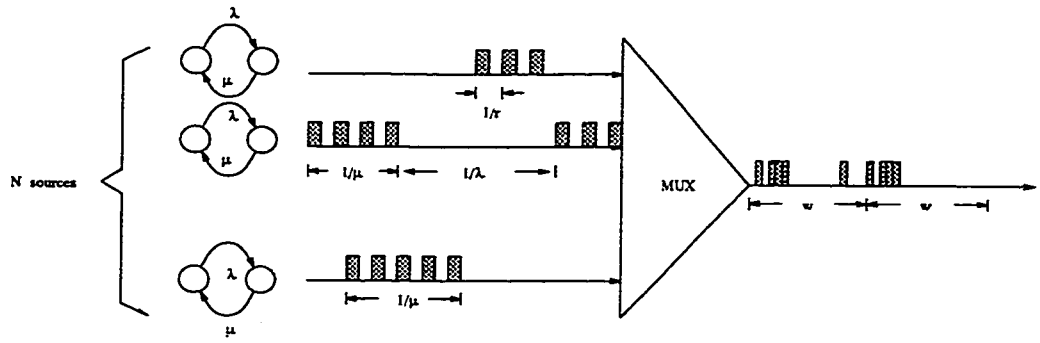

Figure 4.1: The ATM multiplexer at the VP level, loaded with a single type of sources.

$$p = 1 - e^{-\lambda w} \approx \lambda w; \tag{4.1}$$

similarly, the probability that it will become idle, given it was active previously, is given as

$$q = 1 - e^{-\mu w} \approx \mu w. \tag{4.2}$$

The above approximations are valid for $\lambda w \ll 1$

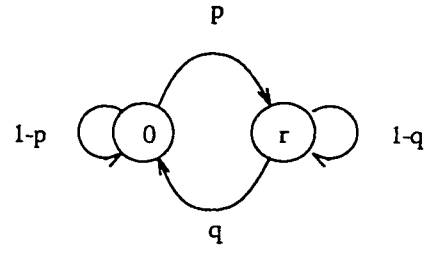

Figure 4.2: The discrete time binary On-Off model

and $\mu w \ll 1$, or in other words when w is much smaller than the mean burst, or mean silence periods of a source. Accordingly, our binary On-Off model is given in

discrete time as in figure 4.2.

We let A_i, the number of sources that are active during the i^{th} time interval, describe the state of our system. A_i is a Markov chain with one step transition probabilities

$$\begin{aligned} p_{lm} &= \Pr(A_{i+1} = m \mid A_i = l) \\ &= \sum_{k=\max\{l-m,0\}}^{\min\{l,N-m\}} \binom{l}{k} q^k (1-q)^{l-k} \binom{N-l}{m-l+k} p^{m-l+k} (1-p)^{N-m-k} \end{aligned} \tag{4.3}$$

From our considerations above for the magnitude of the products λw and μw, and equations (4.1) and (4.2), we have that $p \ll 1$ and $q \ll 1$. Expanding the terms that involve powers of $(1-p)$ and $(1-q)$ in Taylor series around 1 in (4.3), and keeping only terms up to first order in p and q, we have

$$p_{i,i+1} = (N-i)p \tag{4.4}$$

$$p_{i,i-1} = iq \tag{4.5}$$

$$p_{i,i} = 1 - iq - (N-i)p, \tag{4.6}$$

with transitions to other states having probabilities vanishing as p and $q \to 0$. Therefore, A_i becomes a birth-death process.

We monitor the cell activity on the link by counting the number of cells at the link during the time intervals w. We let Y_i be the cell count in the i^{th} observation interval. Y_i will depend on A_i, the number of sources that were active during the

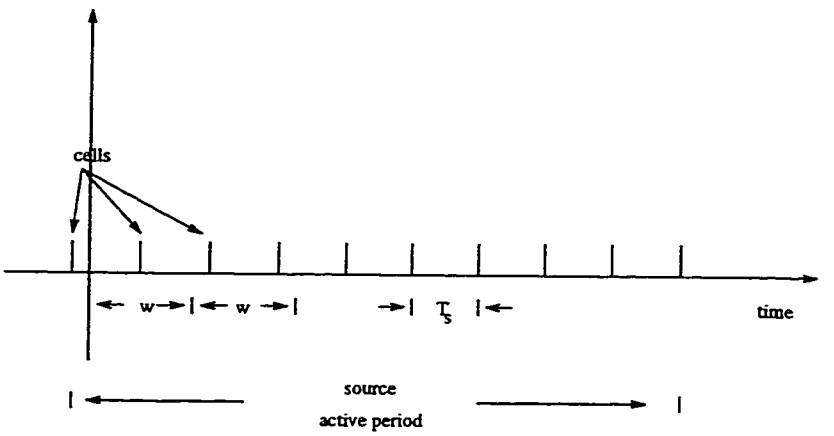

Figure 4.3: Time diagram of cell transmissions on a VP from a single active source.

i^{th} observation interval. Moreover, it will depend on the length w of the observation interval with respect to the source cell generation period $\frac{1}{r}$. Neglecting the effect of the small amount of queueing at the multiplexer, we will consider that the periodic generation of cells during source activity periods is not affected by the statistical multiplexing at the VP input.

In order to characterize quantitatively the relation between Y_i, the number of observed cells in a window w, and the system state A_i we start by considering a single active source transmitting cells on the link (figure 4.3). Denoting by $\lfloor y \rfloor$, $y \in R$, the integer that is not greater than y, the number of cells observed in a slot interval is at least $\lfloor \frac{w}{T_s} \rfloor$, the number of times that a source period $T_s = \frac{1}{r}$ fits into the observation interval w. Additionally, one more cell might be observed depending on the relative phase of the cell generation process to the observation window. Figure 4.3 depicts the time diagram of cell transmissions on the VP from an active source for a particular example; in the first time slot only one cell is observed while in the second we count two.

There is a certain dependence between observations in consequentive time inter-

vals. For instance, in the example depicted in figure 4.3, the number of observations in consecutive windows alternates between one and two, and thus given the number of measurements in one interval, the number of observations during the next interval is determined uniquely. In the sequel, we choose to ignore the interdependence of measurements in consecutive time slots and assume that in every slot we observe either $\lfloor \frac{w}{T_s} \rfloor = \lfloor wr \rfloor$ or $\lfloor wr \rfloor + 1$ cells independently from the number of cells in previous slots.

In every slot, there are at least $\lfloor wr \rfloor$ cells. The probability of observing an additional cell depends on the remaining time within a slot after the subtraction of the time consumed for the transmission of $\lfloor wr \rfloor$ cells, $w - \lfloor wr \rfloor T_s$. The likelihood of observing an additional cell depends on the relative size of this remaining time within a time slot with respect to the source period. Thus, normalizing the remaining time within a slot by the source period, and setting $\pi \triangleq wr - \lfloor wr \rfloor$, the number of cells observed in a slot follows a Bernoulli distribution with parameter π,

$$\Pr(Y_i = k \mid A_i = 1) = \begin{cases} \pi, & k = \lfloor wr \rfloor + 1 \\ 1 - \pi & k = \lfloor wr \rfloor \end{cases} \tag{4.7}$$

The number of cells that a given active sources generates in a time interval w, is independent and identically distributed with the number of cells generated by any other active source during the same time interval. Therefore, the probability distribution of the number of cell counts Y_i, given that $A_i = a$ sources are active, is the a-fold convolution of the Bernoulli distributed random variable in (4.7). However,

the a-fold convolution of a Bernoulli distributed random variable has a binomial distribution; hence,

$$\Pr(Y_i = a\lfloor wr \rfloor + k \mid A_i = a) = \begin{pmatrix} a \\ k \end{pmatrix} \pi^k (1-\pi)^{a-k}. \tag{4.8}$$

Equation (4.8) suggests that the number of cells counted in a observation interval w can be expressed as

$$Y_i = A_i \lfloor wr \rfloor + Z_i, \tag{4.9}$$

with Z_i is a binomially distributed random variable, with its distribution dependent on the value of the random value A_i

$$\Pr(Z_i = k \mid A_i = a) = \begin{pmatrix} a \\ k \end{pmatrix} \pi^k (1-\pi)^{a-k}. \tag{4.10}$$

Equation (4.9), according to estimation theory, is a probabilistic observation model for the state A_i of our system. In other words, there is not an one to one mapping between the system state A_i and the number of counted cells, Y_i. Accordingly, given the number of cell observations in a given slot, Y_i, the number of active sources A_i can not be determined uniquely. We characterize this ambiguity in determining A_i from the measurements Y_i as measurement "noise".

A_i can be estimated from Y_i; however, the accuracy of this estimation increases if we consider apart from the measurement in slot i, the complete history of observations

up to the current time. Towards this end, let M be the order of the current slot. Then, our problem is to estimate the current system state A_M given a complete history of observations Y_i, $1 \leq i \leq M$. Recalling that the process A_i, that describes our system state, is birth-death (and consequently Markov), the estimation problem relates to the estimation of a Markov process through noisy observations.

Equation (4.9), that gives the probabilistic observation model of A_i, is an additive noise model; however, the additive "noise" part Z_i is, neither normally distributed, nor independent of the estimated process A_i. In such non-additive white Gaussian environment, non linear estimation algorithms are optimum; however, in this chapter, we choose to limit ourselves to linear estimation algorithms to estimate A_i, for their simplicity and real time operation, recognizing the fact that these algorithms are possibly suboptimal for our problem.

The Additive White Gaussian Noise Observation Model

Considering linear estimation algorithms, observation noise is relevant only up to its second order statistics (appendix D). Therefore the non-AWGN observation model of equation (4.9), might be replaced by an AWGN model of the form,

$$Y_i = c_i A_i + V_i, \tag{4.11}$$

with V_i a zero mean normally distributed random sequence, and c_i a real scalar.

More precisely, looking into equation (D.2) in appendix D, we see that the relevant second order statistics of Y_i, that are essential in linear estimation, are the autoco-

variance function of the observation data process, $C_{YY}(i,j)$, and the cross-covariance function, $C_{AY}(i,j)$, of the observation data, Y_i, with the estimated process, A_i. In Appendix E we express these quantities in terms of the autocovariance function of A_i, $C_{AA}(i,j)$ as follows:

$$C_{YY}(i,j) = (wr)^2 C_{AA}(i,j) \qquad i \neq j \tag{4.12}$$

$$\sigma^2_{Y_i} = \sigma^2_{A_i}(wr)^2 + E[A_i](1-\pi)\pi, \tag{4.13}$$

and

$$C_{AY}(i,j) = (wr)C_{AA}(i,j). \tag{4.14}$$

Accordingly, the AWGN in (4.11) has to match expressions (4.12), (4.13) and (4.14). Towards this end, we consider the corresponding expressions derived directly from (4.11):

$$C_{YY}(i,j) = c_i c_j C_{AA}(i,j) \quad i \neq j, \tag{4.15}$$

$$\sigma^2_{Y_i} = c_i^2 \sigma^2_{A_i} + \sigma^2_{V_i}, \tag{4.16}$$

and

$$C_{AY}(i,j) = c_m C_{AA}(i,j), \tag{4.17}$$

Comparing these expressions with equations (4.12), (4.13) and (4.14), we conclude

that an AWGN model of the form

$$\tilde{Y}_i = wr\tilde{A}_i + V_i \qquad \forall i \in \{1, 2, \ldots, M\}. \tag{4.18}$$

can be postulated for the data Y_i, with $\tilde{Y}_i$ and $\tilde{A}_i$ in (4.18) the centered parts of Y_i and A_i respectively,

$$\tilde{Y}_i = Y_i - E[Y_i] \quad \text{and} \quad \tilde{A}_i = A_i - E[A_i]. \tag{4.19}$$

Recalling again from the Appendix B, that the mean number of observations in a slot is related to the mean number of active sources in the same slot by $E[Y_i] = wrE[A_i]$, we can postulate the more general model,

$$Y_i = wrA_i + V_i \qquad \forall i \in \{1, 2, \ldots, M\}. \tag{4.20}$$

The variance of V_i is $\sigma^2_{V_i} = E[A_i](1 - \pi)\pi$.

Linear Dynamic System Model

In linear estimation besides the observation data, only statistics up to the second order of the estimated process are relevant as well. Therefore, we can replace the birth-death law, that describes our system state evolution, by a linear dynamic model, that has the same mean and autocovariance function, without affecting linear estimation.

Towards this end we consider, from appendix E.2.3, assuming stationarity of the

system state A_i, its autocovariance function

$$C_{AA}(m) = \sigma_A^2 \delta^{|m|}, \tag{4.21}$$

where $\delta = 1 - p - q$, and its power spectrum $S_A(z) \triangleq \sum_{-\infty}^{+\infty} R_{AA}(m) z^{-m}$, [Papou84],

$$S_A(z) = \sigma_A^2 \frac{\delta^{-1} - \delta}{\delta^{-1} + \delta - (z^{-1} + z)}. \tag{4.22}$$

Since constant terms in $R_{AA}(m)$ do not contribute to the expression of the power spectrum, (4.22) can be considered as the power spectrum of the centered process $\tilde{A}_i = A_i - E[A_i]$ as well.

Deriving a process A_i' that follows a linear dynamic evolution model driven by white noise W_i, and having a power spectrum of the form (4.22), is tantamount to designing a linear time invariant shaping filter $H(z)$ (figure 4.4). Towards this end we perform factorization of the power spectrum of A_i, $S_A(z)$.

From equation (4.22) we see that $S_A(z)$ has two poles, one at δ and the other at δ^{-1}, and no zeros. Keeping the pole inside the unit circle, the system function for the shaping filter is written as

$$H(z) = \sigma_A \frac{\sqrt{1 - \delta^2}}{z - \delta}. \tag{4.23}$$

Writing the difference equation that corresponds to this transfer function, and keeping

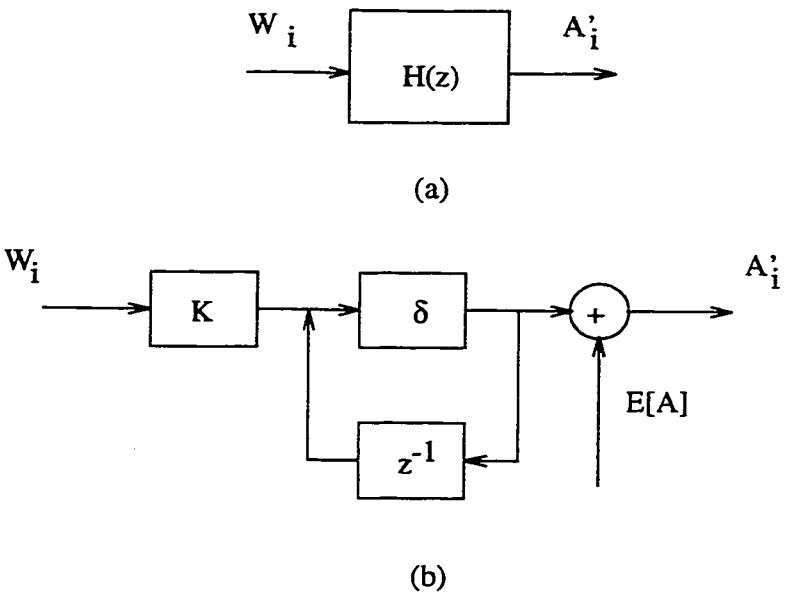

Figure 4.4: The linear time invariant filter for the generation of the approximate state process A'_i; (a) general scheme (b) detailed block diagram ($K = \sigma_A\sqrt{1-\delta^2}$) .

in mind that $S_A(z)$ corresponds only to the centered part of A_i, we have

$$\tilde{A}'_{i+1} = \delta\tilde{A}'_i + (\sigma_A\sqrt{1-\delta^2})W_i, \tag{4.24}$$

where $\tilde{A}'_i$ is the centered part of A'_i. Finally, taking into consideration the non-zero mean of A_i (appendix E.2.1), and matching it with the mean of A'_i we get

$$A'_i = \frac{Np}{p+q} + \tilde{A}'_i. \tag{4.25}$$

4.1.2 State Estimation Using the IPP Source Model

System Description

So far, our discussion was limited to the On-Off source model, according to which,

sources transmit at a constant rate in active state. A similar discussion is valid under IPP modeling of the individual source behavior. According to this model, cells are transmitted with a Poisson rate γ during active source periods. In this case an additive observation model, of the form (4.9), that relates the number of cell observations during an interval w with the state of the network in terms of number of active sources, can only be determined in a probabilistic fashion. Given that $A_i = a$ sources are active during the i^{th} observation interval, Y_i is a Poisson distributed random variable with parameter $aw\gamma$; thus,

$$\Pr(Y_i = k \mid A_i = a) = \frac{(aw\gamma)^k}{k!} e^{-(aw\gamma)}. \tag{4.26}$$

System Modeling

The probabilistic observation model of the system state A_i in equation (4.26) can be replaced by an AWGN model when performing linear estimation of A_i. However, the AWGN model must match the statistics of Y_i up to the second order. To perform the matching, we first consider the second order statistics of Y_i, i.e. its autocovariance function, $C_{YY}(i,j)$, and its cross-covariance function, $C_{AY}(i,j)$, with the network state process A_j, as given by the probabilistic model of equation (4.26). From appendix E.1.2 (equations (E.21) and (E.18)) we get

$$C_{YY}(i,j) = (w\gamma)^2 C_{AA}(i,j) \qquad i \neq j. \tag{4.27}$$

$$\sigma^2_{Y_i} = (w\gamma)^2 \sigma^2_{A_i} + w\gamma E[A_i], \tag{4.28}$$

and from (equation (E.24) in the same Appendix), that,

$$C_{AY}(i,j) = w\gamma C_{AA}(i,j). \tag{4.29}$$

Following similar steps as in the case of On-Off source modeling, the above equations (4.27), (4.28) and (4.29) suggest an AWGN model for the observations data of the form

$$\tilde{Y}_i = w\gamma \tilde{A}_i + V_i \qquad \forall i \in \{1,2,\ldots,M\} \tag{4.30}$$

with $\sigma^2_{V_i} = w\gamma E[A_i]$.

Taking into consideration the first order statistics of the observation data as well, we can write, more generally

$$Y_i = w\gamma A_i + V_i \qquad \forall i \in \{1,2,\ldots,M\}. \tag{4.31}$$

The observation AWGN model in equation (4.31) is similar to the corresponding model of equation (4.20) under On-Off source modeling. The difference is that, under IPP modeling, the cell Poisson arrival rate γ during active source states replaces the uniform cell rate r of the On-Off model in the expression of the observation model. Moreover, the expression of the variance of the additive "noise" in (4.31) is different from its expression in (4.20).

The cell generation process during source active periods is independent of the network state evolution; therefore the linear dynamic model in equation (4.24), derived

for the state evolution in the case of On-Off source modeling, applies intact when cell arrivals during active source periods do not occur at a uniform rate, but follow a Poisson process (IPP model).

4.1.3 Filter Performance

So far we have developed a linear first order autoregressive model for the network state process, and an additive white Gaussian model for the observation data Y_i; we summarize these results by stating them in a form that is typical in the application of the Kalman filtering algorithm. Kalman filtering formulation is given in the case of On-Off source modeling; the formulation under an IPP source modeling parallels the one below, setting γ instead of r.

$$\tilde{A'}_{i+1} = \delta \tilde{A'}_i + (\sigma_A \sqrt{1-\delta^2}) W_i \qquad \text{state update equation} \qquad (4.32)$$

$$\tilde{Y}_i = wr\tilde{A'}_i + V_i. \qquad \text{observation equation} \qquad (4.33)$$

Notice that we consider only the zero mean processes $\tilde{A'}_i$ and $\tilde{Y}_i$; furthermore, we have replaced $\tilde{A}_i$ in equation (4.18) by its equivalent $\tilde{A'}_i$, under a linear dynamic model in equation (4.33).

The Kalman Filtering Algorithm

Given this formulation the Kalman algorithm in its discrete form can be stated [Maybe79] by two sets of equations; the first set describes how the estimate and

variance of the estimate propagates in time

$$\hat{\tilde{A}}_M^- = \delta \hat{\tilde{A}}_{M-1} \tag{4.34}$$

$$\epsilon_M^- = \delta^2 \epsilon_{M-1} + \sigma_A^2(1-\delta^2) \tag{4.35}$$

where $\hat{\tilde{A}}_M^-$ and ϵ_M^- denote the a priori (before the observation information at time M is made available) estimate and error variance of the estimate respectively.

The second set of equations consists of the measurement update equations and gives the a posteriori estimates (after the measurement information is processed) for the system state and variance in relation to the a priori ones,

$$k_M = \frac{wr\epsilon_M^-}{(wr)^2\epsilon_M^- + \sigma_V^2} \tag{4.36}$$

$$\hat{\tilde{A}}_M = \hat{\tilde{A}}_M^- + k_M(\tilde{Y}_M - wr\hat{\tilde{A}}_M^-) \tag{4.37}$$

$$\epsilon_M = (1 - wrk_M)\epsilon_M^- \tag{4.38}$$

Another useful representation of the algorithm results if we combine equations (4.34) and (4.37) as in [Papou81]. Accordingly, $\hat{\tilde{A}}_M$, the centered state estimate at frame M, is given as a linear combination of $\hat{\tilde{A}}_{M-1}$, the centered state estimate at the previous step, and the current observation $\tilde{Y}_M = Y_M - E[Y_M]$,

$$\hat{\tilde{A}}_M = \delta(1 - wrk_M)\hat{\tilde{A}}_{M-1} + k_M\tilde{Y}_M. \tag{4.39}$$

where k_M is the Kalman gain at step M. Using (4.36) and (4.35), k_M can be shown

to depend on the error variance at step $M-1$,

$$k_M = \frac{\delta^2 \epsilon_{M-1} + \sigma_A^2(1-\delta^2)}{(wr)[\delta^2 \epsilon_{M-1} + \sigma_A^2(1-\delta^2)] + \sigma_V^2}. \tag{4.40}$$

Finally combining equations (4.38), (4.36) and (4.35), we get a recursion on M (a scalar Riccati difference equation) for the variance of the estimation error ϵ_M

$$\epsilon_M = \frac{\sigma_A^2(1-\delta^2) + \delta^2 \epsilon_{M-1}}{(wr)^2[(1-\delta^2)\sigma_A^2 + \delta^2 \epsilon_{M-1}] + \sigma_V^2} \sigma_V^2. \tag{4.41}$$

The filter is initialized as follows

$$\epsilon_1 = \frac{\sigma_A^2 \sigma_V^2}{(wr)^2 \sigma_A^2 + \sigma_V^2} \qquad k_1 = \frac{wr\sigma_A^2}{(wr)^2 \sigma_A^2 + \sigma_V^2} \tag{4.42}$$

The long range performance of the filter is given by letting $M \to \infty$ in equation (4.41). Setting $\lim_{M\to\infty} \epsilon_{M-1} = \lim_{M\to\infty} \epsilon_M = \epsilon$, the long term estimation error, we get from (4.41) the following quadratic in ϵ,

$$(wr)^2 \delta^2 \epsilon^2 + (1-\delta^2)\left[(wr)^2 \sigma_A^2 + \sigma_V^2\right] \epsilon - (1-\delta^2)\sigma_A^2 \sigma_V^2 = 0. \tag{4.43}$$

Keeping only the positive root of (4.43), the long term mean square error in state estimation is given as

$$\epsilon = \frac{-(1-\delta^2)\left[(wr)^2 \sigma_A^2 + \sigma_V^2\right] + (1-\delta^2)\sqrt{\left[(wr)^2 \sigma_A^2 + \sigma_V^2\right]^2 + 4\delta^2 \sigma_A^2 \sigma_V^2}}{2(wr)^2 \delta^2} \tag{4.44}$$

The algorithm returns a value for $\hat{A}_M$, that is not necessarily an integer. Therefore, implementing the algorithm, we have included a final stage that rounds-off the estimate $\hat{A}_M$ to its closest integer value.

Simulation Results

Voice Source Estimation

We examined the performance of Kalman filtering in estimating the number of active sources in a voice multiplexing example, using a voice simulation model. N 8-bit PCM encoded voice sources with silence detection are multiplexed on a channel. During active periods stream voice data are packetized into ATM cells, resulting in one ATM cell every 5.9 msec. Active and idle voice source periods were considered exponentially distributed with means $\frac{1}{\mu_{vo}} = 1.01$ sec and $\frac{1}{\lambda_{vo}} = 1.38$ sec respectively [Yatsu82]. Two filters are considered; the first was developed assuming an On-Off voice source model, and the second assuming an IPP model. In developing the filter assuming IPP source modeling, we have used the mean interval method [Ide89], to match each voice source to an Interrupted Poisson Process. According to this method, active and idle source periods are mapped to IPP activity and inactivity in a one-to-one manner. Consequently, the transition probabilities for the IPP model (figure 1.4) have the same values as their respective parameters of the On-Off model (figure 1.3). The third parameter of the IPP model, i.e. the Poisson cell rate γ during the active state was chosen to be equal to the rate r in the active state for the On-Off model.

Figure 4.5 gives the percentage error, $\frac{\epsilon}{N}100\%$, in estimating the number of active voice sources from cells counts using Kalman filtering, as a function of the number of

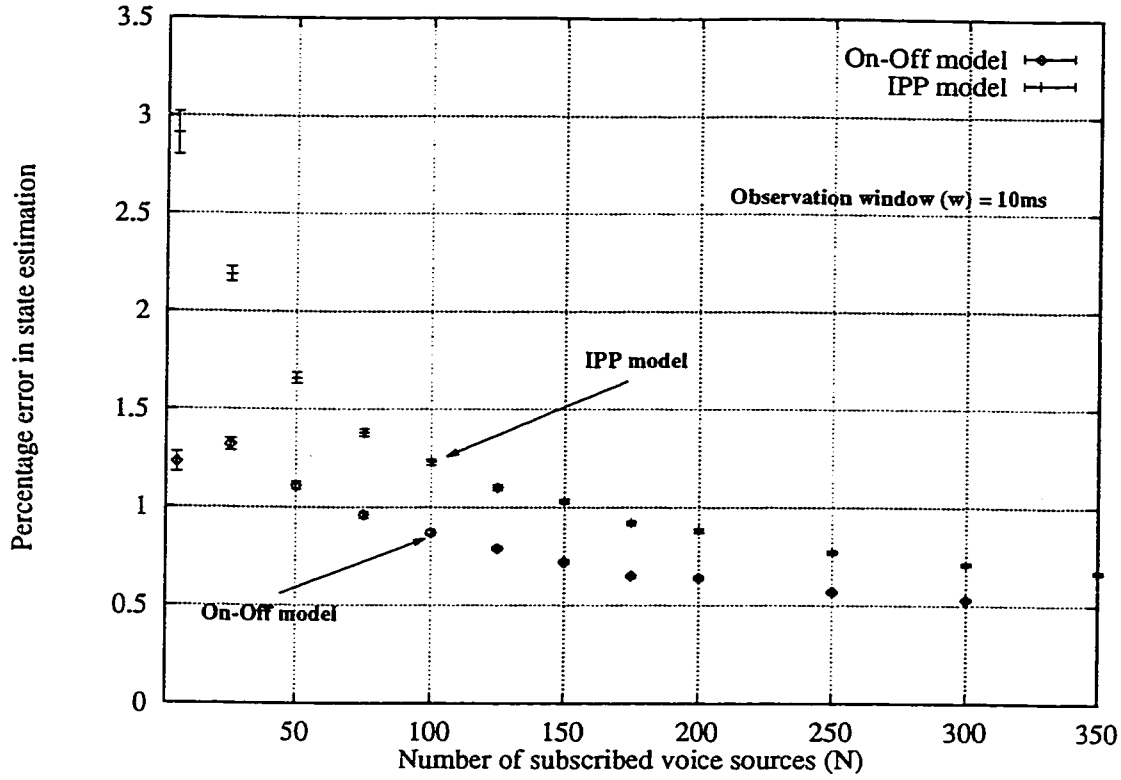

Figure 4.5: State estimation error in statistical voice multiplexing

subscribed voice sources N. The observation time interval w was fixed at 10 ms. 95 % confidence intervals are also shown. For small values of N, the error is dominated by the non-linear effect of rounding-off the estimated state to the nearest integer value. For larger number of subscribed sources, N, the effect of this error diminishes and application of expression (4.44) for the estimation error becomes feasible.

The performance of both filters in terms of the percentage error reaches a fixed value as N increases. This can be explained as follows; from equation (4.44) we see that the error ϵ is a function of the variance of the number of active sources σ_A^2, and the variance of the ambiguity in cell measurements σ_V^2. However, in our example both depend linearly on N. For instance from Appendix C we get that $\sigma_A^2 = \frac{Npq}{p+q}$, and $\sigma_V^2 = \frac{Np}{p+q}(1-\pi)\pi$ for the On-Off model and $\sigma_V^2 = \frac{Np}{p+q}w\gamma$ for the IPP process. By

substituting these two values in (4.44) we see that the long term error depends linearly on N, all other variables remaining fixed. However, for the IPP source modeling the coefficient of linear dependence on N is greater than the corresponding coefficient under the On-Off modeling. Accordingly, the long term estimation error under IPP modeling is greater than the error under On-Off modeling. This is reasonable since the IPP case has an extra dimension of randomness.

Video Source Estimation

Next we examine the performance of the algorithm in determining the activity level of variable bit rate conversational video sources. Video calls have identical

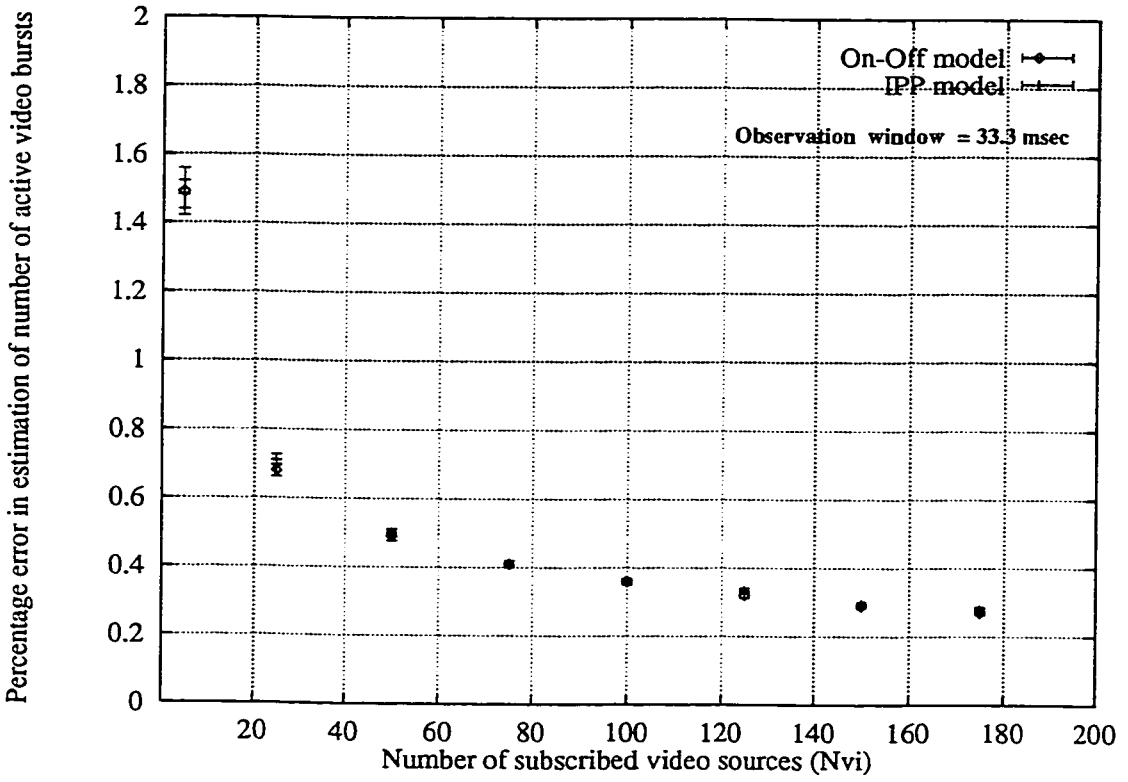

Figure 4.6: State estimation error in statistical video multiplexing

characteristics such as peak bit rate of 10.57 Mbits/s, average bit rate of 3.9 Mbits/s,

and bit rate autocovariance function which decays exponentially with time at a rate of 3.9 sec^{-1} [MASKR88]. Each video call is approximated by a set of $M = 10$ minisources. Figure 4.6 gives the percentage error in estimating the state of a video multiplexing in terms of active video bursts.

4.2 Multiple Source Types

In this section we extend the network state estimation in the case when more than one types of sources are multiplexed on a given VP. In contrast with the homogeneous case, we restrict ourselves only to the case where each source is modeled as a binary On-Off source.

4.2.1 State Estimation Using the On-Off Source Model

System Description

We assume L types of sources multiplexed on a VP. Each source class is characterized by its distinct source dynamics in terms of their On and Off transition probability rates, λ_l and μ_l, and their peak rates r_l at the On state.

As above, we retain the slotted nature of our channel, and we let the slot length w to be small, such that $\lambda_l w \ll 1$ and $\mu_l w \ll 1$ for all classes l, $l \in \{1, 2, \ldots, L\}$. Accordingly, the probability that a given On-Off source of type l will change state from active to idle within this time interval is

$$q_l = 1 - e^{-\lambda_l w} \approx \lambda_l w.$$

Similarly the probability that it will go from idle to active is given as

$$p_l = 1 - e^{-\mu_l w} \approx \mu_l w.$$

Let N_l be the number of subscribed sources of class l. We denote the number of active sources of type l during the i^{th} slot interval by $A_{l,i}$. Then the state of our system becomes a vector[1] $\mathbf{A}_i = (A_{1,i}, A_{2,i}, \ldots, A_{L,i})^T$. $\mathbf{A}_i$ is a L-dimensional Markov chain; however, by allowing the transition probabilities p_l and q_l for all source types to be much less than one, we can show that the transition probabilities for the Markov chain $\mathbf{A}_i$ are significant only for transitions to adjacent states, i.e. states that differ from the current state only by one more or one less active source. Then, $\mathbf{A}_i$ becomes a multidimensional birth-death process. Considering a current state $\mathbf{A}_i = \mathbf{a}$ where $\mathbf{a} = (a_1, a_2, \ldots, a_l, \ldots, a_L)$ and denoting as in chapter 2 $\mathbf{a}_l^+ = (a_1, a_2, \ldots, a_l + 1, \ldots, a_L)$ and $\mathbf{a}_l^- = (a_1, a_2, \ldots, a_l - 1, \ldots, a_L)$, we can write

$$p_{\mathbf{a},\mathbf{a}_l^+} = (N_l - a_l)p_l \tag{4.45}$$

$$p_{\mathbf{a},\mathbf{a}_l^-} = a_l q_l \tag{4.46}$$

$$p_{\mathbf{a},\mathbf{a}} = 1 - (N_l - a_l)p_l - a_l q_l \tag{4.47}$$

As in the single source type environment, we monitor the cell activity on the VP, and we count the number of cells in consecutive time intervals of duration w. We denote by $Y_{l,i}$ the contribution of class l calls during the i^{th} observation interval to

[1]The notation $(.)^T$ denotes the transpose of a vector. We define our system state to be a column vector.

the total cell count Y_i; then,

$$Y_i = \sum_{l=1}^{L} Y_{l,i}. \tag{4.48}$$

From our discussion in the previous section, in the case when only one type of source was multiplexed on the VP, the number of cells observed during the i^{th} window, that belong to a given source class l, can be written as

$$Y_{l,i} = A_{l,i}\lfloor wr_l \rfloor + Z_{l,i}, \tag{4.49}$$

with $Z_{l,i}$ a binomially distributed random variable

$$\Pr(Z_{l,i} = k \mid A_{l,i} = a_l) = \begin{pmatrix} a_l \\ k \end{pmatrix} \pi_l^k (1-\pi_l)^{a_l - k}, \tag{4.50}$$

and $\pi_l \triangleq wr_l - \lfloor wr_l \rfloor$. Accordingly, the total number of observations from all source classes is given as

$$Y_i = \sum_{l=1}^{L} A_{l,i}\lfloor wr_l \rfloor + \sum_{l=1}^{L} Z_{l,i}. \tag{4.51}$$

We see that the number of observations during the i^{th} observation interval, Y_i, depends on the network state $\mathbf{A}_i = (A_{1,i}, A_{2,i}, \ldots, A_{L,i})$, but not in a one to one manner; this is not only due to "noise" part $\sum_{l=1}^{L} Z_{l,i}$ included in (4.51), but to the fact that the same number of observations can be counted when different combinations of sources

of different classes are active as well.

As in the homogeneous case, after observing the number of packets in the M^{th} frame, Y_M, we want to derive $\hat{\mathbf{A}}_M = (\hat{A}_{1,M}, \hat{A}_{2,M}, \ldots, \hat{A}_{L,M})^T$, an estimate of the network state, during interval M. However, in the multiple source type case, the estimated state is a vector process, while the observation data, Y_M, is still a scalar, which implies that we can not distinguish between packets of different source classes. We limit ourselves to linear estimation algorithms, assuming complete observed knowledge of the history of the process up to and including time M.

The Additive White Gaussian Noise Observation Model

Linear estimation of the network state involves only moments up to the second order of the observation data. Therefore we can postulate an AWGN model for Y_i to replace the actual model of equation (4.51) without affecting the linear estimation. The AWGN model will be:

$$Y_i = \sum_{l=1}^{L} c_{l,i} A_{l,i} + V_i \tag{4.52}$$

with V_i a sequence of normally distributed zero mean random variables and $c_{l,i}$ $l \in \{1, 2, \ldots, L\}$ real constants.

The AWGN model in (4.52) has to match the second order statistics of the original data to be adequate for our linear estimation purposes, i.e. the autocovariance function $C_{YY}(i,j)$ of the observation data Y_i and the cross-covariance function $C_{A_lY}(i,j)$ of Y_i with the active sources of class l, A_l, for all $l \in \{1, 2, \ldots, L\}$.

In Appendix (equation (E.10)) we prove using equation (4.51) that,

$$C_{YY}(i,j) = \sum_{l=1}^{L}(wr_l)^2 C_{A_lA_l}(i,j) \qquad i \neq j \tag{4.53}$$

$$\sigma_{Y_i}^2 = \sum_{l=1}^{L}\sigma_{A_{l,i}}^2(wr_l)^2 + \sum_{l=1}^{L}E[A_{l,i}]\pi_l(1-\pi_l) \tag{4.54}$$

and

$$C_{A_lY}(i,j) = wr_l C_{A_lA_l}(i,j) \tag{4.55}$$

with $C_{A_lA_l}(i,j)$ the autocovariance function of $A_{l,i}$.

Similarly, for the AWGN model in equation (4.52) we have:

$$C_{YY}(i,j) = \sum_{l=1}^{L} c_{l,i}c_{l,j}C_{A_lA_l}(i,j) \tag{4.56}$$

$$\sigma_{Y_i}^2 = \sum_{l=1}^{L} c_{l,i}C_{A_lA_l}(i,i) + \sigma_{V_i}^2 \tag{4.57}$$

and

$$C_{A_lY}(i,j) = c_{l,i}C_{AA}(i,j) \tag{4.58}$$

Comparing expressions (4.56), (4.57) and (4.58), derived according to the AWGN model, with the corresponding expressions (4.53) (4.53) and (4.55), derived from our original observation model (equation (4.51)), we see that an AWGN model for the observation data Y_i could be postulated by letting $c_{l,i} = wr_l$ and $\sigma_{V_i}^2 = \sum_{l=1}^{L} E[A_{l,i}]\pi_l(1-$

π_l) in (4.52). Therefore as far as linear filtering of A_l is concerned, the data Y_i can be considered as given by the following AWGN model,

$$\tilde{Y}_i = \sum_{l=1}^{L} wr_l \tilde{A}_{l,i} + V_i. \tag{4.59}$$

with $\tilde{Y}_i = Y_i - E[Y_i]$ and $\tilde{A}_{l,i} = A_{l,i} - E[A_{l,i}]$ the centered parts of Y_i and $A_{l,i}$ respectively.

Linear Dynamic System Model

On the predicament of an AWGN observation model such as the one postulated by equation (4.59), the optimum linear filter for the estimation of the network state $\mathbf{A}_i$ depends only on the second order statistics of the process. Therefore, if keeping the same mean and autocorrelation function, we approximate the original discrete state multidimensional birth-death process, with another one $\mathbf{A}'_i$ that follows a linear dynamic model, we will be able to apply the more efficient Kalman filtering algorithm towards the network state estimation, instead of the transversal filter used in the Appendix.

Going through similar considerations as in the one dimensional case, $\mathbf{A}_i$ is approximated with a first order autoregressive process in the L dimension space. Since the number of active sources for each source type are independent processes, the L dimensional autoregressive approximation to $\mathbf{A}_i$ would be a system of L decoupled one dimensional autoregressive processes, one for every class type. We denote by C_{AA}

the covariance matrix of $\mathbf{A}_i$, i.e. $C_{AA} = E[\mathbf{A}_i \mathbf{A}_i^T]$. Then,

$$C_{AA} = \begin{cases} \sigma_{A_l}^2 & \text{for} \quad i = j \\ 0 & \text{for} \quad i \neq j \end{cases} \tag{4.60}$$

Moreover, we let $\mathcal{D}$ be the diagonal matrix with diagonal elements $\delta_i = 1 - p_i - q_i$, $i \in \{1, 2, \ldots, L\}$

$$\mathcal{D} = \text{diag}\{\delta_1, \delta_2, \ldots, \delta_L\}.$$

Then, assuming stationarity for $\mathbf{A}_i$, the linear dynamic model for $\mathbf{A}_i$ is written as:

$$\tilde{\mathbf{A}}'_{i+1} = \mathcal{D}\tilde{\mathbf{A}}'_i + C_{AA}^{1/2}\left(I_L - \mathcal{D}^2\right)^{1/2}\mathbf{W}_i \tag{4.61}$$

$$\mathbf{A}'_i = E[\mathbf{A}_i] + \tilde{\mathbf{A}}'_i \tag{4.62}$$

with $\mathbf{W}_i$ a $L \times 1$ vector of zero mean Gaussian random sequences, and $\mathcal{I}_L$ the $L \times L$ unity matrix. $E[\mathbf{A}_i]$ is the vector of the per class mean number of active sources

$$E[\mathbf{A}_i] = (E[A_{1,i}], E[A_{2,i}], \ldots, E[A_{L,i}])^T \tag{4.63}$$

with $E[A_{l,i}] = \frac{N_l p_l}{p_l + q_l}$.

4.2.2 Filter Performance

Before describing the form of Kalman filtering applicable to the network state estimation in our case, we summarize our results so far concerning the evolution of our system state and observation model respectively

$$\tilde{\mathbf{A}}'_{i+1} = \mathcal{D}\tilde{\mathbf{A}}'_i + \mathcal{C}_{AA}\left(I_L - \mathcal{D}^2\right)^{1/2}\mathbf{W}_i \qquad \text{state update equation} \tag{4.64}$$

$$\tilde{Y}_i = w\mathbf{r}^T\tilde{\mathbf{A}}'_i + V_i \qquad \text{observation equation} \tag{4.65}$$

In writing equation (4.65) we have introduce the $L \times 1$ column vector $\mathbf{r} = (r_1, r_2, \ldots, r_L)^T$; this notation will be helpful in stating the equations that embody the Kalman filtering algorithm. Moreover, we define the $L \times L$ state estimation error correlation matrix $\mathcal{E}_M$, with elements

$$\mathcal{E}_M(l,m) = E[(A_l - \hat{A}_l)(A_m - \hat{A}_m)] \qquad l,m = 1,2,\ldots,L, \tag{4.66}$$

and the $L \times 1$ Kalman gain vector $\mathbf{k}_M$. Then, the Kalman filtering algorithm is given by the following two sets of equations [Hayki86]; the time update equations,

$$\bar{\hat{\mathbf{A}}}_M = \mathcal{D}\hat{\tilde{\mathbf{A}}}_{M-1} \tag{4.67}$$

$$\bar{\mathcal{E}}_M = \mathcal{D}\mathcal{E}_{M-1}\mathcal{D} + \mathcal{C}_{AA}\left(I_L - \mathcal{D}^2\right) \tag{4.68}$$

and the measurement update equations

$$\mathbf{k}_M = \frac{w\mathcal{E}_M^- \mathbf{r}}{(w^2\mathbf{r}^T\mathcal{E}_M^-\mathbf{r} + \sigma_V^2)} \tag{4.69}$$

$$\hat{\tilde{\mathbf{A}}}_M = \hat{\tilde{\mathbf{A}}}_M^- + \mathbf{k}_M(\tilde{Y}_M - w\mathbf{r}^T\hat{\tilde{\mathbf{A}}}_M^-) \tag{4.70}$$

$$\mathcal{E}_M = (\mathcal{I}_L - w\mathbf{k}_M\mathbf{r}^T)\mathcal{E}_M^-. \tag{4.71}$$

Combining equations (4.70) and (4.67) we get a recursive expression for the estimate at step M:

$$\hat{\tilde{\mathbf{A}}}_M = (\mathcal{I}_L - w\mathbf{k}_M\mathbf{r}^T)\mathcal{D}\hat{\tilde{\mathbf{A}}}_{M-1} + \mathbf{k}_M\tilde{Y}_M \tag{4.72}$$

Expression (4.72) gives the estimate at time M with respect to the estimate in the previous time interval $M-1$ and the current observation Y_M. It requires the knowledge of the Kalman gain vector $\mathbf{k}_M$; however, from equations (4.69) and (4.68) by eliminating $\mathcal{E}_M^-$, we have,

$$\mathbf{k}_M = \frac{w\mathcal{D}\mathcal{E}_{M-1}\mathcal{D}\mathbf{r} + w\mathcal{C}_{AA}\left(I_L - \mathcal{D}^2\right)\mathbf{r}}{w^2\mathbf{r}^T\mathcal{D}\mathcal{E}_{M-1}\mathcal{D}\mathbf{r} + w^2\mathbf{r}^T\mathcal{C}_{AA}\left(I_L - \mathcal{D}^2\right)\mathbf{r} + \sigma_V^2} \tag{4.73}$$

Equation (4.73) in turn requires the knowledge of the estimation error correlation matrix $\mathcal{E}_{M-1}$. Going through similar steps as in the previous homogeneous case, by combining equations (4.71), (4.68), and (4.73), we have a matrix difference Riccati

equation for $\mathcal{E}_M$,

$$\mathcal{E}_M = \mathcal{E}_M \;=\; (\mathcal{I}_L - w\mathbf{k}_M\mathbf{r}^T)\left[\mathcal{D}\mathcal{E}_{M-1}\mathcal{D} + \mathcal{C}_{AA}\left(I_L - \mathcal{D}^2\right)\right] \tag{4.74}$$

The initial filter gain and error matrix are

$$\mathbf{k}_1 = \frac{w\mathcal{C}_{AA}\mathbf{r}}{(w^2\mathbf{r}^T\mathcal{C}_{AA}\mathbf{r} + \sigma_V^2)} \qquad \mathcal{E}_1 = \mathcal{C}_{AA} - w\mathbf{k}_1\mathbf{r}^T\mathcal{C}_{AA} \tag{4.75}$$

As in the homogeneous case, the estimates, $\hat{A}_{M,l}$, of the number of active sources of class l, given by the above filtering algorithm are not necessarily integer valued. For this reason, we round-off the state estimates $\hat{A}_{M,l}$ $l = 1, 2, \ldots, L$, at the output of the Kalman filter, to the nearest integer value.

Simulation Results

We consider a video-image transfer multiplexing example to examine the performance of the Kalman filtering algorithm in a heterogeneous environment. Video sources are modeled as aggregates of $M = 10$ minisources, and have the same statistical characteristics as in the previous video multiplexing example. Image transfer sessions are modeled as On-Off with mean On duration of $\frac{1}{\mu_{\text{im}}} = 1$ sec, and mean Off duration of $\frac{1}{\lambda_{\text{im}}} = 10$ sec. The peak transmission rate during On image periods is 10 Mbits/s.

Figure 4.7 gives the accuracy of the estimate of active video bursts, and figure 4.8 the accuracy of the estimate of active image bursts. For small values of subscribed

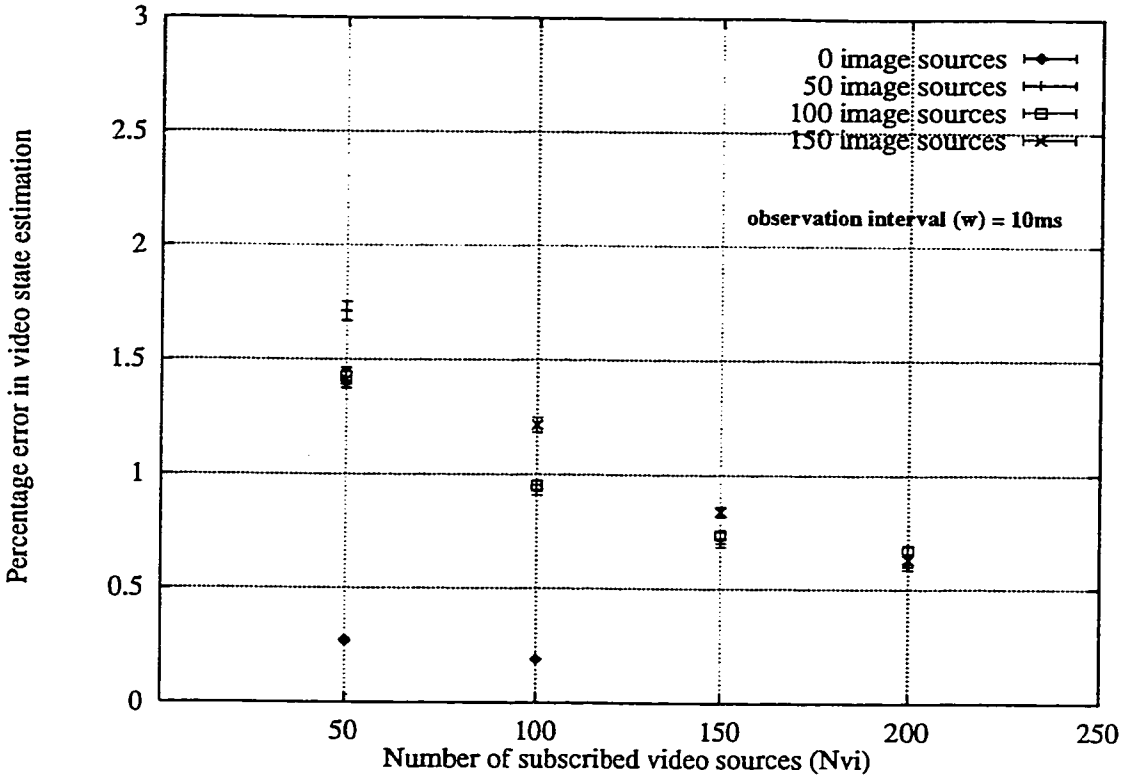

Figure 4.7: Video state estimation error in statistical, video-image transfer, multiplexing

sources the error is dominated by the rounding-off procedure at the filter output.

The error for both estimates is very low, in the order of magnitude of $1 - 2\%$.

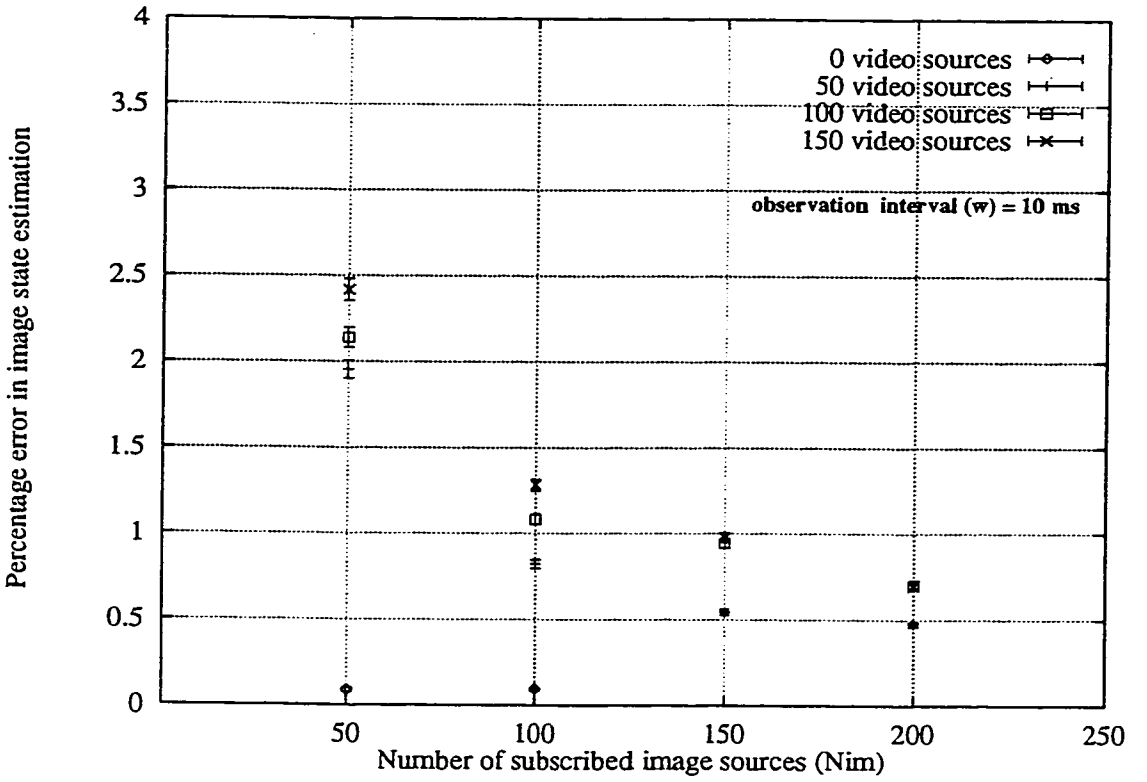

Figure 4.8: Image state estimation error in statistical, video-image transfer, multiplexing

Chapter 5
CONCLUSION AND FUTURE WORK

We have presented a feasibility study of a proactive congestion control approach for broadband networks. The basic idea is to predict congestion inside the network, from a current underload network state and, in case of congestion imminence, shape traffic at the periphery of the network, before it enters. Prediction of network overload can be performed either when network elements are bufferless or when they are equipped with a considerable amount of buffering. The first case corresponds to networks supporting real time services with very tight end-to-end delay requirements, while the second is related to transportation of real services as well but with more relaxed end-to-end performance criteria. Prediction and subsequent proactive measures are possible in these cases because the time scales of the traffic involved are of the same order of magnitude as the network round trip time.

The are two main advantages of the proactive congestion control strategy: first, it allows graceful degradation of the service offered to a call by performing traffic shaping, and accordingly permits to admit more calls into the network; second, it makes it possible to offer performance guarantees to network calls in an easier manner by performing traffic shaping at the entrance of the network rather than inside the network, as in selective discarding in [YinLS90]. Moreover, network resources up to

the congested node are not wasted by the transmission of packets that will be dropped later on with a high probability. Accordingly, in a multihop network these resources could be used for transmission of traffic that is not routed through the bottleneck link.

The proactive congestion control approach will be used together with an admission control policy to guarantee a certain performance level for all the calls being supported. The exact call admission control strategy that will be deployed will depend on the performance requirements of the calls and requires a treatment by itself. Current admission control strategies such as the effective bandwidth approach can be used towards this end [Ross96, Kaufm92, DzioR87, Kouko93].

The proactive congestion control methodology can be extended in several ways. First, the feasibility of the approach in the case of delay tolerant traffic that share the same VP of allocated capacity C, with delay sensitive services can be examined. Characteristic of these cases is that delay sensitive services are usually given higher priority in accessing the VP capacity. As such, the effective VP capacity seen by the delay sensitive services varies in a stochastic manner. Assuming Markovian traffic models for the delay sensitive services, the VP capacity available to the delay tolerant services varies according to a Markovian rule. Therefore we can use a Markov drift process of chapter 3 to model this situation as well, as in [Mitra88].

Moreover, extension of the model in chapter 3 for services that follow On-Off traffic models with non exponential either On or Off periods is required. Services, that are of this type include mainly connectionless data services with long range dependence. It has been recently suggested [WiTSW97] to use On-Off models with at least one

state (either the On or Off state) Pareto-distributed, as models of these services. As a first fitting of our model to the situation of connectionless data multiplexing, we could approximate the Pareto distribution by a hyperexponential distribution [FeldW97]. This leads us to an appropriately defined Markov drift process as well, and thus the approach of chapter 3 for calculating the probability distribution for the time to overload can still be applied.

So far, we presented extension of the model of chapter 3 considering a homogeneous service environment. However, this model can be extended to the case of multiplexing an heterogeneous mix of services as well.

Bibliography

[AnanP95] F. Ananasso and F. D. Priscoli, " The Role of Satellites in Personal Communications Services," *IEEE J. Select. Areas Commun.* , pp. 180–196, Feb. 1995.

[AniMS82] D. Anick, D. Mitra and M. M. Sondhi, " Stochastic Theory of a Data-handling System with Multiple Sources," *Bell Syst. Tech. J.*, pp. 1871–1893, Oct. 1982.

[Armbr95] H. Armbryster, "The flexibility of ATM: Supporting Future Multimedia and Mobile Communications," *IEEE Commun. Mag.*, pp. 76–84, Feb. 1995.

[BaeS91] J. J. Bae and T. Suda, "Survey of Traffic Control Schemes and Protocols in ATM Networks," *Proc. IEEE*, pp. 170–189, Feb. 1991.

[BallC89] R. Ballart and Y-C. Ching, "SONET: Now It's the Standard Optical Network," *IEEE Commun. Mag.*, pp. 8–15, March 1989.

[BSTW95] J. Beran, R. Sherman, M. S. Taqqu and W. Willinger, "Long-Range Dependence in Variable-Bit-Rate Video Traffic," *IEEE Trans. Commun.*, vol. 43, pp. 1566–1579, Feb./March/April 1995.

[BertG92] D. Bertsekas and R. Gallager, *Data Networks*, Prentice Hall, Inc., Englewood Cliffs, NJ, 1992.

[BiaGS80] T. Bially, B. Gold and S. Seneff, "A Technique for Adaptive Voice Flow Control in Integrated Packet Networks," *IEEE Trans. on Commun.*, pp. 325 –333, March 1980.

[BonoF95] F. Bonomi and K. W. Fendick, " The Rate-Based Flow Control Framework for the Available Bit Rate ATM Service," *IEEE Network*, pp. 25–39, March/April 1995.

[Brady69] P. T. Brady, "A Model for Generating on-off Speech Patterns in Two-Way Conversation," *Bell System Technical Journal* , pp. 2445–2472, 1969.

[BurgD91] J. Burgin and D. Dorman, "Broadband ISDN Resource Management: The Role of Virtual Paths," *IEEE Commun. Mag.*, pp. 44–48, Sept. 1991.

[CCITT89] CCITT Recomendation I.121, "Broadband Aspects of ISDN," Blue Book, Geneva, Switzerland, 1989.

[CheLS96] T. M. Chen, S. S. Liu and V. K. Salaman, "The Available Bit Rate Service for Data in ATM Networks," *IEEE Commun. Mag.*, pp. 56–71, May 1996.

[ChiaA96] T. Chiang, and D. Anastassiou, "Hierarchical Coding of Digital Television," *IEEE Commun. Mag.*, pp. 38–45, May 1994.

[CoopP90] C. A. Cooper and K. I. Park, "Toward a Broadband Congestion Control Strategy," *IEEE Network*, pp. 18–23, May 1990.

[COST91] J. W. Roberts, Editor, *COST 224 Performance evaluation and design of multiservice networks*, Directorate-General Telecommunications, Information Industry and Innovation, Commission of the European Communities, Oct. 1991.

[CoxM65] D. R. Cox and H. D. Miller, *The Theory of stochastic processes* New York, Wiley, 1965.

[DePry93] M. De Prycker, *Asynchronous Transfer Mode Solution for Broadband ISDN,*, Ellis Horwood, 1993.

[DzioR87] Z. Dziong and J. W. Roberts, "Congestion Probabilities in a Circuit-Switched Integrated Services Network," *Performance Evaluation*, vol. 7, pp. 267-284, 1987.

[ElwaM93] A. I. Elwalid and D. Mitra, "Effective Bandwidth of General Markovian Traffic Sources and Admission Control of High Speed Networks," *IEEE/ACM Trans. on Networking*, vol. 1, pp. 329–343, 1993.

[ElwaM91] A. I. Elwalid and D. Mitra, "Analysis and Design of Rate-Based Congestion Control of High Speed Networks,I: Stochastic Fluid Models, Access Regulation," *Queueing Systems*, vol. 9, pp. 29–64, 1991.

[FeldW97] A. Feldmann and W. Whitt, "Fitting Mixtures of Exponentials to Long-Tail Distributions to Analyze Network Performance Models," in Proc. *IEEE INFOCOM'97*, Kobe, Japan.

[Ferna95] L. Fernandes, "Developing a System Concept and Technologies for Mobile Broadband Communications," *IEEE Personal Commun.* , pp. 54–59, Feb. 1995.

[FowlL91] H. J. Fowler and W. E. Leland, "Local Area Network Traffic Characteristics, with Implications for Broadband Network Congestion Management, " *IEEE J. Select. Areas Commun.*, pp. 1139–1149, Sept. 1991.

[Fried56] B. Friedman, *Principles and Techniques of Applied Mathematics*, John Wiley and Sons, New York, 1956.

[FriHW96] V. J. Friesen, J. J. Harms and J. W. Wong, "Resource Management with Virtual Paths in ATM Networks," *IEEE Network*, pp. 10–20, Sept./Oct. 1996.

[Garre96] M. W. Garett, "A Service Architecture for ATM: From Applications to Scheduling," *IEEE Network*, pp. 6–14, May/June 1996.

[GarrV93] M. W. Garett and M. Vetterli, "Joint Source/Channel Coding of Statistically Multiplexed Real-Time Services on Packet Networks," *IEEE/ACM Trans. Networking*, pp. 71–80, Feb. 1993.

[GaveL82] D. P. Gaver and J. P. Lehoczky, " Channels that Cooperatively Service a Data Steam and Voice Messages," *IEEE Trans. Commun.*, pp. 1153–1161, May 1982.

[GibbH91] R. J. Gibbens and P. J. Hunt, "Effective Bandwidths for the Multi-type UAS Channel," *Queueing Systems*, vol. 9, pp. 17–28, 1991.

[GitHW92] R. Gitlin, J. F. Hayes and S. B. Weinstein, *Data Communications Principles*, Plenum Press, 1992.

[Hayki86] S. Haykin, *Adaptive Filter Theory*, Prentice-Hall, 1986.

[GoodW91] D. J. Goodman and S. X. Wei, "Efficiency of Packet Reservation Multiple Access," *IEEE Trans. Vehic. Technol.*, pp. 170–176, Feb. 1991.

[Grub91] J. L. Grubb, "The Traveler's Dream Come True," *IEEE Commun. Mag.*, vol. 29, pp. 48–51, Nov. 1991.

[GueAN91] R. Guerin, H. Ahmadi and M. Naghshineh, "Equivalent Capacity and Its Applications to Bandwidth Allocation in High-Speed Networks," *IEEE Journal Select. Areas Commun.*, vol. 9 pp. 968–981, Feb. 1991.

[HeffL86] H. Heffes, D. M. Lucantoni, "A Markov Modulated Characterization of Packetized Voice and Data Traffic and Related Statistical Multiplexer Performance," *IEEE J. Select. Areas in Commun.*, pp. 856–868, Sept. 1986.

[HeyTL96] D. P. Heyman, A. Tabatabai and T. V. Lakshman, "Statistical Analysis and Simulation of Video Teleconference Traffic in ATM Networks," *IEEE/ACM Trans. on Circuits and Syst. Video Technology*, vol. 2, pp. 49–59, March 1992.

[HeyL96a] D. P. Heyman and T. V. Lakshman, "Source Models for VBR Broadcast-Video Traffic," *IEEE/ACM Trans. on Networking*, vol. 4, pp. 40–48, Feb. 1996.

[HeyL96b] D. P. Heyman and T. V. Lakshman, "What Are the Implications of Long-Range Dependence for VBR-Video Traffic Engineering?," *IEEE/ACM Trans. on Networking*, vol. 4, pp. 301–317, June 1996.

[HuLP95] X. Hu, J. F. Lambert and A. Pitsillides, "Fast Backward Predictive Congestion Notification for ATM Networks with Significant Propagation Delays," in *Proc. IEEE GLOBECOM'95*, Boston, MA, pp. 275–279.

[Hui88] J. Y. Hui, "Resource Allocation for Broadband Networks," *IEEE J. Select. Areas Commun.*, vol. 6, pp. 1598–1608, Dec. 1988.

[Hui91] J. Y. Hui M. B. Gursoy and R. D. Yates, "A Layered Broadband Switching Architecture with Physical or Virtual Path Configurations," *IEEE J. Select. Areas Commun.*, vol. 9, pp. 1416–1426, Dec. 1991.

[Ide89] I. Ide, "Superposition of Interrupted Poisson Processes and Its Application to Packetized Voice Multiplexers," ITC-12, 1989.

[Kaufm92] J. S. Kaufman, "Blocking with retrials in a completely shared resource environment," *Performance Evaluation*, vol. 15, pp. 99-113, June 1992.

[Keils64] J.Keilson, "A Review of Transient Behavior in Regular Diffusion and Birth-Death Processes," *J. Appl. Prob.*, pp. 247–266, 1964.

[Keils65] J. Keilson, "A Review of Transient Behavior in Regular Diffusion and Birth-Death Processes. Part II" *J. Appl. Prob.*, pp. 405–428, 1965.

[KeilR65] J. Keilson and S. S. Rao, "A Process with Chain Dependent Growth Rate. Part II: The Ruin and Ergodic Problems," *Adv. Appl. Prob.*, pp. 315–338, 1971.

[KimSY94] J. B. Kim, T. Suda and M. Yoshimura, "International Standardization of B-ISDN," *Computer Networks and ISDN Systems*, pp. 5–27, 1994.

[Klein92] L. Kleinrock, "The Latency/bandwidth Tradeoff in Gigabit Networks," *IEEE IEEE Commun. Mag.*, vol. 30, pp. 36–40, April 1992.

[KolAH94] A. Kolarov, A. Atai and J. Hui, "Application of Kalman Filtering in High-Speed Networks," in *Proc. IEEE GLOBECOM'94*, pp. 624–628.

[KrHBG91] H. Kroner, G. Hebuterne, P. Boyer and A. Gravey, "Priority Management in ATM Switching Nodes," *IEEE J. Sel. Areas Commun.*, pp. 418–427, April 1991.

[Kouko93] V. Koukoulidis, *A characterization of reversible Markov processes with applications to shared-resource environments*, Ph. D. Thesis, Concordia University, 1993.

[Kuczu73] A. Kuczura, "The Interrupted Poisson Process," *Bell Syst. Tech. J.*, vol. 52, pp. 437–448, March 1973.

[KungM95] H. T. Kung and R. Morris, "Credit-Based Flow Control for ATM Networks," *IEEE Network*, pp. 40–48, March/April 1995.

[LeTWW94] W. E. Leland, M. S. Taqqu, W. Willinger, and D. W. Wilson, "On the Self-Similar Nature of Ethernet Traffic (Extended Version)," *IEEE IEEE/ACM Trans. Networking* , vol. 2, pp. 1–15, Feb. 1994.

[MASKR88] B. Maglaris, D. Anastassiou, P. Sen, G. Karlsson and J. Robbins, "Performance Models of Statistical Multiplexing in Packet Video Communications," *IEEE Trans. Commun.*, vol. 36, pp. 834–844, July 1988.

[Maybe79] P. S. Maybeck, *Stochastic Models Estimation and Control, Volume I*, Academic Press, 1979.

[Mitra88] D. Mitra, "Stochastic Theory of a Fluid Model of Producers and Consumers Coupled by a Buffer," *Adv. Appl. Prob.*, vol. 20, pp. 646–676, 1988.

[Nelso95] R. Nelson, *Probability, Stochastic Processes and Queueing Theory*, Springer-Verlag, 1995.

[NoRSV91] I. Norros, J. W. Roberts, A. Simonian and J. T. Virtamo, "The Superposition of Variable Bit Rate Sources in an ATM Multiplexer," *IEEE J. Select. Areas Commun.* pp. 378–387, April 1991.

[Norro95] I. Norros, "On the Use of Fractional Brownian Motion in the Theory of Connectionless Networks," *IEEE J. Select. Areas Commun.* pp. 953–961, Aug. 1995.

[Papou81] A. Papoulis, *Probability, Random Variables and Stochastic Processes*, International Student Edition, McGraw Hill, 1981.

[Papou84] A. Papoulis, *Probability, Random Variables and Stochastic Processes*, McGraw Hill, 1984.

[Rapel95] J. Rapeli, "UMTS: Targets, System Concept, and Standardization in a Global Framework," *IEEE Personal Commun.*, pp. 20–28, Feb. 1995.

[ReiRH96] D. J. Reininger, D. Raychaudhuri and J. Y. Hui, "Bandwidth Renegotiation for VBR Video Over ATM Networks," *IEEE J. Select. Areas Commun.*, vol. 14, pp. 1076–1085, Aug. 96.

[RenKo95] Q. Ren, and H. Kobayashi, "Transient Solutions for the Buffer Behavior in Statistical Multiplexing," *Performance Evaluation*, vol. 23, pp. 65–87, 1995.

[Rober93] J. W. Roberts, "Traffic Control in the B-ISDN," *Computer Networks and ISDN Systems*, pp. 1055–1064, 1993.

[Ross96] K. Ross, *Multiservice Loss Networks,* Springer-Verlag, 1996.

[SiLCG89] M. Sidi, W.-Z. Liu, I. Cidon and I. Gopal, "Congestion Control Through Input Rate regulation," *IEEE Trans. Commun.*, pp. 471–477, March 1993.

[StamH91] G. M. Stamatelos and J. F. Hayes, "Burst Control in Statistical Multiplexing: An Application to Broadband Networks," in *Proc. IEEE GLOBECOM'91*, Phoenix, Ariz., pp. 919–923.

[Snyde75] D. Snyder, *Random Point Processes*, John Wiley and Sons, 1975.

[TeneP63] M. Tenenbaum and H. Pollard, *Ordinary Differential Equations* , Harper & Row, 1963.

[TsiHK94] P. Tsingotjidis, J. F. Hayes and H. S. Kim, "Estimation and Prediction Approach to Congestion Control in ATM Networks," in *Proc. IEEE GLOBECOM'94*, San Francisco, CA, pp. 1785–1789.

[Turne83] J. S. Turner and L.F. Wyatt, "A packet Network Architecture for Integrated Services," *IEEE GLOBECOM'83*, San Diego, CA, pp. 2.1.1–2.1.6.

[SrirW86] K. Sriram and W. Whitt, "Characterizing Superposition Arrival Processes in Packet Multiplexers for Voice and Data," *IEEE J. Sel. Areas Commun.*, vol. 4, pp. 833–846, Sept. 1986.

[Viter92] A. J. Viterbi, "A Perspective on the Evolution of Multiple Access Satellite Communication," *IEEE J. Select. Areas Commun.*, vol. 10, pp. 980–983, Aug. 1992.

[Weis86] A. Weiss, "A New Technique for Analyzing Large Traffic Systems," *Adv. Appl. Prob.*, pp. 507–532, 1986.

[WerAG92] M. Wernik, O. Aboul-Magd and H. Gilbert, "Traffic Management for B-ISDN Services," *IEEE Network*, pp. 10–19, Sept. 1992.

[WiTSW97] W. Willinger, M. S. Taqqu, R. Sherman, and D. Wilson, "Self-Similarity Through High-Variability: Statistical Analysis of Ethernet LAN Traffic at the Source Level," *IEEE/ACM Trans. on Networking*, vol. 5, pp. 71–86, Feb. 1997.

[WuMPP94] W. W. Wu, E. F. Miller, W. L. Pritchard and R. L. Pickholtz, "Mobile Satellite Communications," *Proc. IEEE*, vol. 82, pp. 1431–1448, Sept. 1994.

[YangR95] C-Q. Yang and A. S. Reddy, "A Taxonomy for Congestion Control Algorithms in Packet Switching Networks," *IEEE Network*, pp. 34–45, July/August 1995.

[Yatsu82] Y. Yatsuzuka, "Highly Sensitive Speech Detector and High-speed Voiceband Data Discriminator in DSI-ADPCM Systems," *Trans. Commun.*, pp. 739–750, April 1982.

[YinLS90] N. Yin, S. Li and T. E. Stern, "Congestion Control for Packet Voice by Selective Packet Discarding," *IEEE Trans. Commun.*, vol. 38, pp. 674–683, May 1990.

[YinHl91] N. Yin and M. G. Hluchyj , "A Dynamic Rate Control Mechanism for Source Coded Traffic in a Fast Packet Network," *IEEE J. Select. Areas Commun.*, vol. 9, pp. 1003–1012, Sept. 1991.

APPENDIX A
EIGENVALUES AND EIGENVECTORS OF $\mathcal{C}^{-1}[\mathcal{Q} - s\mathcal{I}]$.

In this section we adapt the procedure of [RenKo95], an extension of the classic work of [AniMS82] to the transform domain, to determine the eigenvalues and eigenvectors of matrix $\mathcal{C}^{-1}[\mathcal{Q} - s\mathcal{I}]$ present in equation (3.31) of chapter 3. The next section gives the eigenvalues, while section A.2 treats the left eigenvectors. In contrast with [RenKo95], we present the left eigenvectors first, since they are the first tractable for our problem, which differs from [RenKo95] in that it is based on the backward Kolmogorov equations rather than the forward.

A.1 Eigenvalues

Consider equation (3.34) that relates the system eigenvalues with the left eigenvectors

$$\zeta_i(s)\mathbf{h}_i(s)^T\mathcal{C} \;=\; \mathbf{h}_i(s)^T[\mathcal{Q} - s\mathcal{I}]. \tag{A.1}$$

This can be also written as

$$\zeta_i(s)\left(\frac{C}{r} - m\right)h_{i,m}(s) \;=\; (N-m+1)\rho h_{i,m-1}(s) - [(N-m)\rho + m + s]\,h_{i,m}(s) + (m+1)h_{i,m+1}(s) \quad 0 \le m \le N, \tag{A.2}$$

where $h_{i,m}(s)$ denotes the m^{th} element of vector $\mathbf{h}_i(s)$. Let $H_i(s,v)$ denote the generating function of $\mathbf{h}_i(s)$, i.e.

$$H_i(s,v) = \sum_{i=0}^{N} h_{i,m}(s)v^m. \tag{A.3}$$

By multiplying (A.2) by v^m and summing over m, we obtain an equation in $H_i(s,v)$ and $\frac{\partial H_i(s,v)}{\partial v}$, (using the relation $\sum_{i=1}^{N} mv^m h_{i,m}(s) = v\frac{\partial H_i(s,v)}{\partial v}$)

$$\frac{\frac{\partial H_i(s,v)}{\partial v}}{H_i(s,v)} = \frac{-\zeta_i(s)\frac{C}{r} - N\rho - s + N\rho v}{\rho v^2 - (\zeta_i(s) - 1 + \rho)v - 1}. \tag{A.4}$$

We define $\sigma_1(s)$ and $\sigma_2(s)$ to be the distinct roots of the quadratic in the denominator of the right-hand side i.e.,

$$\sigma_1(s) = \frac{\zeta_i(s) - 1 + \rho + \sqrt{(\zeta_i(s) - 1 + \rho)^2 + 4\rho}}{2\rho} \tag{A.5}$$

$$\sigma_2(s) = \frac{\zeta_i(s) - 1 + \rho - \sqrt{(\zeta_i(s) - 1 + \rho)^2 + 4\rho}}{2\rho} \tag{A.6}$$

Equation (A.4) may now be written as

$$\frac{\frac{\partial H_i(s,v)}{\partial v}}{H_i(s,v)} = \frac{b_1(s)}{v - \sigma_1(s)} + \frac{b_2(s)}{v - \sigma_2(s)}. \tag{A.7}$$

where the residues are computed to be

$$b_2(s) = N - b_1(s) \tag{A.8}$$

$$b_1(s) = \frac{-\zeta_i(s)\frac{C}{r} - N\rho - s + N\rho\sigma_1(s)}{\rho(\sigma_1(s) - \sigma_2(s))} \tag{A.9}$$

The solution to (A.4) is

$$H_i(s,v) = (v - \sigma_1(s))^{b_1(s)}(v - \sigma_2(s))^{N-b_1(s)} \tag{A.10}$$

where we have assumed that the highest order term of $H_i(s,v)$ in terms of v is $h_{i,N}(s) = 1$.

By definition $H_i(s,v)$ is a polynomial in v of degree N. Since $\sigma_1(s)$ and $\sigma_2(s)$ are distinct, this is possible if and only if $b_1(s)$, defined in (A.9), is an integer in $[0,N]$. Denoting this integer by k, we get

$$H(s,v) = (v - \sigma_1(s))^k(v - \sigma_2(s))^{N-k} \qquad k = 0,1,\ldots,N. \tag{A.11}$$

If in (A.9) we write k for $b_1(s)$, and substitute for the expressions $\sigma_1(s)$ and $\sigma_2(s)$, rearrange, square, then we obtain the family of quadratics (3.46) in the unknown eigenvalue.

A.1.1 Properties of the Eigenvalues

Proof of Theorem 1

We adapt to our case the proof given by Ren and Kobayashi in [RenKo95]. There are two main differences between our case and the one in [RenKo95]: first we deal with the backwards equations; and second we allow loading conditions that are above the

stability point, i.e. $\frac{N\rho r}{1+\rho} > C$.

We consider the derivative of $\zeta(k,s)$ with respect to s,

$$\nabla\zeta(k,s)\frac{d\zeta(k,s)}{ds} = -\frac{\left(\frac{N}{2}-\frac{C}{r}\right)+\left(\frac{N}{2}-k\right)\frac{s+(N-\frac{C}{r})+\frac{C}{r}\rho}{\sqrt{\Delta(k,s)}}}{\left(\frac{C}{r}-k\right)\left(N-k-\frac{C}{r}\right)} \tag{A.12}$$

Then we distinguish two cases according to the value of $\frac{C}{r}$

1. $\frac{C}{r} \leq \frac{N}{2}$; then,

   1.a) When $0 \leq k \leq c$, the roots $\zeta(k,0)$, are negative; we find that $N-k-\frac{C}{r} > 0$, $\frac{C}{r}-k > 0$, $\frac{N}{2}-k > 0$, and

$$\frac{s+(N-\frac{C}{r})+\frac{C}{r}\rho}{\sqrt{\Delta(k,s)}} \geq 1 \qquad \forall s \geq 0.$$

   Then,

$$\frac{d\zeta(k,s)}{ds} \leq -\frac{(\frac{N}{2}-\frac{C}{r})+(\frac{N}{2}-k)}{(\frac{C}{r}-k)(N-k-\frac{C}{r})} < 0.$$

   1.b) When $c+1 \leq k \leq N$, the roots $\zeta(k,0)$, are non-negative;

   1.b–i) if $c+1 \leq k \leq N-c$, it follows that $N-k-\frac{C}{r} > 0$, $\frac{C}{r}-k < 0$, $\frac{N}{2}-k < 0$, and

$$0 \leq \frac{s+(N-\frac{C}{r})+\frac{C}{r}\rho}{\sqrt{\Delta(k,s)}} \leq 1 \qquad \forall s \geq 0.$$

Then,

$$\frac{d\zeta(k,s)}{ds} \geq -\frac{\frac{N}{2}-\frac{C}{r}+(\frac{N}{2}-k)}{(\frac{C}{r}-k)(N-k-\frac{C}{r})} > 0$$

1.b–ii) if $N-c+1 \leq k \leq N$, it follows that $N-k-\frac{C}{r} < 0$, $\frac{C}{r}-k < 0$, $\frac{N}{2}-k < 0$, and

$$\frac{s+(N-\frac{C}{r})+\frac{C}{r}\rho}{\sqrt{\Delta(k,s)}} \geq 1 \qquad \forall s \geq 0.$$

Then,

$$\frac{d\zeta(k,s)}{ds} \geq -\frac{\frac{N}{2}-\frac{C}{r}+(\frac{N}{2}-k)}{(\frac{C}{r}-k)(N-k-\frac{C}{r})} > 0$$

2. $\frac{N}{2} < \frac{C}{r} < N$; then

2.a) When $0 \leq k \leq c$, the roots $\zeta(k,0)$, are negative; We find that $N-k-\frac{C}{r} > 0$, $\frac{C}{r}-k > 0$, $\frac{N}{2}-k > 0$, and

$$\frac{s+(N-\frac{C}{r})+\frac{C}{r}\rho}{\sqrt{\Delta(k,s)}} \geq 1 \qquad \forall s \geq 0.$$

Then,

$$\frac{d\zeta(k,s)}{ds} \leq -\frac{\frac{N}{2}-\frac{C}{r}+(\frac{N}{2}-k)}{(\frac{C}{r}-k)(N-k-\frac{C}{r})} < 0$$

2.b) When $c+1 \leq k \leq N$, the roots $\zeta(k,0)$, are non-negative;

2.b–i) if $c+1 \leq k \leq N-c$, it follows that $N-k-\frac{C}{r} > 0$, $\frac{C}{r}-k < 0$, $\frac{N}{2}-k < 0$, and

$$0 \leq \frac{s+(N-\frac{C}{r})+\frac{C}{r}\rho}{\sqrt{\Delta(k,s)}} \leq 1 \qquad \forall s \geq 0.$$

Then,

$$\frac{d\zeta(k,s)}{ds} \geq -\frac{\frac{N}{2}-\frac{C}{r}+(\frac{N}{2}-k)}{(\frac{C}{r}-k)(N-k-\frac{C}{r})} > 0$$

2.b–ii) If $N-c+1 \leq k \leq N$, it follows that $N-k-\frac{C}{r} < 0$, $\frac{C}{r}-k < 0$, $\frac{N}{2}-k < 0$, and

$$\frac{s+(N-\frac{C}{r})+\frac{C}{r}\rho}{\sqrt{\Delta(k,s)}} \geq 1 \qquad \forall s \geq 0.$$

Then,

$$\frac{d\zeta(k,s)}{ds} \geq -\frac{\frac{N}{2}-\frac{C}{r}+(\frac{N}{2}-k)}{(\frac{C}{r}-k)(N-k-\frac{C}{r})} > 0$$

The above observations can be summarized as follows:

- Consider those roots that are positive at at $s=0$. There exist $N-c-1$ such roots. Their derivatives $\frac{d\zeta(k,s)}{ds}$ are always positive.

- Consider those roots that are negative at $s=0$. There exist $c+1$ such roots. Their derivatives $\frac{d\zeta(k,s)}{ds}$ are always negative for $s \geq 0$.

- The root that corresponds to $k = N$ intersects the origin at $s = 0$: $u(N, 0) = 0$. Its derivative $\frac{d\zeta(N,s)}{ds}$ is always positive.

A.2 Left Eigenvectors

The generating function of the left eigenvector is given by equation (A.11). Expanding (A.11), yields the coefficients of the given polynomial, and thus the eigenvector coefficients. Thus the m^{th} component of the i^{th} eigenvector is given as,

$$h_{i,m}(s) = (-1)^{N-m} \sum_{j=0}^{k} \begin{pmatrix} k \\ j \end{pmatrix} \begin{pmatrix} N-k \\ m-j \end{pmatrix} \sigma_1(s)^{k-j} \sigma_2(s)^{N-k-m+j} \quad \text{(A.13)}$$
$$0 \leq m \leq N.$$

We see that for the determination of the elements of the eigenvector knowledge of $\sigma_1(s)$ and $\sigma_2(s)$ is required. We recall that these are given as solutions to the quadratic at the denominator of (A.4) by expressions (A.5) and (A.6) respectively.

A problem with the calculation of $\sigma_1(s)$ and $\sigma_2(s)$ as seen from (A.5) and (A.6), is the square root in the numerator of both expressions. However, using equation (A.9), and setting $b_1(s) = k$ on its LHS, we can show by substitution of the expressions for $\sigma_1(s)$ and $\sigma_2(s)$ and subsequent rearrangement that

$$\sqrt{(\zeta(k,s) - 1 + \rho)^2 + 4\rho} = \frac{s + \zeta(k,s)\left(\frac{N}{2} - \frac{C}{r}\right) - \frac{N}{2}(\rho + 1)}{k - \frac{N}{2}}. \quad \text{(A.14)}$$

Accordingly, $\sigma_1(s)$ and $\sigma_2(s)$ are expressed as follows

$$\sigma_1(s) = \frac{\zeta(k,s)\left(k-\frac{C}{r}\right)+k(\rho-1)+s-N\rho}{2\rho\left(k-\frac{N}{2}\right)} \tag{A.15}$$

$$\sigma_2(s) = \frac{\zeta(k,s)\left(k+\frac{C}{r}-N\right)+k(\rho-1)-s+N}{2\rho\left(k-\frac{N}{2}\right)} \tag{A.16}$$

Having found $\sigma_1(s)$ and $\sigma_2(s)$ for a particular value of k we use (A.14) to yield the coefficients of the given polynomial and thus the eigenvector coefficients. A further simplification comes from the observation that depending on the value of k, m and N, the terms in the summation (A.14) may involve the product of $\sigma_1(s)\sigma_2(s)$ raised to the appropriate power, times a power of $\sigma_1(s)$ or $\sigma_2(s)$. However, since $\sigma_1(s)$ and $\sigma_2(s)$ are given as solutions of the quadratic in the denominator of the RHS in (A.4), their product is

$$\sigma_1(s)\sigma_2(s) = -\frac{1}{\rho}, \tag{A.17}$$

independent of s. Moreover, any power of either $\sigma_1(s)$ or $\sigma_2(s)$ will only involve a polynomial in s, and polynomials of s multiplied by $\sqrt{\Delta(k,s)}$. Hence, the general form of the elements $h_{i,m}(s)$ of the left eigenvectors $\mathbf{h}_i(s)$ is

$$h_{i,m}(s) = p(s) + q(s)\sqrt{\Delta(k,s)} \tag{A.18}$$

where $p(s)$ and $q(s)$ are polynomials in s.

A.3 Right Eigenvectors

In contrary with [AniMS82], we have started with the evaluation of the left eigenvectors, since this is the only tractable approach in our case due to the backward form of the equation 3.31. However, we are more familiar with right eigenvectors, and in order to express the solution of our problem in a more convenient way, we continue by deriving the column right eigenvectors as well.

There is a diagonal matrix $\mathcal{S}$ that symmetrizes $\mathcal{Q}$ i.e., with $\mathcal{S}_{mm} = \sqrt{\rho^m \binom{N}{m}}$. Moreover,

$$\mathbf{h}_i(s) = (\mathcal{S}^{-1})^2 \mathbf{f}_i(s),$$

and thus elementwise,

$$f_{i,m}(s) = \rho^m \binom{N}{m} h_{i,m}(s). \tag{A.19}$$

APPENDIX B
EIGENVALUES AND EIGENVECTORS OF $\mathcal{C}^{-1}\mathcal{Q}$

We start with the equation that involves the left eigenvector

$$z_i \bar{\psi}_i^T \mathcal{C} \;=\; \bar{\psi}_i^T \mathcal{Q}. \tag{B.1}$$

Equation (B.1) is similar to the relevant equation in [AniMS82], with the only differences being that in our case we are dealing with the left eigenvectors, while Anick et al. deal with the right ones, and our matrices $\mathcal{Q}$ and $\mathcal{C}$ are the transpose and negative respectively of the relevant matrices in [AniMS82]. These differences are brought about, as mentioned earlier, on the fact that we use the backward Kolmogorov equations in the formulation of our first passage problem, while Anick et al. use an approach based on the forward equations.

Therefore, to find z_i as well as $\bar{\psi}_i$, we can directly use their results, adapted to our case. Taking the transpose of both sides of (B.1) and incorporating the negative of matrix $\mathcal{C}$ in it,

$$-z_i\,(-\mathcal{C})\,\bar{\psi}_i \;=\; \mathcal{Q}^T \bar{\psi}_i. \tag{B.2}$$

Comparing this with the relevant equation in [AniMS82], we see that our eigenvalues

are the negative of theirs and our left eigenvectors are their right eigenvectors. Similar comments apply to our right eigenvectors.

A further point that introduces one more change in the results of [AniMS82] as applied to our case, is that that in our case the multiplexer operates with an average input load that is greater than the channel capacity, i.e., $\frac{N\rho r}{1+\rho} > C$. This by itself forces one of the negative eigenvalues in [AniMS82] to switch sign and become positive (see appendix of [AniMS82]).

Taking into consideration this final comment and the results of [AniMS82], we conclude that there are $N - c - 1$ positive positive eigenvalues for our system, one at at 0, and $c + 1$ negative eigenvalues.

APPENDIX C
A PARTICULAR SOLUTION OF THE SYSTEM OF DIFFERENTIAL EQUATIONS (3.55)

In this appendix we use the method of variation of parameters [TeneP63] to derive a particular solution of the inhomogeneous system of first order linear differential equations in equation (3.55),

$$C\frac{d\mathbf{M}_n^+(\xi_0)}{d\xi_0} = \mathcal{Q}\mathbf{M}_n^+(\xi_0) + n!\mathbf{M}_{n-1}^+(\xi_0). \tag{C.1}$$

From (3.59), the general solution of the homogeneous system is

$$\mathbf{M}_{n_{gh}}^+(\xi_0) = \sum_{i=0}^{N} u_{ni} e^{z_i(\xi_0 - B')}\bar{\phi}_i. \tag{C.2}$$

According to the method, we treat u_{ni} as being functions of the independent parameter ξ_0; accordingly the general form of a particular solution for the inhomogeneous system (C.1) is

$$\mathbf{M}_{n_{pi}}^+(\xi_0) = \sum_{i=0}^{N} u_{ni}(\xi_0) e^{z_i(\xi_0 - B')}\bar{\phi}_i. \tag{C.3}$$

In order to determine the exact form of $u_{ni}(\xi_0)$, we must substitute (C.3) in the

original differential equation (C.1). Accordingly,

$$\sum_{i=0}^{N} \mathcal{C}\frac{d}{d\xi_0}\left(u_{ni}(\xi_0)e^{z_i(\xi_0-B')}\right)\bar{\phi}_i = \mathcal{Q}\sum_{i=0}^{N} u_{ni}(\xi_0)e^{z_i(\xi_0-B')}\bar{\phi}_i + n!\mathbf{M}^{+}_{n-1}(\xi_0) \qquad \text{(C.4)}$$

Performing the differentiation on the left hand side of (C.4), and taking into account that

$$\mathcal{C}u_{ni}(\xi_0)\frac{d}{d\xi_0}\left(e^{z_i(\xi_0-B')}\right)\bar{\phi}_i = \mathcal{Q}\sum_{i=0}^{N} u_{ni}(\xi_0)e^{z_i(\xi_0-B')}\bar{\phi}_i \qquad \text{(C.5)}$$

we have,

$$\sum_{i=0}^{N} \mathcal{C}\frac{du_{ni}(\xi_0)}{d\xi_0}e^{z_i(\xi_0-B')}\bar{\phi}_i = n!\mathbf{M}^{+}_{n-1}(\xi_0) \qquad \text{(C.6)}$$

Further multiplying (C.6) on the left by the left eigenvector $\bar{\psi}_i^T$, and using the fact that $\bar{\psi}_i^T\mathcal{C}\bar{\phi}_j = 0$, for $i \neq j$, we get

$$\bar{\psi}_i^T\mathcal{C}\frac{du_{ni}(\xi_0)}{d\xi_0}e^{z_i(\xi_0-B')}\bar{\phi}_i = n!\bar{\psi}_i^T\mathbf{M}^{+}_{n-1}(\xi_0). \qquad \text{(C.7)}$$

Integrating with respect to ξ_0,

$$u_{ni}(\xi_0) = n!\int_0^{\infty} \frac{\bar{\psi}_i^T\mathbf{M}^{+}_{n-1}(\xi_0)}{\bar{\psi}_i^T\mathcal{C}\bar{\phi}_i}e^{-z_i(\xi_0-B')}d\xi_0. \qquad \text{(C.8)}$$

By substituting (C.8) in (C.3) (3.60) follows.

APPENDIX D
DEPENDENCE OF THE OPTIMUM LINEAR FILTER ON THE OBSERVATION DATA AND ESTIMATED PROCESS STATISTICS

In this Appendix we discuss the dependence of linear estimation on the statistics of the observation data and the estimated process. Although the results discussed here are general, we will present them in the context of our estimation problem, namely the estimate of the network state in a ATM network given cell count observation data.

We start by highlighting the derivation of the discrete form of the Wiener-Hopf equation for our problem. From this equation, it is seen that linear estimation depends only on the second order statistics of the observation data and their statistical relation to the estimated process. Moreover, in the case of an additive white and Gaussian observation noise, only the second order properties of the estimated process are relevant as well.

Towards this end, let M be the current observation interval, $A_{l,M}$ the network state in terms of active sources of class l, and Y_i, $i \in \{1, 2, \ldots, M\}$ our observation data, in terms of number of cell arrivals, for the past M consecutive observation intervals. At this point we do not make any specific assumption about the source of the observations; they can either correspond to all traffic types on the VP or they can be the number of observations from a single source type. We perform linear

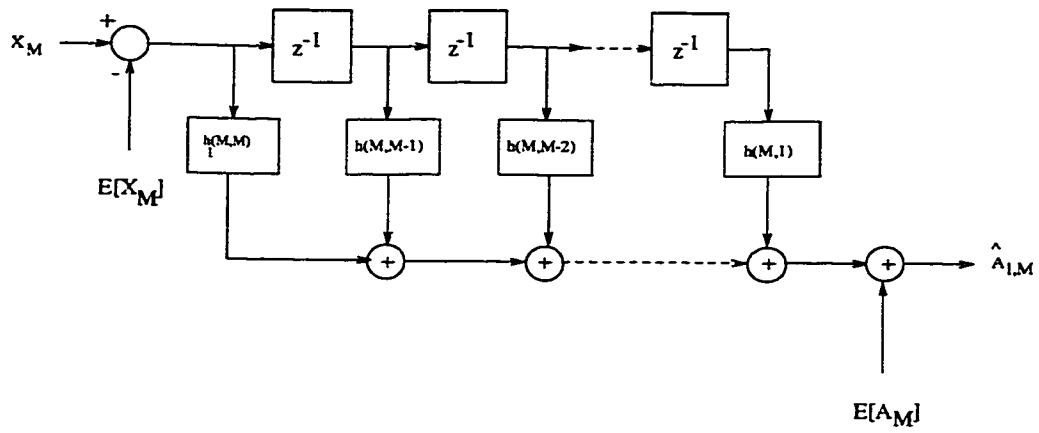

Figure D.1: The linear filter structure

estimation of $\tilde{A}_{l,M} = A_{l,M} - E[A_{l,M}]$, given the M observations $\tilde{Y}_i = Y_i - E[Y_i]$, $i \in \{1,2, \ldots, M\}$. Then the estimate $\hat{\tilde{A}}_{l,M}$ of $\tilde{A}_{l,M}$ is written as

$$\hat{\tilde{A}}_{l,M} = \sum_{i=1}^{M} h_l(M,i)\tilde{Y}_i.$$

We allow the linear filter coefficients, $h_l(M,i)$, to depend on both the current time and the order of the filter coefficient, allowing possible time variant solutions of the optimality problem.

Minimization of $\epsilon_M = E\left[\left(\tilde{A}_{l,M} - \hat{\tilde{A}}_{l,M}\right)^2\right]$, the mean square error of the estimator, results in the orthogonality principle [Papou84], according to which, the estimation error of the optimal filter must be orthogonal to all data,

$$E\left[\left(\tilde{A}_{l,M} - \sum_{i=1}^{M} h_l^o(M,i)\tilde{Y}_i\right)\tilde{Y}_m\right] = 0 \qquad \forall m \in \{1,2,\ldots,M\} \qquad \text{(D.1)}$$

$h_l^o(M,i)$ being the coefficients of the optimum linear filter. We expand (D.1) and recalling that $\tilde{A}_{l,i}$ and $\tilde{Y}_i$ are centered processes derived from $A_{l,i}$ and Y_i respectively,

we write

$$C_{A_l Y}(M,m) = \sum_{i=1}^{M} h_l^o(M,i) C_{YY}(i,m) \qquad \forall m \in \{1,2,\ldots M\}. \tag{D.2}$$

with $C_{YY}(i,m)$ the autocovariance function of the observation data, and $C_{A_l Y}(M,m)$ the crosscovariance function of the observation data with the estimated process A_l. From equation (D.2) we see that the filter coefficients of the optimal linear filter depend on the second order statistical properties of the observation data.

Moreover, by assuming an AWGN for the observation data Y_i, i.e. of the form (4.11),

$$\tilde{Y}_i = c_{l,i}\tilde{A}_{l,i} + V_i \tag{D.3}$$

with $c_{l,i}$ some real constants, and V_i a zero mean Gaussian noise sequence, the optimal linear filter depends on the second order statistical properties of the estimated process. Clearly, under the assumption of the observation model in (D.3), equation (D.2) is written as

$$c_{l,m} C_{A_l A_l}(M,m) = \sum_{i=1}^{M} \sum_{l=1}^{L} c_{l,i} c_{l,m} h_l^o(M,i) C_{A_l A_l}(i,m) + \sigma_{V_i}^2. \tag{D.4}$$

APPENDIX E
OBSERVATION DATA AND ESTIMATED PROCESS STATISTICS

E.1 Statistics of the Observation Data

In this section we give statistics up to the second order of the cell count process at the output of a multiplexer. More precisely, we are interested in the autocovariance function of the observation data, and the cross-covariance function of the data with the network state process. We derive these expressions in terms of the cross-covariance function of the network state process A_i, assuming two models of cell generation during active source periods: a) deterministic, with uniform fixed rate (On-Off source model); and b) probabilistic, with exponentially distributed cell interarrival times (IPP source model).

We base our derivations on tagging a particular class of sources. In a multiple source type environment the number of packet counts in a time slot Y_i can be written as $Y_i = \sum_{l=1}^{L} Y_{l,i}$, where $Y_{l,i}$ is the contribution to the packet count of the l^{th} class of sources. The actions of the sources being independent, $Y_{l,i}$ are independent random variables; as such, the statistics of their sum, Y_i, are simply expressed as sums of the individual per class statistics.

Mean Number of Observations in a Time Interval

We tag a certain source type l. Using the observation model in equation (4.51) and conditioning on the state of the source, the mean number of cells observed during the i^{th} time interval belonging to the tagged class, is given as

$$E[Y_{l,i} \mid A_{l,i} = a_l] = a_l \lfloor wr_l \rfloor + E[Z_{l,i} \mid A_{l,i} = a_l]. \tag{E.1}$$

However, $Z_{l,i}$ given $A_{l,i} = a_l$ is binomially distributed (equation (4.50)), with mean $E[Z_{l,i} \mid A_{l,i} = a_l] = a_l \pi_l$. Substituting in (E.1), and taking into consideration that $\pi_l = wr_l - \lfloor wr_l \rfloor$, we have

$$E[Y_{l,i} \mid A_{l,i} = a_l] = a_l wr_l. \tag{E.2}$$

Finally unconditioning on $A_{l,i}$,

$$E[Y_{l,i}] = E[A_{l,i}] wr_l. \tag{E.3}$$

For L class types,

$$E[Y_i] = \sum_{l=1}^{L} E[A_{l,i}] wr_l. \tag{E.4}$$

Variance of the Number of Observations in a Time Interval

We start by deriving $E[Y_{l,i}^2]$, the mean square of the number of observations in a time slot, that belong to class l. Conditioning on the number of active sources of type l, $A_{l,i} = a_l$, and taking into consideration equation (4.51), we write

$$E[Y_{l,i}^2 \mid A_{l,i} = a_l] =$$

$$(a_l \lfloor wr_l \rfloor)^2 + E\left[Z_{l,i}^2 \mid A_{l,i} = a_l\right] + 2a_l \lfloor wr_l \rfloor E[Z_{l,i} \mid A_{l,i} = a_l] \qquad \text{(E.5)}$$

However, given that a_l sources of class l are active, $Z_{l,i}$ is binomially distributed; thus, its mean and mean square are,

$$E\left[Z_{l,i}\right] = a_l \pi_l, \qquad \text{(E.6)}$$

$$E\left[Z_{l,i}^2 \mid A_{l,i} = a_l\right] = a_l^2 \pi_l^2 + a_l \pi_l (1 - \pi_l) \qquad \text{(E.7)}$$

respectively. Substituting (E.6) and (E.7) in (E.5) we get,

$$E[Y_{l,i}^2 \mid A_{l,i} = a_l] = (a_l \lfloor wr_l \rfloor)^2 + a_l^2 \pi_l^2 + a_l \pi_l (1 - \pi_l) + 2a_l \lfloor wr_l \rfloor a_l \pi_l. \qquad \text{(E.8)}$$

Completing the square in the RHS of equation (E.8),

$$E[Y_{l,i}^2 \mid A_i = a_l] = (a_l wr_l)^2 + a_l \pi_l (1 - \pi_l),$$

and unconditioning on $A_{l,i}$,

$$E[Y_{l,i}^2] = E[A_{l,i}^2](wr_l)^2 + E[A_i]\pi_l(1-\pi_l).$$

Finally, using (E.3),

$$\begin{aligned}\sigma_{Y_{l,i}}^2 &= E[Y_{l,i}^2] - E[Y_{l,i}]^2 \\ &= \sigma_{A_{l,i}}^2(wr)^2 + E[A_{l,i}]\pi_l(1-\pi_l). \end{aligned} \tag{E.9}$$

For L source types, since the number of observed cells belonging to different classes are independent from each other,

$$\sigma_{Y_i}^2 = \sum_{l=1}^{L} \sigma_{A_{l,i}}^2(wr_l)^2 + \sum_{l=1}^{L} E[A_{l,i}]\pi_l(1-\pi_l). \tag{E.10}$$

Autocovariance Function of the Observation Data

We again tag a certain source type l. By definition, the autocovariance function of the observation data, belonging to the tagged class, is given as

$$C_{Y_lY_l}(i,j) = E[Y_{l,i}Y_{l,j}] - E[Y_{l,i}]E[Y_{l,j}] \tag{E.11}$$

with arguments i and j denoting the i^{th} and j^{th} observation intervals. We only consider $C_{Y_lY_l}(i,j)$ for $i \neq j$, since $C_{Y_lY_l}(i,i) = \sigma_{Y_{l,i}}^2$, and has been derived above (equation (E.9)).

Equation (E.11) involves the joint mean of the number of observations in intervals i and j, $E[Y_{l,i}Y_{l,j}]$. Conditioning on the number of active sources during the i and j time slot, $Y_{l,i}$ and $Y_{l,j}$ are independent; thus, using equation (E.2)

$$\begin{aligned} E[Y_{l,i}Y_{l,j} \mid A_{l,i} = a_l, A_{l,j} = a_m] &= E[Y_i \mid A_{l,i} = a_l]E[Y_j \mid A_{l,j} = a_m] \\ &= a_l a_m w^2 r_l^2. \end{aligned}$$

Unconditioning on $A_{l,i}$ and $A_{l,j}$,

$$E[Y_{l,i}Y_{l,j}] = E[A_{l,i}A_{l,j}](wr_l)^2 \tag{E.12}$$

Finally substituting (E.12) in (E.11) and using (E.3) we get

$$C_{Y_lY_l}(i,j) = (wr_l)^2 C_{A_lA_l}(i,j) \qquad i \neq j$$

with $C_{A_lA_l}(i,j)$ the autocovariance function of A_l, the number of active sources of type l. For L source types

$$C_{YY}(i,j) = \sum_{l=1}^{L} (wr_l)^2 C_{A_lA_l}(i,j) \qquad i \neq j \tag{E.13}$$

Crosscovariance function of the Observation Data with the State Process

We again tag a certain source type l. By definition, the crosscovariance of the network state process, in terms of active sources of class l during the i^{th} time interval,

with the number of observations during the j^{th} time slot.

$$C_{A_l Y}(i,j) \triangleq E[A_{l,i} Y_j] - E[A_{l,i}]E[Y_j] \tag{E.14}$$

Equation (E.14) involves the joint mean $E[A_{l,i}Y_j]$. Conditioning on $A_{l,j} = a_l$,

$$\begin{aligned} E[A_{l,i}Y_j \mid A_{l,j} = a_l] &= E[Y_j \mid A_{l,j} = a_l]E[A_{l,i} \mid A_{l,j} = a_l] \\ &= wr_l a_l E[A_{l,i} \mid A_{l,j} = a_l] \end{aligned}$$

Further, unconditioning on $A_{l,j}$,

$$E[A_{l,i}Y_{l,j}] = wr_l E[A_{l,i}A_{l,j}] \tag{E.15}$$

Finally, substituting (E.15) in (E.14),

$$C_{A_l Y}(i,j) = wr_l C_{A_l A_l}(i,j) \tag{E.16}$$

E.1.2 IPP Source Model

We continue by deriving the statistics of the observation data in the case of the IPP source model. In contrast with above we give results for a single source type for brevity.

Mean Number of Observations in a Time Interval

Conditioning on the state of A_i during the i^{th} source interval, Y_i is Poisson distributed (equation (4.26)). Therefore its mean is given as

$$E[Y_i \mid A_i = a] = aw\gamma.$$

Unconditioning on A_i,

$$E[Y_i] = E[A_i]w\gamma. \tag{E.17}$$

Variance of the Number of Observations in a Time Interval

The derivation of the variance of Y_i starts with finding its mean square first. Conditioning on $A_i = a$, Y_i is Poisson distributed with rate $aw\gamma$ (equation (4.26)); accordingly its mean square is given as

$$E[Y_i^2 \mid A_i = a] = aw\gamma + (aw\gamma)^2.$$

Unconditioning on $A_i = a$,

$$E[Y_i^2] = E[A_i]w\gamma + E[A_i]^2(w\gamma)^2.$$

Finally, using (E.17)

$$\begin{aligned} \sigma_{Y_i}^2 &= E[Y_i^2] - E[Y_i]^2 \\ &= E[A_i]w\gamma. \end{aligned} \tag{E.18}$$

Autocovariance Function of the Observation Data

The autocovariance function of the observation process, is given by definition as

$$C_{YY}(i,j) \triangleq E[Y_iY_j] - E[Y_i]E[Y_j] \tag{E.19}$$

with arguments i and j denoting the i^{th} and j^{th} observation intervals. We only consider $C_{YY}(i,j)$ for $i \neq j$, since $C_{YY}(i,i) = \sigma_{Y_i}^2$ and has been derived above (equation (E.18)).

Equation (E.19) involves the joint mean $E[Y_iY_j]$. Conditioning on the number of active sources during the i and j time slot, Y_i and Y_j are independent and Poisson distributed; thus

$$\begin{aligned} E[Y_iY_j \mid A_i = a_i, A_j = a_j] &= E[Y_i \mid A_i = a_i]E[Y_j \mid A_j = a_j] \\ &= a_ia_jw^2\gamma^2. \end{aligned}$$

Unconditioning on A_i and A_j,

$$E[Y_iY_j] = E[A_iA_j](w\gamma)^2. \tag{E.20}$$

Finally substituting (E.20) in (E.19) we get

$$C_{YY}(i,j) = (w\gamma)^2 C_{AA}(i,j) \qquad i \neq j \tag{E.21}$$

with $C_{AA}(i,j)$ the autocovariance of the network state process.

Crosscovariance function of the Observation Data with the State Process

The crosscovariance of the state process, in terms of number of active sources during the i^{th} time slot, and the number of observations during the j^{th} time slot is defined as

$$C_{AY}(i,j) \triangleq E[A_i Y_j] - E[A_i]E[Y_j] \tag{E.22}$$

Equation (E.22) involves the joint mean $E[A_i Y_j]$. Conditioning on $A_j = a$, Y_j is Poisson distributed with rate $aw\gamma$

$$\begin{aligned} E[A_i Y_j \mid A_j = a] &= E[Y_j \mid A_j = a]E[A_i \mid A_j = a] \\ &= aw\gamma E[A_i \mid A_j = a] \end{aligned}$$

Further, unconditioning on A_j,

$$E[A_i Y_j] = w\gamma E[A_i A_j]. \tag{E.23}$$

Finally, substituting (E.23) in (E.22),

$$C_{AY}(i,j) = w\gamma C_{AA}(i,j) \tag{E.24}$$

E.2 Statistics of the Stationary State Process

We derive the first and second order statistics of the network state process, i.e. the process that characterizes the number of active sources; results are given considering a single source, and assuming stationarity. The actions of the sources being independent, results for more than one sources, and for different source types, stand as simple generalizations of the expressions for a single source.

E.2.1 Mean Number of Active Sources

The mean of A_i, for a single source, is simply the steady state probability that a source is in the active state during a time slot, $\pi_{on} = \frac{p}{p+q}$. Moreover, given N sources of the same type,

$$E[A_i] = \frac{Np}{p+q}. \tag{E.25}$$

E.2.2 Variance of the Number of Active Sources

The variance of A_i, for a single source, is the variance of steady state distribution

of the activity of a single source, $\sigma = \frac{pq}{p+q}$. Consequently, for N identical sources,

$$\sigma_A^2 = \frac{Npq}{p+q}. \tag{E.26}$$

E.2.3 Autocovariance Function of the Number of Active Sources

We follow an adaptation of the approach taken in [Papou84] for the generalized telegraph signal, assuming that time is discrete.

By definition,

$$\begin{aligned} C_{AA}(m) &\triangleq E[A_i A_{i+m}] - E[A_i]E[A_{i+m}] \\ &= E[A_i A_{i+m}] - \left(\frac{p}{p+q}\right)^2 \end{aligned} \tag{E.27}$$

where we have used the result in section E.2.1. However, since our system state can assume only two values, $A_i = 1$, when the single source is active, and $A_i = 0$, when is idle,

$$\begin{aligned} E[A_i A_{i+m}] &= \sum_{k,l} kl \Pr(A_i = k, A_{i+m} = l) \\ &= \Pr(A_i = 1, A_{i+m} = 1) \\ &= \Pr(A_{i+m} = 1 \mid A_{i+m} = 1)\pi_{on} \end{aligned} \tag{E.28}$$

We denote the conditional probability at the RHS of (E.28) by $p_{11}(m)$,

$$p_{11}(m) = \Pr(A_{i+m} = 1 \mid A_i = 1)$$

Similarly, we denote by $p_{10}(m)$ the probability that A_i goes from the active to idle in m steps. With the above definition we can formulate the Chapman-Kolmogorov equations that relate the state of A_i at times $i+m-1$, and $i+m$, given that at time i, $A_i = 1$.

$$p_{11}(m) = p_{11}(m-1)(1-q) + p_{10}(m-1)p \tag{E.29}$$

$$p_{10}(m) = p_{11}(m-1)q + p_{10}(m-1)(1-p) \tag{E.30}$$

Equations (E.29) and (E.30) comprise a system of difference equations which in matrix form is written as

$$\mathbf{p}_1(m) = \mathcal{P}\mathbf{p}_1(m-1) \tag{E.31}$$

with $\mathbf{p}_1(.) = (p_{11}(.), p_{10}(.))^T$ and

$$\mathcal{P} = \begin{bmatrix} 1-q & p \\ q & 1-p \end{bmatrix} \tag{E.32}$$

The solution of equation (E.31) for $p_{11}(m)$ can be expressed using the eigenvalues of matrix $\mathcal{P}$, $1-p-q$ and 1, as

$$p_{11}(m) = k_1(1-p-q)^m + k_2 1^m \tag{E.33}$$

with k_1 and k_2 constants to be determined. Constant k_2 is the steady state probability

that the source is active; this can be justified simply by taking the limit of $p_{11}(m)$ for $m \to \infty$. The remaining constant k_1 is determined from the initial condition, $p_{11}(0) = 1$. The final solution then becomes

$$p_{11}(m) = \frac{q}{p+q}(1-p-q)^m + \frac{p}{p+q} \tag{E.34}$$

Substituting (E.34) in (E.28) and considering that $\pi_{on} = \frac{p}{p+q}$, we finally get,

$$C_{AA}(m) = \frac{pq}{(p+q)^2}(1-p-q)^m \tag{E.35}$$

Equation (E.35) gives the autocovariance function of A_i in the case of a single source. For N identical sources,

$$C_{AA}(m) = N\frac{pq}{(p+q)^2}(1-p-q)^m. \tag{E.36}$$